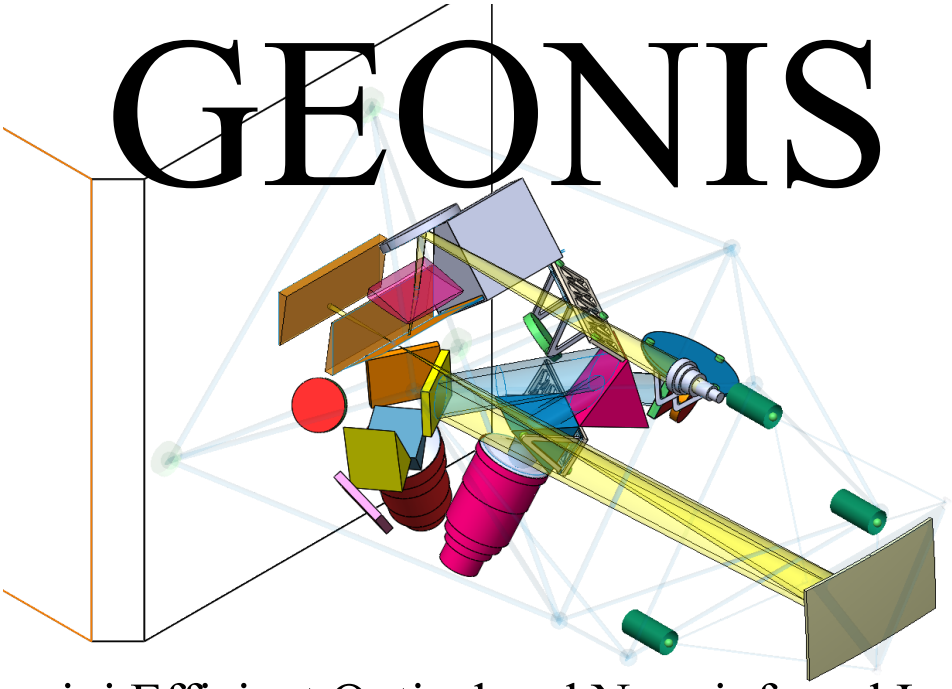
GEONIS



Gemini Efficient Optical and Near-infrared Imager and Spectrograph

J. M. Desert (CU Boulder)
D. Fox (Penn State)
M. Kasliwal (project scientist, Caltech)
M. van Kerkwijk (Toronto)
N. Konidaris (principal investigator, Caltech)
J. Masiero (JPL)
T. Matheson (NOAO)
D. Reiley (project manager, Caltech)

in collaboration with Gemini staff:
M. Close, S. Goodsell, R. Mason, B. Rambold

A Executive Summary

The astronomical landscape in the coming decade will be dominated by next generation wide-field synoptic surveys at every wavelength: optical (TESS, ZTF, LSST), infrared (JWST, NeoWISE, NEOCAM, WFIRST), ultraviolet (ULTRASAT), radio (LOFAR, LWA, SKA, ALMA). Experience with current surveys (e.g. SDSS, PTF) has shown that spectroscopic follow-up holds the key to unraveling the astrophysics and hence, realizing the science from discoveries by synoptic surveys.

A comparative analysis of various instruments on large aperture telescopes has shown that the primary workhorse (in units of papers, citations, and time usage) is the spectrograph[1]. Thus, the success of an observatory is closely tied to the quality and efficiency of its instrumentation with the highest bar being set for its spectrographs.

To determine the science requirements of a next generation spectrograph, we studied three ongoing large and long term programs at Gemini: near earth asteroids (PI Masiero), extrasolar planets (PI Desert) and transients (PI Kasliwal).

Driven by the science requirements, we propose GEONIS — a spectrograph designed with the goal of maximizing every iota of efficiency while enabling a breadth of new science. GEONIS will deliver wavelength coverage spanning 400 nm to 1,600 nm with a tunable resolution leveraging high-speed low-read-noise detectors. To boost instrument efficiency, GEONIS will have a slit-viewing camera, atmospheric dispersion compensation system, and flexure compensation system that will maximize the fraction of time Gemini is collecting science photons and minimize overhead.

GEONIS capitalizes on Gemini's unique strengths. In particular, Gemini's successful queue observing mode is well-suited to rapid response classification of events discovered by synoptic surveys. We propose to operate GEONIS in classification-driven observing mode such that on-the-fly reduced spectra directly determine the next steps in the panchromatic follow-up sequence. This opens up a new paradigm of minute-timescale response to the fastest relativistic explosions, the youngest supernovae and the rarest neutron-star mergers.

Our vision is that GEONIS leads the way in leveraging the science potential of discoveries from the James Webb Space Telescope (JWST), Large Synoptic Survey Telescope (LSST), advanced Laser Interferometer Gravitational-Wave Observatory (aLIGO), Transiting Exoplanet Survey Satellite (TESS), and the Wide-Field infrared Survey Telescope (WFIRST).

The GEONIS concept meets the aforementioned science requirements and fits within the cost cap of \$12 M (projected at \$10.4M, with a variance up to \$12.4 M), mass limit of 2 ton (projected at 1.6 ton, without contingency), and volume limits of Gemini instrumentation. From start to first light GEONIS is projected to take almost six years.

[1] `http://www.astro.caltech.edu/~srk/KeckInstruments.pdf`

Contents

A Executive Summary 1

B Science Objectives, Science Case, and Science Requirements 5
- B.1 GEONIS and Time Domain Astronomy . . . 5
  - B.1.1 Flash Spectroscopy of Newborn Supernovae . . . 5
  - B.1.2 Relativistic Explosions . . . 7
  - B.1.3 GEONIS in the Era of Low Latency Astrophysics . . . 8
  - B.1.4 GEONIS in the advanced LIGO era . . . 9
- B.2 GEONIS and Near Earth Asteroids . . . 10
- B.3 GEONIS and Exoplanetology . . . 12
- B.4 Scope & Risk: Science Team's Role . . . 14
- B.5 GEONIS in the LSST era . . . 14
- B.6 Science Requirements . . . 16

C Operations Concept Document 17
- C.1 Science Priorities . . . 17
  - C.1.1 Simplicity . . . 17
  - C.1.2 Spectral Resolution . . . 17
  - C.1.3 Throughput . . . 17
- C.2 Instrument Concept Overview . . . 17
- C.3 Summary of Requirements . . . 18
  - C.3.1 Modes of Operation . . . 18
  - C.3.2 Instrument Control . . . 18
  - C.3.3 Atmospheric Dispersion Corrector . . . 18
  - C.3.4 Guiding . . . 18
  - C.3.5 ADC+Guiding . . . 19
  - C.3.6 Slitmasks . . . 19
  - C.3.7 Field of View . . . 19
  - C.3.8 Dichroic Beam Splitter . . . 19
  - C.3.9 Spectroscopic Resolution . . . 19
  - C.3.10 Wavelength Range . . . 19
  - C.3.11 Image quality, uniformity, and stability . . . 19
  - C.3.12 Distortion . . . 20
  - C.3.13 Throughput . . . 20
  - C.3.14 Observing efficiency . . . 20
  - C.3.15 Instrument flexure . . . 20
  - C.3.16 Sensitivity . . . 20
  - C.3.17 Stray light control . . . 21
- C.4 Observing Scenarios . . . 21
  - C.4.1 Generic Observing Steps . . . 21

C.4.2 Transient Events . . . 21
C.4.3 Exoplanets . . . 22
C.4.4 Near-Earth Objects . . . 23
C.5 General Calibration . . . 24
C.5.1 Sky Subtraction . . . 24
C.5.2 Geometric Distortion . . . 24
C.5.3 Flat-field and Bias . . . 24
C.5.4 Wavelength Calibration . . . 24
C.5.5 Flux Calibration . . . 24
C.5.6 Linearity . . . 25
C.5.7 Dark Current . . . 25
C.5.8 Telluric . . . 25

D Feasible Technical Requirements and Instrument Design 26
D.1 Flowdown of Requirements . . . 27
D.1.1 Science Case: Transients . . . 30
D.1.2 Science Case: Exoplanets . . . 31
D.1.3 Science Case: Near-Earth Objects . . . 32
D.1.4 Non-Science Requirements . . . 33
D.1.5 Compliancy Summary Matrix . . . 34
D.2 Design Summary . . . 36
D.3 GEONIS' Approach to the Required Variable Spectral Resolution . . 38
D.4 Real Time Object Acquisition & Guiding . . . 38
D.5 Real Time Data Reduction Pipeline . . . 39
D.6 Systems Engineering . . . 40
D.6.1 Throughput . . . 40
D.6.2 Image Quality Budget . . . 46
D.6.3 Precision Budgets . . . 46
D.6.4 Mass Estimates and Budgets . . . 47
D.6.5 Compliance and Problems with Interface Control Documents . 48
D.7 Details of Instrument Subsystems, Feasibility, & Next Steps . . . 50
D.7.1 System Structure . . . 50
D.7.2 Atmospheric Dispersion Corrector . . . 52
D.7.3 Slitmask Removal System . . . 54
D.7.4 Slit-viewing Camera System . . . 55
D.7.5 Collimator . . . 60
D.7.6 Spectrograph/Imager layout . . . 63
D.7.7 Camera Lens Mounting . . . 70
D.7.8 Optical Camera System . . . 73
D.7.9 Near-Infrared Camera System . . . 75
D.7.10 Optical / Near Infrared Detector System . . . 76
D.7.11 Open-Loop Flexure Compensation System . . . 77

D.7.12 Electronic and Interfaces Design 78
D.7.13 Control Software 81
D.7.14 Data Reduction Pipeline 84
D.8 Design Orthogonality 84
D.9 EMCCDs - Mass, Budget, and Risk Savings 86
D.10 Description of Known Risks for GEONIS 92
D.11 GEONIS is a Workhorse Instrument 93
D.12 Optical Drawing Tree 93
D.13 Organization of Mechanical Drawings 94
D.14 Summary of Changes from GEONIS Proposal 94

E Budget, Schedule, & Risk 97
E.1 Cost estimate and Work Breakdown Structure 97
E.2 Schedule 98
E.3 Management Risks 101
E.4 Special Facilities 102
E.5 Major Items & Long Lead Items 103
E.6 WBS Dictionary 104

B Science Objectives, Science Case, and Science Requirements

GEONIS is a versatile instrument that will enable a wide variety of astrophysics. Our science team (project scientist: M. Kasliwal, J.M. Desert, D. Fox, M. van Kerkwijk, J. Masiero, T. Matheson) has selected highlights from the science case for time domain astronomy, asteroids and exoplanetology. Next, we present the synergy between GEONIS and next generation facilities such as advanced Laser Interferometer Gravitational Wave Observatory (LIGO) and Large Synoptic Survey Telescope (LSST).

B.1 GEONIS and Time Domain Astronomy

We are in the midst of a boom in the field of time domain astronomy. Synoptic surveys with wide-field charge-coupled devices (CCD) cameras on telescopes ranging from 16-inch to 8-m are undertaking optical surveys for purposes ranging from near-earth asteroids to weak lensing. In time domain astronomy alone, the phase space of transients now has a dozen entirely new classes of explosions discovered only in the past few years (Figure 1). Surveys are now pushing to uncover rarer transients (1 per 10^4 years per galaxy) and shorter timescale transients (< 1 day).

Next generation surveys are poised to uncover transient events per night (EPN) by an unfathomable two orders of magnitude more than today. Specifically, the discovery rate will be of the order of 10^5 EPN with the Zwicky Transient Facility (ZTF; starting 2017) and of the order of 10^6 EPN with the LSST (starting 2023). The study of transients is entirely dependent on prompt spectroscopy of the scientifically interesting needles-in-the-haystack of discovery.

Currently, Gemini (the leading ground-based queue-scheduled observatory) with the Gemini Multiobject Spectrograph (GMOS) in the rapid Target of Opportunity mode is playing an important role in enabling time domain astronomy. However, with the next generation of surveys, we will need an extremely efficient and optimized spectrograph. We propose the GEONIS instrument that would uniquely position Gemini to lead the charge of spectroscopic follow-up in the ZTF and LSST era. Next we describe some examples of science cases and how they motivate the instrument design.

B.1.1 Flash Spectroscopy of Newborn Supernovae

Mapping the supernova flavor to the progenitor star type remains a major outstanding question in supernova research. Traditionally, it has been possible to make the links observationally only for supernovae within 10 Mpc, where pre-explosion imaging was available from Hubble Space Telescope (HST) and bright progenitors could be identified. Recently, we demonstrated with iPTF13ast that we can directly identify progenitors out to 100Mpc using a flash spectrum obtained within a day of explosion (Gal-Yam et al., 2014, Nature). At this young phase, the supernova flash ionizes its immediate surrounding and temporarily powers emission lines diagnostic of the

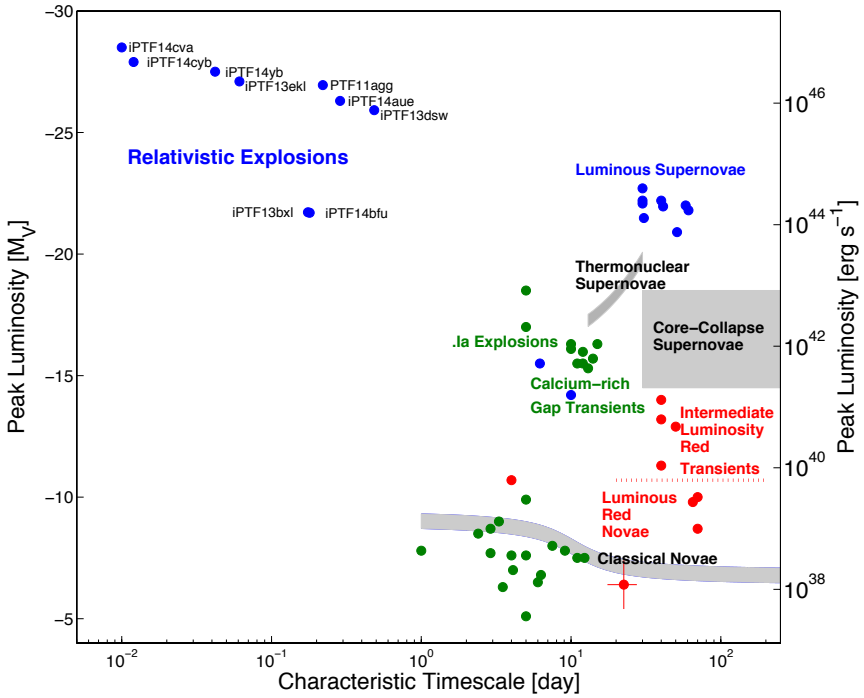


Figure 1: Phase space of cosmic transients illustrating the luminosity gap between novae and supernovae (-10 to -16 mag, especially at t $<$ 10 days). Gray bands denote the three classes known in 2005. Recent discoveries are already bridging this gap with multiple populations representing new stellar physics. Next generation surveys such as ZTF and LSST will probe even shorter timescales and even rarer transients. GEONIS can play a vital role in spectroscopically characterizing this phase space. [Updated from (Kasliwal, 2011, Ph.D. Thesis)]

progenitor wind composition (Figure 2). Note that this signature disappears if we wait until the next night. We showed that the Type IIb supernova iPTF13ast was an exploding WNh-type Wolf Rayet Star. With ZTF, we can obtain a flash spectrum of a newborn supernova within hours of explosion every single night. At this young phase, we need to maximize sensitivity (SR6) and tune resolution (SR2). To do this every night, we need the observations to optimize efficiency (SR6, SR8, and SR9). To detect high ionization lines without confusion with sky line residual, we need clean sky subtraction (SR7).

Based on hundreds of hours of observing experience, the team agrees that slit lengths longer than 20″ are required for precise sky subtraction. Given that GEONIS has an infrared arm, and A-B spectroscopy may be required, a 20″ slit allows for plenty of room for multiple observations along the slit (recall that if one observes A-B there is a $\sqrt{2}$ noise penalty). As the number of positions along the slit increases, the shot noise decreases (2 positions is a 1.41 penalty (A-B), 3 positions is a 1.31 penalty (A-(B+C)/2), and 4 positions is a 1.26 penalty (A-(B+C+D)/3)).

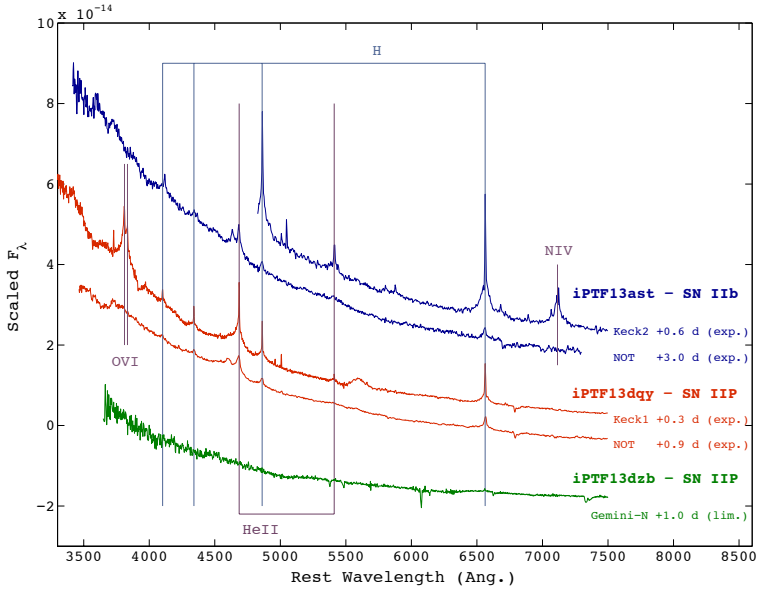


Figure 2: Flash spectroscopy of three Type II supernovae within one day of explosion shows a diversity of progenitor composition and mass-loss for the different flavors of explosion. iPTF13ast (Type II-b) showed N IV emission lines which are the hallmark of a Wolf-Rayet WNh progenitor [Gal-Yam et al. 2014, Nature]. On the other hand, iPTF13dqy shows O VI emission and iPTF13dzb shows neither oxygen nor nitrogen [Khazov et al. 2015, Yaron et al. submitted]. Note that these lines disappear once the blast wave sweeps up the immediate vicinity of the explosion. GEONIS can obtain a flash spectrum of one newborn supernova discovered by ZTF every night!

B.1.2 Relativistic Explosions

Although the less-than-a-day regime is hitherto uncharted territory, our discoveries thus far bode well for this new transient phase space (Figure 2). The most luminous and relativistic known class of such "fast" extragalactic transients are the afterglows of gamma-ray bursts (GRBs; initial Lorentz factor $\Gamma_0 > 100$). Medium- or high-resolution spectroscopy of GRB afterglows, across the broadest possible bandpass, serves as the single critical observation enabling an impressive swath of associated extragalactic science and cosmology.

First, the most compelling science opportunity here is the discovery of "orphan" afterglow-like transients that lack high-energy emission altogether, either due to beaming effects or due to the suppression via pair production. We may have uncovered one such "dirty" fireball (PTF11agg; Cenko et al. 2013). Unfortunately, due to the lack of prompt spectroscopy, the identification remains somewhat ambiguous. In another case, iPTF has detected an on-axis optical afterglow entirely independent of any high-energy trigger. iPTF14yb was revealed to be at z = 1.98, and only following our discovery announcement (Cenko et al. 2014) was a corresponding high-energy transient identified by the InterPlanetary Network of gamma-ray detectors. Theoretical estimates suggest that orphan afterglows should outnumber on-axis GRBs by at

least a factor of three to one (Totani & Panaitescu, 2002). With the high cadence of ZTF, we expect to detect one orphan afterglow per month (or we will need to radically alter our picture of beaming in GRBs). Prompt spectroscopy covering a wide redshift range will be essential to determine the nature of the discovery. Here, the wide wavelength coverage of GEONIS extending into the near-infrared so that we can see absorption lines such as Mg II 2800 Å as far as z=4.7 is needed (SR1).

Second, gamma-ray bursts offer a unique capacity for high-quality absorption-based abundance measurements of the gas in star-forming galaxies across the full range of redshifts where GRBs are routinely identified, $0.5 < z < 8$. Such measurements are possible only for GRB afterglows and, rarely, for intervening DLA systems along quasar lines of sight Prochaska et al. (2007); Chen et al. (2009); Laskar et al. (2011). Abundance datasets, once collected, will then serve as references for high-redshift host galaxy studies for years and even decades beyond the nights of their collection.

Third, prompt spectroscopy of high-redshift afterglows has provided a unique tool for identifying $z > 6$ star-forming galaxies independent of galaxy luminosity, and localizing them precisely in three dimensions Tanvir et al. (2009); Cucchiara et al. (2011); Tanvir et al. (2012); Chornock et al. (2013). The great majority of high-redshift galaxies currently under study have been gathered from deep HST fields, where they are identified by photometric analyses alone.

Gamma-ray bursts, by contrast, serve to illuminate star formation at these redshifts wherever it is happening, whether in massive galaxies or – with increasing probability at increasing redshifts – low-luminosity dwarfs.

Fourth, at redshifts beyond the epoch of reionization, bright afterglows offer unique diagnostics of the reionization process itself. High signal-to-noise ratio spectra that cover the Lyman-alpha transition at these redshifts are capable of measuring the column depths of neutral hydrogen both in the host galaxy and in the intergalactic medium beyond Miralda-Escudé (1998), Mesinger & Furlanetto (2008); McQuinn et al. (2008); Chornock et al. (2013).

The IGM column serves as a direct measurement of the progress of reionization at the burst redshift along that line of sight; multiple such measurements would thus serve to map the cosmic reionization in full. At the same time, the host galaxy column directly measures the escape fraction of reionizing photons from high-redshift star-forming regions – a crucial input to models of reionization, with competing groups of theorists and galaxy-formation simulations continuing to differ even as to its order of magnitude. With redshifts from $6 \leq z \leq 12$ being useful for reionization studies, these measurements require high-efficiency medium-resolution spectroscopy at the Lyman-α transition over this range of redshifts, i.e., up to 1.6 μm (SR1).

B.1.3 GEONIS in the Era of Low Latency Astrophysics

A rapid response classification spectrum within a few hours of discovery drives new science: flash spectroscopy of infant supernovae, looking for interaction of a SN Ia with

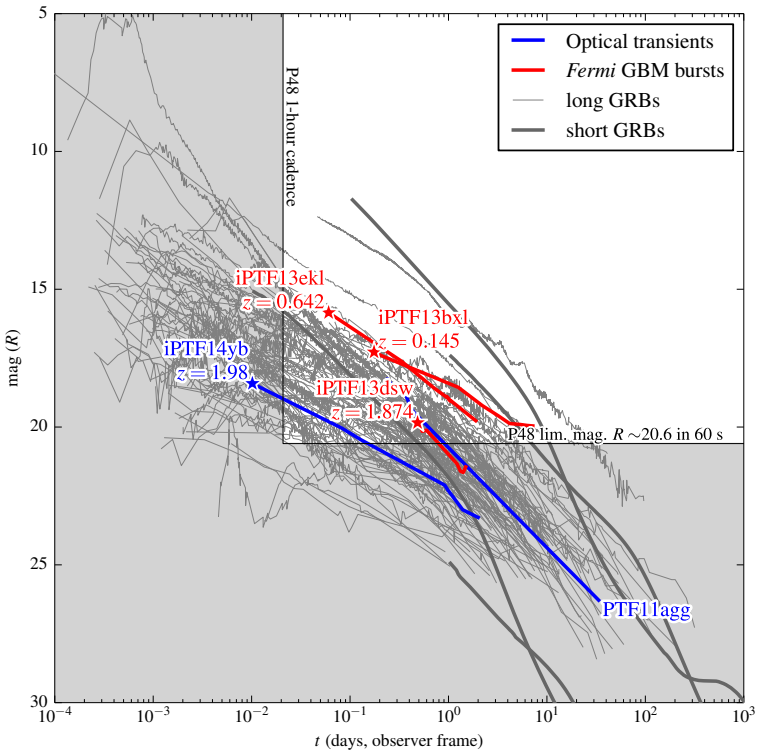


Figure 3: iPTF has discovered relativistic explosions that fade on hour timescales. Two were optical afterglow discoveries completely independent of any high energy trigger (blue) [Cenko et al. 2013, Cenko et al. 2015]. Three were optical afterglows triggered by searching hundred deg^2 around the Fermi-GBM localization (red) [Singer et al. 2013, Singer et al. 2015]. Here, we compare them to a sample of canonical afterglows of GRBs (black).

companion, relativistic explosions and electromagnetic counterparts of gravitational waves that fade quickly. The combination of iPTF and the Gemini large program has resulted in one such same-night spectrum every ten days on average. The combination of GEONIS and more powerful discovery engines (ZTF, LSST) will improve this by more than an order of magnitude in both number and latency; we could get classification spectra within minutes of discovery, multiple times a night, every night.

B.1.4 GEONIS in the advanced LIGO era

With the imminent commissioning of advanced LIGO and Virgo, ramping up in sensitivity from 2015 to 2019 (Aasi et al. 2013), enormous resources are being invested into discovering the electromagnetic counterpart of gravitational waves. The key astrophysics question is whether or not neutron star mergers are the long-sought sites of r-process nucleosynthesis and thus, the mines of heavy element production (i.e., half the elements in the periodic table heavier than iron including gold, platinum, uranium). Recent opacity calculations of lanthanides show that the electromagnetic emission will peak in the near-infrared. Furthermore, the emission fades on timescales

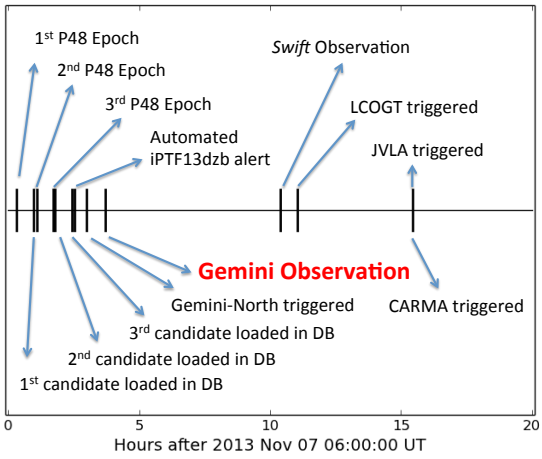


Figure 4: Example timeline for panchromatic follow-up of a young core-collapse supernova, iPTF13dzb, within hours of discovery. We obtained the Gemini spectrum within 1 hour of the automated iPTF transient discovery alert. Swift, JVLA, CARMA and LCOGT were triggered for follow-up within 24 hours. The decision to undertake panchromatic follow-up requires the classification-driven observing mode. In addition to flash spectroscopy of infant supernovae, the relativistic explosions and the gravitational wave follow-up science cases described above rely on this mode.

of hours to days. This motivates why we need a near-IR arm to GEONIS (SR1).

B.2 GEONIS and Near Earth Asteroids

The Gemini telescopes provide a unique asset for investigation of newly discovered near-Earth asteroids (NEAs). In particular, the large aperture, accessibility of queue-scheduling, and constant availability of all instrumentation make it an ideal tool for rapidly responding to new discoveries. Current surveys focus predominantly on discovery and orbit characterization of NEOs, addressing the impact question, with physical properties being obtained for only a fraction of all known objects. Future surveys, however, will discover objects too faint and too frequently for the currently existing followup assets. Observations from surveys such as LSST will provide sufficient data to show that the majority of objects discovered will not hit the Earth. However, the data from LSST alone will not be able to make a definitive assessment of the fraction of a percent of objects that remain as "virtual impactorsÓ (a class of object that has some Monte Carlo simulations resulting in Earth impact). For this, a followup telescope that can regularly track objects of interest at magnitudes near the LSST limit will be critical to determine precise orbital trajectories, and thus their hazard.

As part of a Gemini Large and Long program (PI Masiero) the Near-Earth Ob-

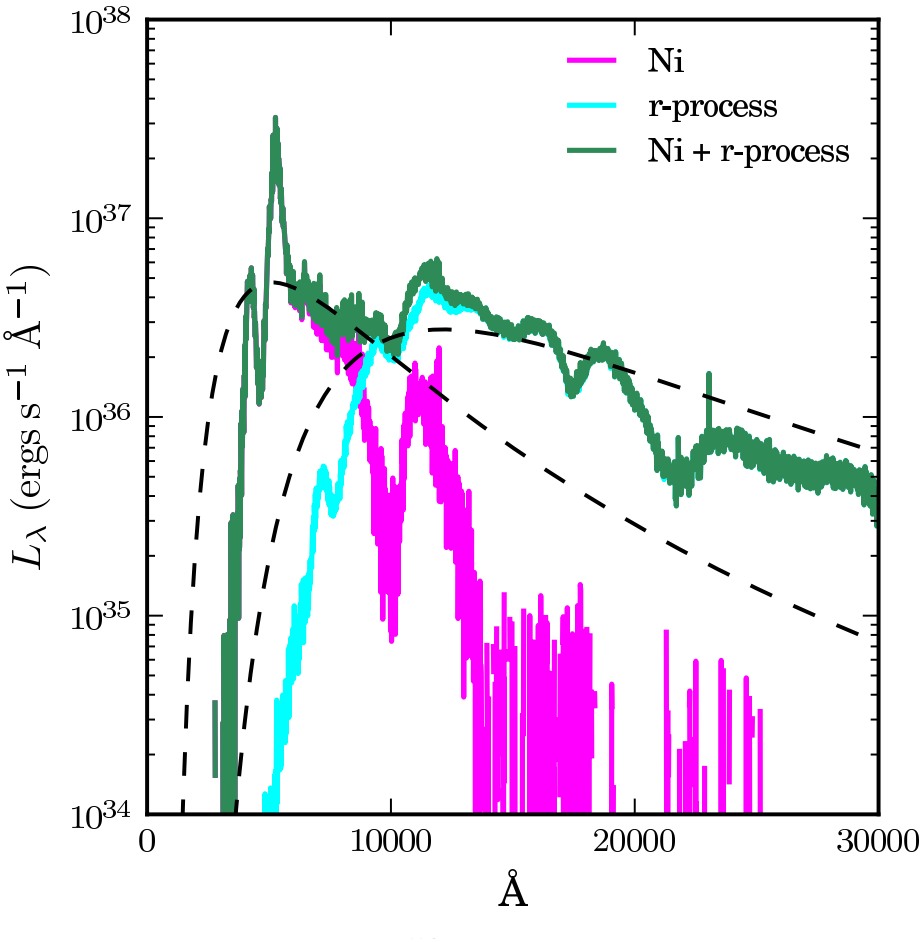


Figure 5: Theoretical prediction of the spectrum of electromagnetic counterparts to neutron star mergers (Kasen et al., 2013; Barnes & Kasen, 2013). The quantity of Nickel-56 powering the blue peak is much debated (magenta line). The "guaranteed" emission is from radioactive decay of heavy elements synthesized by the r-process (cyan). Due to the opacities of heavy elements, the spectrum peaks in the near-infrared. GEONIS is perfectly suited to characterize the chemical composition and ejecta masses of neutron star mergers.

ject Wide-Field Infrared Survey Explorer (NEOWISE) team has been using Gemini-South/GMOS for critical followup of faint NEAs that other telescope cannot observe. When an NEA is discovered by NEOWISE, it typically has 5-10 detections spanning $\sim$1 day. These measurements are sufficient to calculate a preliminary orbit that will allow for future positions to be predicted, however the uncertainty region spanned by the predictions grows rapidly over the days following the last observation, and can reach a degree or more within a week without further followup astrometry. GMOS is used in imaging mode to make astrometric measurements of NEA candidates, which improve the orbits that can be determined and thus reduces future positional uncertainties. However, the GMOS field of view is 5' x 5', which is usually smaller than

the uncertainty region for many objects. These objects then require tiled observations mapping the uncertainty region, each of which is charged setup and acquisition time. Uncertainty regions expand exponentially with time from the last observation, but are strongly influenced by the length of observation arc already obtained. With future surveys such as LSST, observation arc length will be shorter so followup will need to happen within two days. Larger fields of view permit more time between last detection and followup trigger (SR4). Centroid ability on a NEA scales with image diameter/SNR. To maintain high-efficiency operations, GEONIS must not degrade the image quality of Gemini by more than 10% (SR15).

Our proposed instrument would reduce the overhead time needed to acquire the position and pointing (SR8), while simultaneously maintaining the field of view (SR4). GEONIS must maintain the aperture advantage of Gemini (SR6). These two features would improve the ability of Gemini to make critical followup measurements of faint, newly discovered NEAs, a need that will only increase as next-generation surveys such as NEOCam and LSST begin (both slated for the 2020-2022 timeframe). Further, GEONIS will enable studies of colors and spectra of asteroids, which probe the surface composition and can be used to link objects back to their formation in the Main Belt. Presently the general pathways are known, but it is difficult to link specific objects to their source region. Improved population statistics will enable a more complete understanding of the asteroids from their formation and collisional evolution to their present day orbits.

decreasing stress on the followup system. For this reason, we attempted to maximize the field-of-view of GEONIS.

B.3 GEONIS and Exoplanetology

Exoplanet transit spectroscopy measurements have primarily been achieved using space telescopes like HST and Spitzer. This has primarily been due to the requirement that very-high relative precisions (at least 10^{-3}) have to be obtained over timescales of hours (i.e., the timescale of a transit). However, we recently opened the door of using large ground-based telescopes equipped with multi-object spectrograph with custom slit-masks to observe a transit event . The key elements of the technique are simultaneous observation of a reference star for calibration of variations in the Earth's atmospheric transmission, and using very wide slits to avoid time-variable and differential slit losses. In this context, the Gemini telescopes, with their large apertures and accessibility of queue-scheduling, and equipped with the GMOS instruments provide a unique asset for investigation of exoplanet atmospheres. The current state-of-the-art for transit spectroscopy observations on the Gemini telescopes with the GMOS instruments is from our NOAO Survey Program (PI J.-M. Desert). This is the first ground-based survey of exoplanet atmospheres: we are currently surveying 9 close-in gas giant exoplanets. Our goal is to make repetitive measurements (about four transits per object) in order to improve the precision, but more importantly to understand our (systematic) errors and limitations. Our experience shows that we

can achieve precision about twice photon-noise, corresponding to approximately few 100 ppm (SR10) at a resolving power R=50 (SR11), for bright host stars (Vmag=8). This allows us to detect atomic and molecular features in the transmission or thermal emission spectra of hot planets with hydrogen-dominated atmospheres.

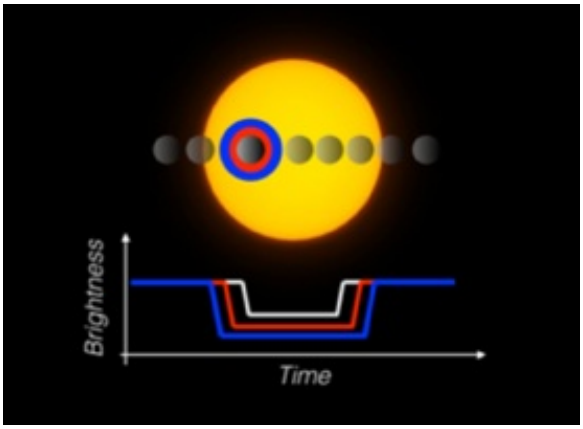


Figure 6: Measurements of the transit depths at different wavelength inform us about the atmospheric properties and composition of transiting exoplanets. The atmosphere's depth is a wavelength-dependent phenomenon as indicated by the various colors on the above figure. The wavelength-dependent length of a transit is a key property to measure.

The proposed instrument will provide significant improvements compared to the GMOSs. We will be able to secure spectra from 0.4 μm to 1.6 μm in a single exposure (SR1). This is important because our measurements are relative in time and in wavelength, and because the full spectrum of the planet is required to make measurements (this is currently a limit in our own program; Figure 6). GEONIS will significantly improve the duty cycle (currently 50%), thanks to the frame transfer device on the detector. This is important because the transit duration is limited in time (about 3 hours). Each observation requires to gather data before, during and after the transit (typically about 5 hours), and to remain as stable as possible (SR5). During that time, lots of parameters are varying (e.g., airmass, seeing) and we try to minimize and characterize the variability wherever possible. Currently, our GMOS survey suffers from flexure. That is one of the main factors that limits the precision we can achieve. Our instrument will significantly improve this precision by being very stable with the addition of active flexure compensation. Because each transit is only a few hours, and each exposure is on order of one minute, minimizing detector readout time is essential. Current detectors limit the observing duty cycle to some 50%. With GEONIS it is possible to improve duty cycle to 90% by transferring images into the frame store (SR14).

We require that GEONIS in its single longslit mode has a slit long enough such that it can be oriented to include both the reference star and the planet and wide enough to capture the full flux (SR3). Based on simulations performed with the Sloan Digital Sky Survey, we recognize that the slit must be larger than 6 $'$ (SR12) in

order to have coverage of most Transiting Exoplanet Survey Satellite (TESS) planet candidates, while at the same time observing a spectrophotometric reference star. To have the best spectrophotometric precision, GEONIS is required to have a 12″ wide longslit (SR13) based on similar observations using GMOS.

There is a strong synergy between GEONIS and James Web Space Telescope (JWST) since these two instrument are complementary in terms of bandpasses. While JWST will provide information on exoplanet atmosphere GEONIS composition in the IR at high resolution, the low-resolution of GEONIS will provide information on the atomic composition and baseline pressure from Rayleigh and Mie scattering that will be measured from the visible to the NIR bandpass. Overall, the wavelength domain covered in a single shot, combined with the stability and new efficient detectors of GEONIS will allow to move the field of exoplanet from detecting of atoms and molecules in hot-Jupiter atmospheres (currently with GMOS) to making astrophysical measurements (abundances, temperature, metallicity) and also to detect atmosphere of lower mass planets. These will represent important steps for exoplanetology.

B.4 Scope & Risk: Science Team's Role

The science case and instrument concept were and will continue to be developed together. As the technical case for the instrument advances, the cost and risk of GEONIS's key subsystems will become better understood. Our baselined instrument will require a change of scope, and the role of the science team is to work with the technical team on any instrument changes.

B.5 GEONIS in the LSST era

One of the GSTAC principles for the GIFS instrument call is synergy with upcoming capabilities. The LSST is a prime example of a new capability that will begin survey operations in a time frame commensurate with the deployment of the GIFS instrument. LSST is a ugrizy imaging survey that provides much of its own photometric follow up, but is devoid of a spectroscopic component. Almost all of the LSST science cases can be enhanced with spectroscopic follow up. There are two basic modes with broad scientific appeal: 1) massively multiplexed, wide-field spectroscopy to characterize enormous samples and 2) high-throughput, wide-wavelength single-object spectroscopy to study rare objects (see Matheson et al. (2013) for a more detailed discussion). The narrow-field design of the Gemini telescopes precludes their cost-effective use as a platform for wide-field, multi-object capabilities. A high-throughput, wide-wavelength spectrograph, though, augments the strengths of the Gemini Observatory.

One of the four main science goals of the LSST project is the study of time-domain astronomy. Every night, a few million alerts will be generated by LSST for objects whose brightness or position has changed. Many of these will be known variables or asteroids, but hidden among them will be rare and interesting objects. The information provided by LSST about alerts will be limited so spectroscopic follow

up will be necessary to identify and study these unusual cases. For objects that require immediate (within 30 minutes) follow up, there are few facilities with the necessary capabilities. Mauna Kea is too far west and the North American and South African observatories can only access a fraction ($\sim$20%) of the fields at the same time that LSST observes them (based on our own analysis of LSST Operations Simulator runs). Only Chilean observatories are well positioned for extremely rapid follow up and Gemini South is in the best position of all. Only a few hundred meters from the LSST site, with a large aperture and a proven track record of rapid response, Gemini South is an ideal platform for this high-throughput, high-efficiency spectrograph. This combination amplifies the strengths of instrument and observatory to provide a capability that maximizes the synergy with LSST.

Beyond the time domain, there are many science cases for non-variable objects described in Matheson et al. (2013) for which a high-throughput, wide-wavelength spectrograph is an ideal instrument. These are generally objects with a low surface density, but study of even a handful will be scientifically significant. Examples include high-redshift galaxies, high-redshift AGN, vetting Galactic stars with unusual metallicities, tests of the extinction law through the Galaxy and the Magellanic clouds, and monitoring of weather on brown dwarfs.

B.6 Science Requirements

- SR1. Wavelength range will be maximized and span at least 400 nm to 1600 nm. This would enable detection of [O II] at z 0.1, Mg II at z 4.7 for relativistic explosions and be sensitive to lanthanides in neutron-star mergers.
- SR2. Spectral resolution will be selectable and span at least R≈500 to R≈4,000 with a 1-arcsecond slit.
- SR3. A slit width of two pixels must subtend the best 20% of seeing of about 0.4 arcsecond. With this sampling, the instrument will deliver a 1-arcsecond-wide slit into five pixels. The maximum allowed width of longslit will be long enough for comparative exoplanetology.
- SR4. Pixel scale to cover a large FOV for the NEO astrometry case.
- SR5. Exoplanet atmospheres require high instrument stability so that the amount of flexure achieved is a fraction of a pixel over the length of a transit (hours).
- SR6. Highest possible throughput.
- SR7. Excellent sky subtraction.
- SR8. Maximize open-shutter time on science time by (a) High acquisition efficiency, (b) No nighttime "shut" calibrations (Wavelength or flat), (c) Fast locking of loops.
- SR9. Rapid reduction of data to enable on-the-fly classification of supernovae.
- SR10. Exoplanet atmospheres requires precision of 200 ppm.
- SR11. Exoplanet atmosphere measurements require a resolution R>50 with a wide slit.
- SR12. Exoplanet atmospheres require slit length $> 6'$ in order to observe the majority of TESS events.
- SR13. Exoplanet atmospheres require slit width $> 12''$ in order to achieve high spectrophotometric precision.
- SR14. To maximize science efficiency, keep readout overhead to less than 10% in a 50-second exposure.
- SR15. GEONIS must not degrade telescope image quality by more than 10% over GEONIS' field.

C Operations Concept Document

C.1 Science Priorities

The science priorities for the GEONIS instrument are guided at the highest level by the Gemini STAC principles [2]. It will be a workhorse instrument with broad capabilities highly desired by the community. Synergy with LSST, located just a few hundred meters from Gemini South, is the chief scientific goal of GEONIS. It specifically addresses the STAC principles that the instrument be highly efficient and provide a wide-wavelength moderate-resolution spectrographic capability. The design of GEONIS itself was guided by three main principles.

C.1.1 Simplicity

While the cost cap for the instrument favors a simple design, there are many other advantages for a simple instrument that still fulfills the overall science priorities. The minimization of moving parts and support of limited number of modes lead directly to a more efficient observational practice. This efficiency reduces overhead, specifically calibration time, and thus increases open shutter time.

C.1.2 Spectral Resolution

Wide-wavelength coverage is a high priority for GEONIS, especially for transient follow-up in the era of LSST. A moderate spectral resolution of R$\sim$4000 is also highly desirable. A large fraction of the proposed GEONIS wavelength range is dominated by bright OH emission lines from the night sky. A resolution of $\sim$4000 effectively splits these OH features and allows for the detection of faint sources between the sky lines. The nature of the EMCCDs and the design of the data reduction package will allow users to select lower-resolution outputs.

C.1.3 Throughput

The STAC principles and the science cases all stress the need for high throughput. For GEONIS, this is considered as a system problem, not just one of optics. The highest possible efficiency for the optical components is the first consideration, but other factors in the GEONIS design combine with this to maximize throughput in the broadest sense of the term. In addition to passing as many photons as possible through the instrument, GEONIS speeds up target acquisition, applies flexure compensation to preserve PSF fidelity, and reduces calibration overhead with a simple and solid design.

C.2 Instrument Concept Overview

GEONIS is an optical (400 – 800 nm) and near infrared (800 – 1600 nm) spectrograph and imager. A dichroic splits the incoming beam and directs the light to the two different detectors. Dispersion for spectroscopy will be accomplished with a grating

[2] https://www.gemini.edu/node/12266

whose orders are then cross-dispersed with a prism. GEONIS will use large 4K × 4K detectors with 15 μm pixels that yield a scale of $\sim$0.19″ on each arm. It will use a CCD (or EMCCD) on the optical arm and a Hawaii 4RG on the infrared arm. The imaging field is 8.5′× 3′. The spectral resolution is R$\sim$4000 with a 1.0″ × 20″ slit while lower resolution spectra can be obtained via rebinning in the data reduction phase. A lower-resolution mode with a 6′ slit is also available. A guiding camera will provide rapid and automatic acquisition. Flexure compensation will ensure high stability and minimize calibration images. The instrument will include an atmospheric dispersion corrector (ADC) that adjusts automatically to account for zenith distance of the telescope to ensure that the positions of targets are achromatic over the 400 – 1600 nm wavelength range.

C.3 Summary of Requirements

C.3.1 Modes of Operation

GEONIS will have three modes of operation: imaging, low-resolution spectroscopy for exoplanets, and moderate-resolution spectroscopy (the general purpose mode). The instrument will be able to switch between modes rapidly.

C.3.2 Instrument Control

The instrument will be controlled remotely to move prisms and gratings. It will be scriptable within the standard Gemini instrument control system. The EMCCD allows for readout of the data and real-time reduction to assess the signal-to-noise ratio of the data.

C.3.3 Atmospheric Dispersion Corrector

As GEONIS will operate over a wide wavelength range, an atmospheric dispersion corrector (ADC) is essential. It will reduce dispersion losses and enable observations at larger airmasses. In addition, this eliminates the need for rotation to the parallactic angle for each observation and helps to reduce overhead.

The current ADC concept is a linear pair of prisms. As the linear pair of prisms pistons, the telescope also repoints and refocuses (see §D.7.2 for details). Because the amount of piston and offset are predetermined, the telescope control system will have to be modified to both repoint the telescope as the ADCs are actuated. Also note that this shift in piston also shifts the rotation axis of the instrument as the prisms are displaced.

C.3.4 Guiding

Guiding is accomplished by the slit-viewing camera looking at light reflected off the slit. The guider software must be able to provide motion commands relative to the slit. The guider is essential to ensure that light from objects is concentrated into as small an area as possible.

Note that the ADC has the effect of repointing the telescope. The slit viewing camera will remove pointing offsets from the ADC.

C.3.5 ADC+Guiding

The ADC and slit-viewing/guider units together are an essential for ensuring high throughput and maximizing the efficiency of the data reduction pipeline.

Figure 7 illustrates the power of ADC and slit-viewing camera working together. The slit viewer, aside from acquiring the object, ensures that the object is fixed at a known location on the slit. The ADC ensures light from the object stays either in the slit, or parallel to order trace. If the ADC is disabled and the airmass is high, one can predict the orientation of the trace; however, we cannot correct the loss of contrast that is attendant with atmospheric dispersion.

C.3.6 Slitmasks

The general-purpose moderate-wavelength mode will uses long-slit masks with a length of $20''$. For the low-resolution, exoplanet mode, the masks will uses slits of $6'$. The slitmask has an optical surface on one side that reflects light into the slit-viewing camera.

C.3.7 Field of View

The field of view for GEONIS is $8.5' \times 3'$, as large as the optical design will allow.

C.3.8 Dichroic Beam Splitter

GEONIS will use a dichroic to split the incoming beam and send the optical and infrared portions to the appropriate cameras.

C.3.9 Spectroscopic Resolution

The spectroscopic resolution with be R$\sim$4000 for the general-purpose mode, and R$\sim$50 for the exoplanet mode.

C.3.10 Wavelength Range

The simultaneous wavelength coverage will be 400 – 800 nm for the optical arm and 800 – 1600 nm for the infrared arm. The science team prefers to extend wavelength coverage as much as possible.

C.3.11 Image quality, uniformity, and stability

GEONIS is designed such that it contributes very little to the delivered PSF. If the variations in PSF shape or FWHM are significant compared to the image size (in spectroscopic mode), errors in wavelength calibration (and decreased slit throughput) result. Such systematic errors can be exacerbated when the seeing is especially good. It is required that the PSF in the instrument focal plane should be uniform over the full field at the level of 0.5% in FWHM for median seeing conditions across the $30''$ slit.

For exoplanetology, atmospheric PSF variations are taken out through differential comparison of the target to a slit standard. To observe exoplanets, the object is held to a fixed position on the detector. By insisting the object is held in this way, the uniformity of the PSF across the field is not important.

C.3.12 Distortion

Field distortion at the camera image must be small enough so as not to contribute to instrument inefficiency. To satisfy this requirement, the distortion must be characterizable so that the mapping of the telescope focal plane (including the guiders/WFSs) to instrument focal plane is consistent. We have not determined the level to which these must be held.

C.3.13 Throughput

GEONIS is a workhorse instrument that must maintain Gemini's large aperture advantage. It must maintain excellent throughput over its full wavelength and field range.

C.3.14 Observing efficiency

GEONIS is designed from the ground up for maximum observing efficiency. We have specified the use of the following items:

- ADC – No need rotate the instrument to the parallactic angle. GEONIS observers do not need multiple observations to capture all the light in cases where the slit cannot be rotated.
- Slit viewing camera – the slit viewing camera is designed with a large enough field that slit alignment is robotic.
- The instrument has designed for open-loop flexure correction so that we do not have to wait for the control loops to settle.
- The detectors are baselined to be readout quickly, so read time is minimized.
- Control software – all mechanisms move in a coordinated fashion (no need to wait for sequential moves).

C.3.15 Instrument flexure

GEONIS will have an active flexure compensation system. This software will monitor the roll/pitch/yaw of GEONIS and adjust the position of the detectors via piezoelectric detector mounts operating in an open control loop.

C.3.16 Sensitivity

GEONIS sensitivity must be limited by shot noise for long integrations. GEONIS has been designed against this goal (slit spectrograph, flexure correction, fast cameras, and efficient operations). The sensitivity requirement flows down to achieve high signal-to-noise flat-field images, and to perform precise background-subtraction for very faint objects.

In general, the best sky subtraction is achieved with some kind of dithering; either with nod and shuffle or with multiple nods along the slit (though there is an attendant increase in shot noise).

C.3.17 Stray light control

GEONIS has two arms. The near infrared arm has the potential for a large scattered-light background signal; however, scattered light can be a problem in the optical. WFOS will require appropriate baffles and stray light guards. Proper stray light suppression will ensure that stray light is less than a few percent of the dispersed night-sky continuum level over the full field. In this way, we ensure excellent background subtraction for faint targets.

C.4 Observing Scenarios

C.4.1 Generic Observing Steps

Daytime observations will provide much of the calibration for all the observing scenarios. GEONIS has been designed to use the Gemini calibration system.

1. A series of bias frames for each mode.
2. A series of flat-field frames for each mode
3. Arc-lamp spectra for each spectroscopic mode.
4. Twilight flat-fields for each mode (may not be necessary for spectroscopic modes).

C.4.2 Transient Events

The LSST will generate millions of alerts per night, but a large fraction of these will be stellar variables or solar system objects. There will still be hundreds of thousands of astrophysical transients, a large number of which would greatly benefit from spectroscopy. As a concrete example, LSST will reveal a new supernova in almost every image. It will not be necessary to obtain a spectrum of every supernova, but there will be unusual and interesting objects among the supernovae found. A specific example is spectroscopy as early as possible, the so-called flash spectroscopy. The science goal is to see the effect of the UV flash as the shockwave reaches the surface of the star. This flash illuminates and ionizes the material around the star, revealing the composition of the wind and thus the progenitor itself.

The telescope will slew to the field, and the slit-viewing camera will take an image of the field. A local cache of astrometry.net will provide an astrometric solution of the field. Using this solution and the known position of the supernova, the telescope will offset to put the supernova into the slit.

Most of the calibrations necessary derive from the daytime calibrations. Only a telluric standard matched in airmass is necessary for nighttime calibration. The data reduction pipeline can operate in real time and assess the signal-to-noise ratio of the spectrum.

Given the volume and rate of alerts generated by LSST, there will need to be an automated process to winnow down the number of alerts to a level commensurate with

human interaction and the amount of follow-up resources. A software infrastructure system that processes data while adding value and then transmits the appropriate subset on to a customer is typically referred to as a broker. An example is the Arizona-NOAO Temporal Analysis and Response to Events System (ANTARES), a collaboration between NOAO and the University of Arizona Computer Science Department (Saha et al., 2014). The more information such a system has, the better decisions it can make about the nature of the astrophysical alert and how important follow up might be. Feeding information back to a broker is valuable and doing it automatically is even more so. The real-time reduction capability for GEONIS is of key importance here. The direct feedback will enable better decision making by the broker, especially in the case of high-value, short-lived events such as electromagnetic counterparts to LIGO detections.

The requirements on the facility are that instrument be available on any given night and that a rapid-response mode exist that can accommodate requests for an immediate observation. This kind of observing strategy is the default mode at Gemini and is one of the strengths of the Observatory. The ability to transmit the information from the real-time reduction is also critical.

These techniques apply to most point-source observations, bright and faint, although some may not need to take advantage of the ability to execute time-critical procedures. For bright enough sources, such as standard stars, it may be possible to eliminate the need for an astrometric solution and instead just move the brightest source in the acquisition image into the slit. This method has been used effectively with the FLOYDS spectrographs on the LCOGT 2m telescopes.

C.4.3 Exoplanets

Characterization of exoplanets remains one of the great problems of modern astronomy. Spectroscopic observation of an exoplanet during a transit reveals signatures of the exoplanet's atmosphere. The key elements of the technique are simultaneous observation of a reference star for calibration of variations in Earth's atmospheric transmission and using very wide slits to avoid time-variable and differential slit losses. In this context, the Gemini telescopes, with their large apertures and accessibility of queue-scheduling provide a unique asset for investigation of exoplanet atmospheres. GEONIS will have a low-dispersion (R$\sim$50) mode that incorporates a long slit ($6'$) that can include a reference star. We can then detect atomic and molecular features in the transmission or thermal emission spectra of hot planets with hydrogen-dominated atmospheres.

The GEONIS exoplanet atmosphere spectroscopy mode is designed around the upcoming Transiting Exoplanet Survey Satellite (TESS) survey. Today, only three known exoplanets orbit bright stars, TESS will bring this total number to several thousand. Given the typical orbital period of known exoplanets, once TESS completes its mission there should be several stars with transiting exoplanets available for characterization every night.

Based on the SDSS bright star catalog, we have determined that a slit of $6'$ allows GEONIS to observe over half of the exoplanets discovered by TESS. As the slit length increases, the fraction increases. For the maximum $8'$ slit length that GEONIS allows, the total fraction could be as much as 80%.

In this exoplanet atmosphere spectroscopy mode, the typical exposure time will be $\sim$50s. The EMCCDs employ frame transfer, allowing charge to be moved on the detector once an exposure is complete and a new exposure to begin immediately. This efficient use of the electronics will provide high duty-cycle observations for the exoplanet atmosphere exposures and thus better time resolution. The slit width is relatively wide at $12''$ to enable high spectrophotometric precision. The spectra can cover a wide variety of wavelength ranges, thus enabling the study of different atomic and molecular components of the exoplanet atmosphere.

It is worth noting that for this science case, instrumental precision dominates the signal. Thus there is a direct correlation between instrument precision and yield. It is clear that non-common-path errors are an essential contributor to loss of precision; however, there are a series of simulations and trades needed in the future, including:

1. Should GEONIS operate with or without the ADC during exoplanet measurements? The ADC will ensure that the trace stays on the same pixels of the detector; however, as the ADC moves the optical path changes. Do the gains of the ADC outweigh its negatives?

2. Should the FCS operate during exoplanet measurements? Like the ADC, the FCS ensures that a fixed set of pixels participate in the spectral image; however, the FCS also induces optical path changes. How is the precision of staying on a constant set of pixels offset by the optical path wander?

C.4.4 Near-Earth Objects

The Gemini telescopes provide a unique asset for investigation of newly discovered near-Earth objects (NEOs). In particular, the large aperture, accessibility of queue scheduling, and constant availability of all instrumentation make it an ideal tool for rapidly responding to new discoveries. GEONIS will be used in imaging mode to make astrometric measurements of NEO candidates, which improve the orbits that can be determined and thus reduce future positional uncertainties.

The imaging-mode observations are straightforward. Once the slit mask is removed, objects and then be directly imaged. Calibrations can be done during the day.

The facility requirements are that instrument be available on any given night and that a rapid-response mode exist that can accommodate requests for an immediate observation. In addition, non-sidereal tracking should be available.

C.5 General Calibration

C.5.1 Sky Subtraction

GEONIS will be used to observe faint sources so accurate background subtraction will be a key element of the data reduction process. Many elements of the instrument design enable better sky subtraction. The moderate spectral resolution that splits the night sky OH emission lines diminishes the portion of the spectrum directly contaminated by the lines. The limited fringing of the EMCCD will also enable better sky subtraction. In addition, the flexure compensation system, and thus the high stability of the instrument, will provide more consistent sky subtraction.

C.5.2 Geometric Distortion

The acquisition system envisioned for GEONIS will automatically apply an astrometric solution to the images obtained with the slit-viewing camera system and then use this information to position the desired target in the slit. These calculations will require knowledge of the transformations necessary to map sky coordinates to detector plane coordinates and these transformations will be derived via commissioning data.

C.5.3 Flat-field and Bias

Flat-field observations are necessary to calibrate the relative pixel-to-pixel response of the detector. A bias frame taken with no light on the detector is necessary to determine the electronic pedestal for the detector. Given the active flexure compensation and high stability of the instrument, day time calibration frames will be usable for observations throughout the night, thus saving the overhead normally spent on these calibrations. In addition, spectroscopic flat fields must match the science observations in wavelength coverage and resolution. For GEONIS, there are only two spectroscopic modes, so there is a finite set of calibrations necessary.

C.5.4 Wavelength Calibration

GEONIS will use arc-line exposures to provide a mapping between pixel position and wavelength for spectroscopic observations. Again, the high stability of the instrument and the limited spectroscopic modes mean that the day time arc-line exposures will be usable for observations throughout the night. Night-sky emission lines in the science frames can be used to tweak the solution for the science data and this can be applied during the data reduction process.

C.5.5 Flux Calibration

Flux calibration uses a source with a known spectra energy distribution to take the counts reported by the detectors and turn them into (relative) flux densities. The limited number of spectral modes means that any standard observed during the night can be used to calibrate all of the programs. It would be best to match airmass as well, so more than one standard may be necessary.

C.5.6 Linearity

The linearity of the detectors will be tested with observations of a constant flux source with a variety of exposure times.

C.5.7 Dark Current

Dark current should be a negligible source of noise for GEONIS.

C.5.8 Telluric

Correction for telluric absorption is critical for the infrared arm of GEONIS and extremely useful for the optical arm. These corrections can be obtained via observations of smooth-spectrum stars at a similar airmass to the science data. As with other calibrations, the high stability and limited number of spectroscopic modes enables reuse of telluric standards, although the variable nature of water vapor absorption through the night can add complications to this plan. Each Gemini site has access to water vapor monitoring equipment, so there is a mechanism for assessing the calibration plan on any given night.

D Feasible Technical Requirements and Instrument Design

Six months ago, the GEONIS team embarked on the Gemini Instrument Feasibility Study. Here we present the concept for a powerful workhorse spectrograph and imager that is cost-capped at $12 M USD and fits within Gemini's mass and volume envelope. Our approach is to focus the design on scientific areas that are on the forefront of astrophysics in the coming decade: transients, exoplanets, and near-earth objects. In these observational applications, GEONIS enhances Gemini's leadership in queue-based observing. To take advantage of queue-based observing, we advocate for a rapid-data-reduction capability.

GEONIS is a dual-arm optical (400 nm – 800 nm) and near-infrared (800 nm – 1,600 nm) spectrograph and imager. In imaging mode, GEONIS covers a 8.5′ by 3′ field (with some corner vignetting). GEONIS' pixel scale is 0.17″ which will sample Gemini's 0.45″ best quartile seeing well. In spectroscopy mode, GEONIS will operate in: "echelette" mode at spectral resolution $R = \frac{\lambda}{\Delta\lambda} \sim 4,000$ or "long slit" mode at $200 < R < 1,000$, with a 1.0″ wide slit. The instrument is designed for high total system throughput by combining fast-readout detectors, atmospheric dispersion correction, a slit viewing camera, and flexure compensation system into a single package. Our top-down cost estimate shows that GEONIS (without contingency) is ∼$10 M USD (see §E).

Parameter	Value
Wavelength Coverage	400 nm – 1,600 nm. Dual band split at 800 nm.
Pixel scale	>0.15″ in imaging mode
Field size	8.5′ slit length, 3′ slit width
Spectral Resolution (echelette)	4,000 (hardware), software selectable to lower values. 20″×1″ slit.
Spectral Resolution (lowres)	200 - 1,000 over 6.7 ′ for a 1″ slit. (Will be seeing limited for exoplanets.)
Image quality	Design delivers < 0.25″ FWHM images over all wavelengths without refocus.
Stability	< 0.1 pixel residual flexure in a 2-h observation. Open loop compensation with tip/tilt mirror
Slit viewer	Optical CCD slit viewer and guider.
Detectors	High readout speed EMCCD and Hawaii 4RG

In this section (§D) we summarize the technical aspects of the GEONIS spectrograph. This section is organized as follows: We describe the flow of requirements (§D.1) including the compliance summary matrix. The design is then summarized in §D.2 and we describe how we take advantage of our fast-readout detector (§D.3) to achieve our key science requirement of both classification and diagnostic science. We describe how to maximize the scientific returns of Gemini with a real time pipeline

(§D.5). This section also describes systems engineering (§D.6) and the system structure (§D.7). We conclude the technical requirements with a list of known risks (§D.10). Details about the zemax layout are described in §D.12. For reference a summary of our design evolution compared against the proposal (§D.14) is provided.

D.1 Flowdown of Requirements

In the following subsections we describe the flowdown of requirements for observing transients (§D.1.1), exoplanets (§D.1.2), and nearth-earth objects (§D.1.3). The key constraining non-science requirements are listed in §D.1.4. The GEONIS compliance matrix is listed in §D.1.5.

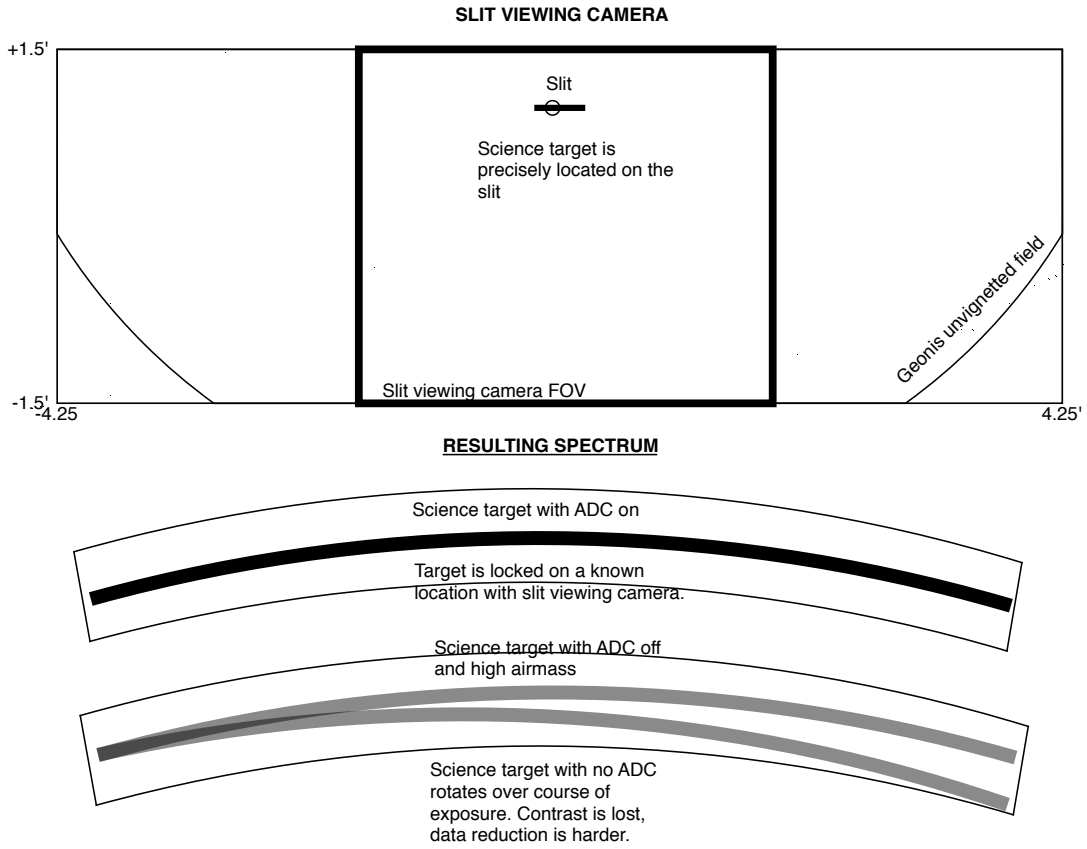


Figure 7: A cartoon diagram indicates the importance of the slit viewing camera and ADC. Top panel: shows the usable field of view of GEONIS in the faint rectangle. The thick dark rectangle indicates the slit-viewing camera field of view. The slit's position is illustrated on the slit mask and a science target is placed about 3/8 of the way into the slit. Bottom panel: shows a single order from the echelette mode (though the effect is the same in all spectroscopic modes) observed with the ADC on or with the ADC off. When the ADC is off, the object can be dispersed by the atmosphere across the slit and the spectrum processes as shown.

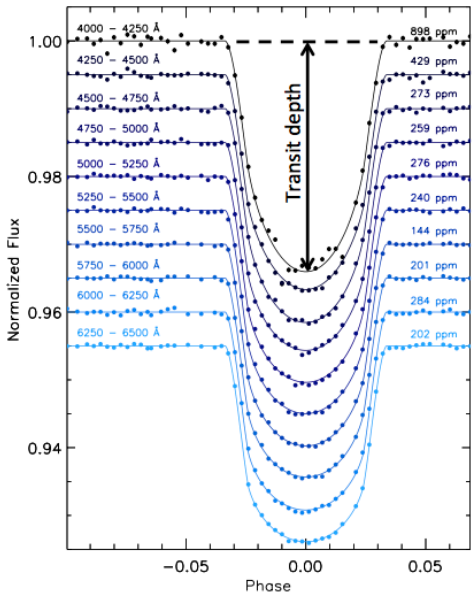


Figure 8: The transit depth at different wavelengths probes various scale heights and molecular bands in the exoatmosphere. Here we show the average flux in a wavelength bin with a width of about 250 Å. The normalized flux ratio (before/during transit) is shown on the vertical axis. Residual RMS is expressed in parts per million on the right

.

D.1.1 Science Case: Transients

The transient observational case requires an instrument with high overall system throughput, and the ability to both classify (low spectral resolution) and diagnosis (high spectral resolution) transient events discovered by programs like LSST. The science requirements include maximizing acquisition efficiency (slit viewing camera), maximizing system throughput (we use modern detectors, coatings, and materials), and a rock solid spectral format (ADC, and flexure compensation system) so that the spectral traces can be extracted with no human intervention.

We also advocate for a instant-look reduction pipeline that allows for a robotic system to classify transient events.

Table 1: Transients technical requirements.

Transients			
Parameter	Value	Source	Justification
Measurement	Echelette	Instrument	Workhorse mode.
Wavelength range	400 - 1,600 nm	§B.1.2/SR1 §B.1.4/SR1	Broadest range within desired risk posture and expected UV performance.
Spectral Resolution	500 - 4,000	§B.1.1/SR2	Will perform both discovery and diagnostic science.
Slit-to-detector Throughput	>30%	§B.1.1/SR7	Must meet or exceed current generation of instruments with a one-arcsecond slit.
Atmospheric dispersion correction	<0.25″ to airmass 2	§B.1.1/SR7	ADC correction maximizes throughput.
Slit viewing camera	Yes	SR9	Slit viewing camera maximizes throughput. Simplifies DRP.
Plate solve time (acquisition)	< 10 s	§B.1.1/SR9	Required to maintain high system throughput. The slit viewer allows us to keep the object fixed on the slit for fast reductions.
Pixel scale	>0.15″	§B.1.1/SR4	Fast cameras mean short exposures.
Image quality	∼0.3″	§B.1.1/SR3	Do not degrade Gemini's excellent delivered image quality by more than 10%.
Slit length	>20″	§B.1.1/SR8	Excellent sky subtraction and slit nods.
Quick look reduction	Yes	§B.1/SR10	Desire quick-look data reduction pipeline to determine SNR.
RMS Residual Flexure	< 0.1 pix	SR2, SR3, SR7, SR8	Impacts image quality, quick-look pipeline, and final pipeline ease
Instant look reduction	Desired	§B.1.3/SR10	Maximizes observatory throughput, see discussions.

D.1.2 Science Case: Exoplanets

The measurement of exoplanet atmospheres demands high precision and system throughput. The primary source of targets will be from missions like TESS. To achieve this goal requirements focus on a stable instrument (flexure compensation), and the ability to perform differential spectrophotometry on a reference star and a science target (long slit). Targets are bright, and so typical exposure times are short at one minute. To maintain high observing efficiency, the exoplanet case requires high-duty-cycle detectors with low noise (frame transfer or muxed).

Table 2: Exoplanet science case technical requirements.

Transients

Parameter	Value	Source	Justification
Measurement	Long slit	Instrument	Must observe science target and fiducial target simultaneously.
Wavelength range	400 – 1,600 nm	§B.3	Covers Na I, K I, H_2O, TiO, and VO species.
Spectral Resolution	200 – 1,000	§B.3/SR11	Sufficient for exoplanet atmosphere
Precision	200 ppm	§B.3/SR10	To measure exoatmospheres as they pass in front of their host star.
Slit length	$>6'$	§B.3/SR12	Cover more than 50% of TESS exoplanets.
Slit width	$> 13''$	§B.3/SR13	Ensure most light from science target enters slit.
Frame transfer duty cycle	$> 90\%$	§B.3/SR14	Ensures operational efficiency of $> 90\%$
Flexure correction	subpixel	§B.3/SR5	Ensures high stability and precision.

D.1.3 Science Case: Near-Earth Objects

The Near Earth Object science case is derived from the requirement to provide followup observations for objects discovered by missions like NEOWISE. Gemini's queue and instrument suite enable measurement of critical orbital information that would otherwise be lost. NEO observations require a large field.

The biggest design tension for GEONIS has been delivering a large imaging field of view. GEONIS is baselined with a $22'^2$ field whereas the telescope delivers a $78'^2$ field. In our GIFS proposal, we attempted to address this enormous field. The proposed GEONIS had a 400-mm-diameter field lens starting at the keep-out-zone the instrument support structure reimaging spectrograph. We explored such a design, but could not find a way to fold the spectrograph and meet the mass and cost requirements. Thus, the GEONIS design shifted towards a reflective collimator, and its $22'^2$ field of view.

Note that the most NEO observations take place using a single filter, we have budgeted for a filter wheel and a variety of filters.

Table 3: NEO technical requirements.

Transients

Parameter	Value	Source	Justification
Measurement	Wide field imaging	Instrument	For ephemeris of NEAs.
Wavelength range	400 – 1,600 nm	§B.2	Peak of SED in the near-optical range is 1 μm.
Throughput	$> 50\%$	§B.2/SR7	Must meet or exceed current generation of instruments.
Frame transfer duty cycle	$> 90\%$	Throughput	Ensures high operational efficency.
Image quality	0.3"	§B.2/SR15	Centroid uncertainty is proportional to image quality.
Atmospheric Dispersion Corrector	Yes	Image quality	ADC requirement flows from image quality requirement.
Field of view	$8'$x $3'$	§B.2/SR4	Largest possible imaging FOV.

D.1.4 Non-Science Requirements

As per ICD 1.5.3/1.9 we excerpt:

> The instrument builder is responsible for providing the frame to interface with the ISS, for providing sufficient weight and design of weights for balancing purposes, and for generally ensuring the instrument is compatible with the specifications provided in document [ICD 1.5.3/1.9].

Gemini observatory places over 100 technical requirements on the instrument builder that cover documentation, shipping, storage, operating environment, interfaces, consumable use, operations, safety, etc. We intend to meet almost all of these requirements, except for a short list of exceptions described in the systems engineering section below (§D.6.5).

For GEONIS there are three non-science requirements that we identified as design-driving, and these requirements are enumerated in Table 4.

Table 4: Non scientific technical requirements. ICD1.5.3/1.9 refers to documents provided by Gemini observatory.

Technical Requirements			
Parameter	Value	Source	Justification
Mass limit	2 metric ton	ICD 1.5.3/1.9	ICD
Dollar Budget	$12 M USD	Gemini	Gemini

D.1.5 Compliancy Summary Matrix

Table 5: Compliance Summary Matrix

Req	Transients	Exoplanets	NEOs	Achieved
Mode	Echelette	Long slit	Imaging	Yes
Sensitivity	High sensitivity to faint sources	High precision on bright sources	High sensitivity to faint sources	Yes
Wavelength Range	360 (desired) - 1,600 nm	400 - 1,600 nm	400 - 1,600 nm	400-1,600 nm
... Dual Beam	Flows from λ-range requirement			Yes
Total system throughput	Maximized	Maximized for 50-s exposures	Maximized for short exposures	Yes
... Detectors	Fast readout	Fast readout	Fast readout	Yes
Echelette Resolution	Classification (100) - Diagnosis (4,000) with a $1''$ slit			Yes, via software
Longslit resolution		> 50 (with a wide slit)		200 - 1,000 (with a $1''$ slit)
Imaging Resolution		> 5		Yes
... Beam Diameter	> 100 mm			118 mm
Field	$20''$	$8\,'$	Largest possible	Yes
Pixel scale	$> 0.15\,''$	$> 0.15\,''$	$> 0.15''$	$0.17''$
Image quality	Does not degrade Gemini best seeing by more than 10% ($0.25''$)			Optical achieves $0.25''$. IR will meet, but is now $\sim 0.3''$.
Flexure requirement	0.1 pixel RMS	0.1 pixel RMS		Ok for transients, unsure if moving pupil does more harm to precision than flexure.
Maximize light into slit	Yes	Yes		ADC and slit-viewing camera
... ADC	Yes	Tentative yes	Yes	Yes, but limited to airmass 1.56
... Slit Viewing System	Yes	Yes		Yes
Ultrahigh precision		200 ppm		Preliminary results promising.
Real Time Classification	Desired		Desired	No reqs, see §D.5

D.2 Design Summary

A block-diagram layout of GEONIS is shown in Figure 9. Light enters from the Gemini 8-m telescope and passes through a linear ADC, polychromatic light is brought to a sharp focus on the telescope focal plane. In spectroscopic mode a reflective slit is placed on the focal plane and the slit diverts a $5' \times 3'$ field into the slit viewing system. In imaging mode, the slitmask is retracted and the focal plane is clear. After the telescope focal plane, the beam travels through the instrument structure to the collimator. The collimator forms a pupil image below the focal plane, and also carries the flexure compensation system. Before the pupil is formed, a dichroic splits the beam into the two spectrograph channels: the infrared and the optical. Both channels are near identical and operate in one of three modes: echelette mode ($20''$ slit, R$\sim$4,000), longslit mode ($6.5'$slit, R$>$100), or imaging. GEONIS' design has evolved since the proposal, and a summary of changes is near the end of this section (§D.14).

The instrument solid model is shown in Figure 10. For clarity the model highlights the optical channel of the instrument. The instrument support structure is shown as thin faint blue rods, and GEONIS is mounted to its bosses via three hockey pucks. Light propagates from the ISS through the ADC and follows the light path shown in the block diagram of Figure 9. The slit-viewer camera beam is shown as a single field point on the slit mask. Here, one can see the beam propagating from the focal plane, reflecting off of the collimator, and being diverted (as blue light) into the optical spectrograph (the IR beam is suppressed for clarity).

Guiding our design approach is that GEONIS is simple to use, and thus the instrument acts as an efficient system. A lot of thought has gone into ensuring that our observing overheads are low (acquisition, setups, readouts, control loops, etc.). Furthermore, given the cost cap, given GMOS, and given the array of multi-object spectrographs that exist or will exist in both hemispheres, we have designed GEONIS as a single object spectrograph of unparalleled efficiency. We highlight these efficiencies below:

Simple Data Reduction – By using fast cameras (faster than f/2.2), an acquisition system that keeps the object in the slit, an ADC that maximizes light into the slit, and an open-loop flexure compensation system, we ensure ease of data reduction. Spectra are background limited within minutes and stay fixed on the detector.

High acquisition efficiency - Our instrument is designed with high-speed detectors and a slit-viewing camera for efficient target acquisition and guiding (see Table 6 below). The slit-acquisition system should be robotic, requiring no human intervention from operators. The slit will not need to be rotated to the parallactic angle as we use an atmospheric dispersion corrector.

High calibration efficiency - The instrument is designed to operate only two spectroscopic modes and one imaging mode. There is not a large suite of gratings that needs calibration. The grating modes cover the entire wavelength range in a single shot, so there is no need to articulate the grating to tune towards the bandpass of

interest. Nightly calibration requires the minimum number of standard star observations.

High stability - GEONIS uses an open-loop flexure compensation system to ensure that calibrations taking during the day are applicable over the entire night. The flexure compensation system both increases throughput and enables our exoplanet atmosphere science case.

High speed - By using electron multiplying CCDs (EMCCDs) the instrument is able to take short exposures (fraction of a second) with high duty cycle. The instrument can degrade well if we descope to traditional EMCCDs.

High throughput - The instrument is designed to have high throughput materials, coating, and to minimize the stray light background.

Gemini's queue based observing is unique in 8-meter-class telescopes. Thus Gemini is viewed as our team's go to facility for targets of opportunity. Indeed, our science team has multiple target of opportunity observers (PS: Kasliwal, Fox, Masiero, & Matheson) that are now serviced with the GMOS. In addition to targets of opportunity, GEONIS will be used for monitoring of time-variable sources, thus acquisition efficiency is essential for our system throughput. Given spectroscopic exposures of between 30 minutes to a few hours, the net loss of science time can be up to 50% to 10%.

Our current time budget of observations is shown in Table 6 below. The contents of the below are based on a document by A. Lopez and D. Coulson of Gemini, who break out the average overhead on GMOS.

Table 6: List of overheads, the amount of overhead in minutes, and the amount we aim to achieve with GEONIS. The overheads for GMOS are from the Lopez & Coulson document. Typical exposure times for target of opportunities is between 30 m to 1 h, and so savings here will make a dramatic impact on instrument efficiency. The most important efficiency gain is the "extra" standard star observation, which is achieved by having a simple instrument design with a single spectroscopic observing mode.

	Overheads on Gemini Today	Predicted with GEONIS
Slew / dome	3 min	3 min
Close guide loops	3 min	3 min
Acquire	2 min	1 min
Slit confirmation image	5 min	0 min
Arclamp + flat	3 min	0 min (FCS)
Standard star	$\sim$ 16 min	0 min (no reconfiguration)
Total	16 min (32 min with standard)	7 min

Guiding will be accomplished using our slit-viewing camera with a frame-transfer CCD (based on our experience on Keck, Palomar, and other telescopes).

D.3 GEONIS' Approach to the Required Variable Spectral Resolution

The spectral resolution requirement states that the instrument deliver a range of spectral resolutions. It is possible to meet such a requirement in hardware or software. The traditional hardware approach is to provide a mechanism that mechanically moves gratings in and out of the beam. But mechanisms take tens of seconds to adjust and can fail, and we lose valuable science time; the mechanism moving mass also must be considered in the dynamic mass budget; finally, an array of gratings can be expensive in terms of cost and mass. Another approach is to bin high-resolution spectra (down) to the resolution of interest. The problem with the software approach is that traditional CCDs deliver some 3 to 5 e- of read noise per pixel. At GEONIS R$\sim$4,000, the optical night sky is faint (0.01 e-/s) requiring tens of minutes to reach the regime where sky shot noise dominates over read noise ("background limited").

Our approach with GEONIS is to select spectral resolution during data reduction. First we use an echelette grating, which is the most efficient spectrograph configuration as spectra are always "on blaze". Next, we have fast cameras that allow us to achieve background-limited operation in about five minutes. In the optical, for bright objects where the total exposure time needed at $R \sim 500$ is only a few minutes, we solve the read-noise problem by using the EMCCDs in photon-counting mode where the detector gain is turned up to 1,000 or more. In this mode, the probability of read noise triggering a measurement is a negligible fraction of the probability of detecting a photon. Thus, even at $R \sim 4,000$ the instrument is background limited in a fraction of a second and it is profitable to bin the high-resolution spectrum to the required resolution. In the NIR the sky background is so high that the signal is background limited in a matter of minutes.

Based on discussions with E2V, EMCCDs of the size (CCD282) we need to have an associated development risk. E2V has given us confidence that they will make their CCD282 reliable by the end of 2016. If GEONIS is selected and CCD282 is not available, there is a large format frame-transfer non-electron multiplying device that we could still use. The main disadvantage would be a decrease of total rate of classifications on order of 10%. The attendant loss comes from an estimated 10% decrease in delivered signal to noise due to increased read noise.

D.4 Real Time Object Acquisition & Guiding

To maximize system throughput, and to ensure that the object's location is well known in the slit (for real-time data reduction), object acquisition must be accurate, precise, and automated. A number of automated astrometric calibration systems will refine the astrometric calibration of an image header to deliver a high-precision alignment to a reference catalog (for example, Valdes et al. 1995; Mink 2006; Bertin 2006, Lang et al. 2010). These systems are reliable and robust, and produce excellent results with a RA/Dec guess from the telescope control system. These systems will yield sub-pixel astrometric solutions across the entire field. We thus require a wide-field-of-view acquisition system.

There may be observing cases where the coordinates of the object are not known relative to a well-known reference catalog and a finding chart is supplied, in this case the Gemini astronomer will observe as per normal.

Based on experiments with astrometry.net, it seems that to identify the vast majority of fields when operating on fields of $\sim (16')^2$. A field size requirement is passed to the acquisition and guider system.

Differential flexure between the acquisition system and the slit will reduce photon throughput, and make real-time processing of data more challenging. For these reasons, we conclude that the acquisition and guiding system must look at light reflected near the slit and that the guiding software work by using the slit as the reference position.

D.5 Real Time Data Reduction Pipeline

GEONIS will be spending a good fraction of its time classifying supernova and answering the question "is this object interesting or not?". Today, Gemini is the "go to" observatory for classification of transient sources. In the future, the demand for such service will increase by factors at least ten, which is more than what our community can keep up with (even with super efficient instruments like Geonis). Our community will benefit from any gains in efficiency that Gemini brings to the table. In this subsection we offer some suggestions on how to maximize the detection to classification efficiency in the era of LSST.

To our knowledge, facility-class observatories consider exposure time to be the fundamental delivery unit. The exposure-time-driven approach works well when an observatory allocates its time based on "nights". Queue based observatories want to use signal-to-noise as the fundamental unit of allocation, which is a refinement of the exposure time unit. Real time processing, of course, enables such an approach.

Instruments like GEONIS, designed from the beginning to be stable and allow simple data reduction, allow on the fly reductions (with appropriate software). Instead of the astronomer reducing data, a data reduction robot (responsibility of the observatory) would provide on the fly results available on the internet. A classification robot (responsibility of the observer) would consume the on-the-fly reductions and provide feedback to the observatory. To help our entire community with the deluge of data, we may insist that if the object is not of interest to the team, its classification must be shared with the world.

The evolution of exposure time driven, to signal to noise driven, to classification driven observatories is shown in Figure 11.

The only way real time reduction works is if the instrument pipeline can be automated. This means that wavelength calibration must be automatic, and the trace's position is well known on the slit. GEONIS has been designed with a slit viewing camera such that spectra are at a known location on the slit, and with a ADC so that we know the orientation of the spectra with respect to the trace. Figure 7 in the OCD (§B) demonstrates the importance of these components. Night sky and host galaxy

subtraction are often steps that require human intervention; however, it is generally possible to classify a supernova even with some host galaxy contamination.

Gemini can work within the LSST broker framework (see §C.4.2) where the observatory communicates with external classification robotic systems. The key functionality is for the observatory to broadcast a "we are beginning your observation" message to an observer's robotic system. That message kicks off the observer's robot to start pulling reduced data from Gemini. The observer's robot will assess the data against some objective criteria, for example, 90% confidence that this is a type Ia supernova after max light. Once that criteria is met, the observatory robot will tell Gemini to stop observing. The power of GEONIS is that if the object is exciting, observations can continue without switching any observing modes.

D.6 Systems Engineering

In this section, we report on our throughput prediction (D.6.1) to indicate what we expect an instrument like GEONIS would achieve. We then describe the systems engineering allocations for GEONIS: mass, instrument precision, image quality flowdown, and high-level requirements.

D.6.1 Throughput

Throughput expresses the total efficiency of the instrument when accounting for losses at interfaces (2 ADC, collimator mirror, dichroic, 8 element camera, and filters), vignetting at the cameras (amounts to about 4% at corners), and at gratings (here we assume the light in various orders is summed with no penalty). In this subsection we describe the total system throughput of GEONIS. These numbers do not represent a budget (which is a top-down allocation), but the current system prediction.

For our throughputs, we consider the following: the Gemini observatory atmospheric extinction model at airmass 1.2, three bounces off Gemini's mirrors, two ADC prisms assuming a Sol-Gel coating (which is better than a single-layer MgF2 coating), 20% slit losses, a Gemini-observatory coated collimating mirror, 90% dichroic, gratings simulated via GSOLVER at proper angles of incidence, prisms and cameras simulated in zemax with realistic coatings, and values from E2V and Teledyne for the QE of their respective detectors. The throughput is summarized graphically in Figure 12 below.

GEONIS should deliver excellent signal to noise in a half-hour exposure as listed in Table 7.

Table 7: Signal to noise in half an hour per resolution element (1-arcsecond slit). GEONIS maintains the current high-throughput, but also improves the overall instrument efficiency (which is not included in this table). Results for GMOS and GNIRS based on Gemini Integration Time Calculator (ITC) web page. Results for GEONIS based on scaling ITC sky background signals and expected quantum efficiency, read noise, and dark current.

	S/N in 30-min exposure with 1-arcsec slit			
	GEONIS ($V \sim 20.5$)	GMOS	GEONIS ($H \sim 19.5$)	GNIRS
$R \sim 4,000$	6	not possible	5	not possible
$R \sim 2,500$	9	8	7	4
$R \sim 1,000$	14	13	11	8 ($R \sim 500$)

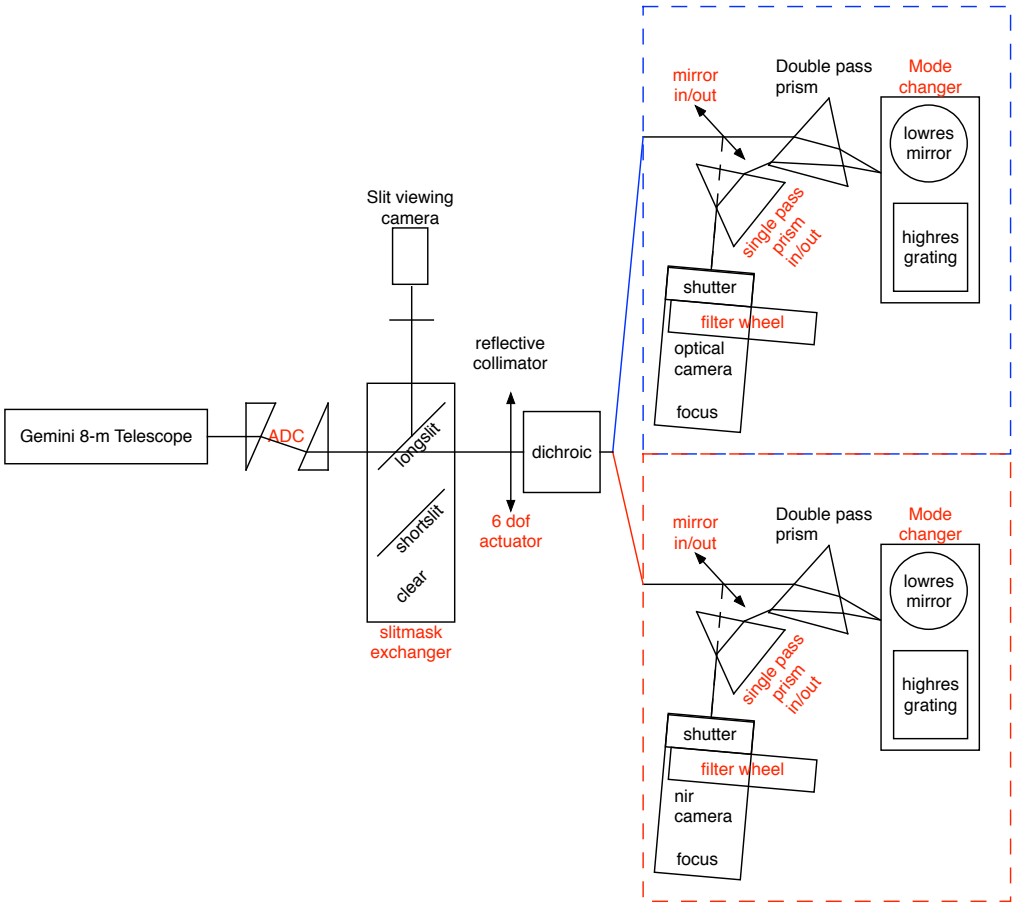


Figure 9: GEONIS functional block diagram. Mode switching elements are highlighted in red. The light path begins at the Gemini telescope and works to the right as follows: atmospheric dispersion corrector (ADC), slitmask exchange unit (one of either longslit, shortslit, or clear), the six-degree-of-freedom reflective collimator, to dichroic. At the dichroic, the beam splits to the optical and IR spectrographs which are both functionally similar. There is a "short-slit" echelette mode for classification (R$\sim$100) and diagnostic science (R$\sim$4,000); a high-precision "long-slit" mode for exoplanet characterization; and an "imaging" mode.

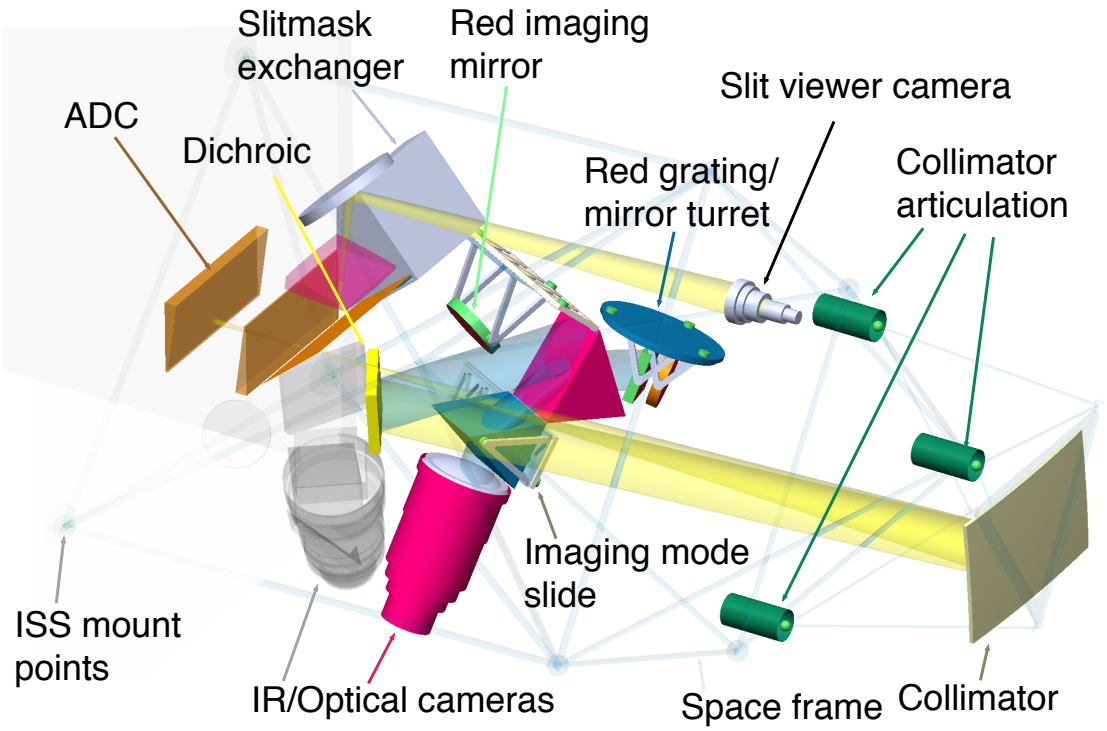


Figure 10: The solid model of GEONIS's systems. Here we see the space frame, moving optical systems, and two light paths. The top path is that of the slit-viewer camera focused (to a single point) on the slit mask. The beam through the spectrograph starts yellow, is collimated, and then is partially reflected by the collimator (where the yellow beam turns blue). GEONIS is configured as shown in panels (a) and (b) of Figure 19.

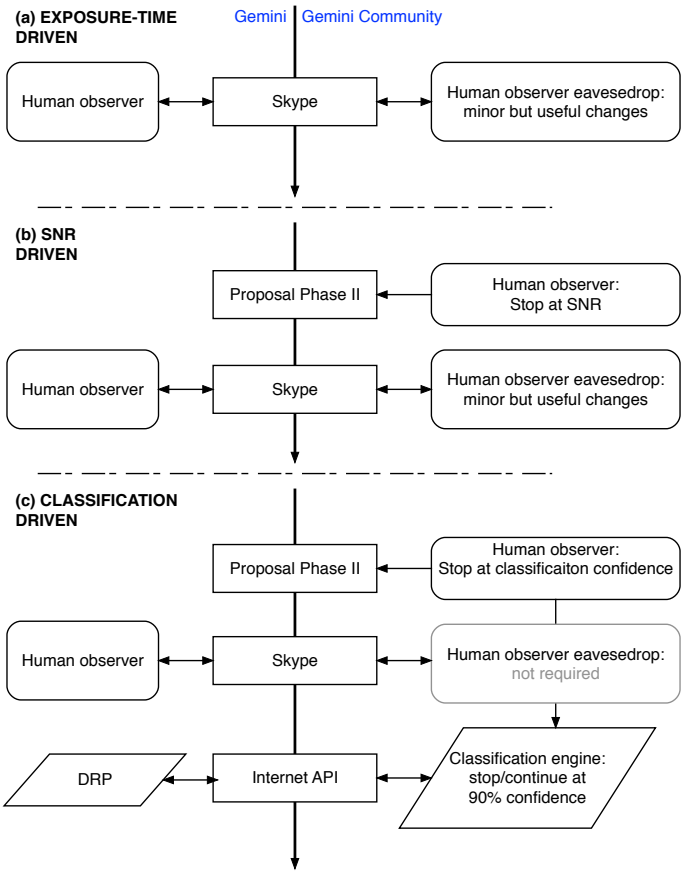


Figure 11: Three flowcharts indicating relationships of Gemini Observatory and the Gemini Community to impact object classification spectroscopy. Panel (a) indicates traditional exposure-time driven observations. In this case, the fundamental deliverable is an image of some predetermined exposure time. It is possible for the observer to make minor changes through the eavesdropping program. Panel (b) indicates signal-to-noise (SNR) driven observations, where the astronomer asks for observations to end after a specific SNR is achieved. In Panel (c) we show classification-driven observing. The key idea here is that observers are allowed real-time access to data reduction. These data are consumed via a classification engine every few minutes, and the classification engine drives the observations.

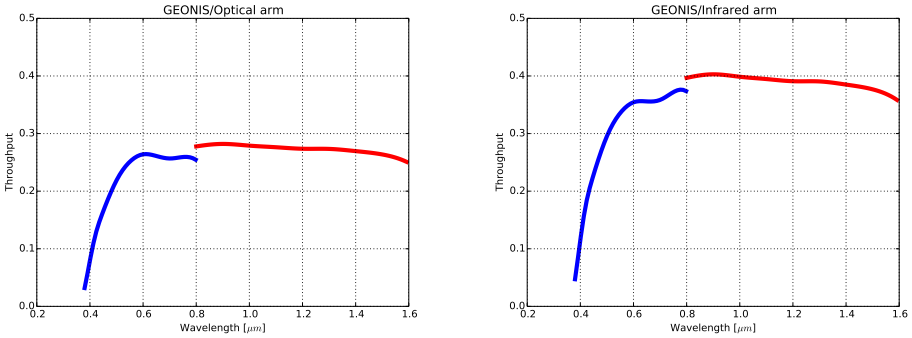


Figure 12: Left: Echelette object-to-detector throughput of GEONIS for typical observing conditions (airmass 1.2, 20% slit losses). Almost all of the loss below $\lambda 0.58$ μm is mirror reflectivity and CCD throughput. Right: Longslit object-to-detector throughput of GEONIS for typical observing conditions (airmass 1.2, 20% slit losses).

D.6.2 Image Quality Budget

Image quality requirements are budgeted at the top level and flow down to subsystems. Excellent image quality is critical for workhorse instruments, especially those that operate in a background-limited regime (typical for a workhorse spectrograph). As expected, better image quality challenges optical design and fabrication, and in general, better image quality requires more mass, volume, and dollars. Thus, we use adopt a formal budgeting process to allocate image quality budget to various subsystems. The numbers here represent allocations, and we have demonstrated that these allocations are reasonable (even though we did not achieve the required image quality for the infrared camera, as described later).

According to Gemini's delivered image quality web page[3] indicates that the best quartile of image quality delivered is 0.45″ across optical and near-infrared bands. GEONIS constrains itself to not degrade the best quarter of image quality by more than 10%. The flowdown of these requirements and their distribution to various systems is shown in Table 8 below. Given that the image quality requirement maps to the same size as a single pixel, the camera and collimator image quality needs to be tested with a microscope that can sample the delivered point-spread function.

Table 8: Image quality budget requirements. Note that the canonical FWHM=2.355 RMS relationship is modified in the two-dimensional case to be $\sqrt{2}$ FWHM=2.355 RMS.

Element	Fraction of budget	FWHM (arcsec)	RMS (″)	RMS (μm)
Requirement	100%	0.25	0.15	12.5
ADC	5%	0.06	0.03	2.8
Collimator + Telescope	30%	0.14	0.08	6.8
Camera	48%	0.17	0.10	8.6
Grating	0%	0.00	0.00	0.0
Rotator	0%	0.00	0.00	0.0
Guider	0%	0.00	0.00	0.0
Flexure	0%	0.00	0.00	0.0
Fabrication (and margin)	10%	0.08	0.05	3.9
Dynamic	7%	0.07	0.04	3.3
Total, FWHM, or RMS value	100%	0.25	0.15	12.5

D.6.3 Precision Budgets

GEONIS is expected to be a powerful exoplanet-atmosphere machine. The ability to measure exoplanet atmosphere is dominated by the systematics within the spectro-

[3]http://www.gemini.edu/node/10781#ImageQuality

graph. These systematics are communicated in parts per million (ppm). The science team's goal is to achieve a precision of better than 200 ppm.

If GENOIS is kept at a constant temperature and gravity vector, it would impart no systematic residual signal. But GEONIS lives in a varying gravity vector and this means that both an ADC (moving optics) and a flexure compensation system are needed. The instrument itself has electronics, cooling, and the like, and will thus have thermal variations that impart small signals to the measurements.

The main contributors to these systematics come from three main contributions: the ADC piston motion causes the collimator's exit pupil to shift inside the spectrograph, the FCS corrects for bulk motion of elements with respect to one another, but as baselined also shifts the collimator's exit pupil, and any nonlinearity in detectors will impart these signals. Our aim is to keep the thermal time constant of GEONIS to be about 12 h, considering the typical exoplanet transit of 4 h. GEONIS' heat capacity is about $10^6 J/^\circ C$, and for a ΔT of $10^\circ C$ (typical value over a night at Cerro Pachon) we must limit the total heat flux to about 25 $watt/m^2$ over the $\sim$ 12 m^2 outer shell, which can be maintained by 75 mm of foam with a fiberglass shell.

The motion of the pupil as a result of ADC and FCS motions is similar enough that both can be simulated together, these are discussed in §D.7.6. The CCD nonlinearity is less of a concern. Based on measurements from other e2v devices, CCD precision is not a driving factor here. Furthermore, with the slit-viewing camera, we will be able to keep the science target fixed on the detector a to fraction-of-a-pixel level.

For future phases a full precision budget should be flowed down from the 200 ppm requirement to individual subsystems.

D.6.4 Mass Estimates and Budgets

Gemini has tight requirements on mass and center of mass. At Keck Observatory, the Cassegrain-style mounted instruments ESI and MOSFIRE both are 2.5 ton in mass, and thus far exceed the 2 ton mass allocation of Gemini. GEONIS aims to combine aspects of both instruments into a single instrument that is less massive. Furthermore, Gemini's instrument support structure requires the center of mass be 1 m from the instrument support structure. Thus, we recognized from the beginning that total mass will be a primary driver to the instrument design.

At this feasibility level, we aimed for an instrument mass of 1.5 ton, in order to carry a 30% mass contingency budget. The reason for this high contingency, is that we are allocating mass based on analogy to other instruments, which has an inherit uncertainty and risk. In our experience, as the instrument design is better understood, mass tends to increase (usually by about 30% from concept to pre-ship review).

Our current mass estimates are derived from two sources: for all optical elements we used the baselined design to estimate mass. For mechanical elements, we use the as-built masses from either ESI or MOSFIRE. For the space frame, we assume 15-mm-diameter invar rod and the mass estimate is thus based on invar's density and

Table 9: Mass budget.

System	Mass (% of total)	Mass (kg)
GEONIS	100%	2000 kg
Space Frame	14%	289 kg
Cooling	8%	150 kg
Mirror inserters	8%	150 kg
Grating Turrets	5%	100 kg
Acquisition mechanics	5%	100 kg
Electronics cabinet	5%	100 kg
Electronics	5%	100 kg
Filters and wheel	4%	85 kg
Mask exchanger	4%	80 kg
Camera barrels	3%	66 kg
Camera glass/crystal	2%	43 kg
Double pass prisms	1%	26 kg
ADC	1%	26 kg
Dewars	1%	22 kg
Collimator mirror	1%	20 kg
Single pass prisms	1%	19 kg
Insulating Foam	1%	12 kg
Acquisition	0%	8 kg
Gratings	0%	2 kg
Lowres mirrors	0%	2 kg
Dichroic/mirrors	0%	2 kg
Total	80%	1590 kg of 2000 kg

the total expected length of rod. There are various multiplicative factors that have been applied after conversations with colleagues, these factors are always larger than 1. The mass budget and estimate is provide as Table 9.

As can be seen from our table, we have already accounted for 80% of the mass budget of the instrument and we missed our contingency mark. Likely GEONIS will be over the 2 ton budget. During the next stages of design GEONIS' mass will be monitored through systems engineering. Note that for the Gemini planet imager, a mass exception of 200 kg was allowed. If we assume GEONIS will be granted such an exception, then we do carry a 30% contingency.

D.6.5 Compliance and Problems with Interface Control Documents

The GEONIS team has studied Gemini's requirements and we are in general agreement with almost all the requirements. Many requirements (e.g., the shipping requirements) are passed to our Keck observatory instruments. We have made note of

the following exceptions:

Exception 1. Caltech mechanical engineering has standardized on Solidworks, and we cannot switch our mechanical designers to Inventor. Based on some experiments exporting to Inventor, we do not believe the export feature will provide a valuable result for Gemini. We understand how important good documentation is for an observatory, and will discuss how this can be best accomplished in future phases.

Exception 2. Caltech uses a variety of thermal analysis programs, we may not be able to conform to only Excel or ANSYS file formats.

Exception 3. GEONIS' baselined detectors are ITAR restricted. Caltech and our attorneys have experience with ITAR, and have worked through a variety of restricted instruments with colleagues in China and India.

Exception 4. GEONIS will require an exception to the volume requirement for the atmospheric dispersion compensator (ADC). The ADC will likely penetrate the keep out zone between the instrument and the ISS on order of a few tens of millimeter. This issue is described in §D.7.2. Note that when the instrument is being installed on the telescope, the ADCs will be retracted and the ADC prism will not penetrate the keep out zone (though its supporting members may penetrate).

Exception 5. GEONIS cannot allow easy access to detector controllers. The Hawaii series of detectors have an ASIC controller that is mounted next to the detector in the cryostat. On the optical side, depending on the final controller selected, it is not clear how accessible such a controller will be.

Exception 6. GEONIS may need a mass exception to 2.2 T (see §D.6.4).

Exception 7. As the ADC trombones, the optical image delivered on the telescope focal plane is shifted, in effect repointing the telescope. For best guiding, the Gemini TCS will need to be modified to accept this term.

D.7 Details of Instrument Subsystems, Feasibility, & Next Steps

This subsection (§D.7) describes all of GEONIS' subsystems. For each subsystem we describe the current state of the design, as well as any risks or issues associated with the current design. The systems are ordered following the light path:

D.7.1 System Structure

The key requirements affecting the structure are imposed by Gemini (mass, volume, interfaces), but also by our flexure compensation system that requires 0.1 RMS residual flexure. These high-level requirements flow to technical requirements requiring an efficient (high stiffness per unit mass) structure with little mechanical hysteresis. To achieve high structural efficiency, we have designed a determinate space frame(e.g. Nelson, 2005; Vogt et al., 2014).

Although we settled on a space-frame design, we approached this problem by examining two monocoque structure strategies. Here we explain the two reasons why we decided against using such the monocoque design.

First, monocoque structures are less efficient that space frames. Monocoque structures require plates under shear to maintain stiffness. A simple 0th-order design using thick steel shear plates indicates that one exceeds the 2 metric-ton mass limit if such a system is adopted. We then considered light-weighted honeycomb benches from Newport. A light-weighted Newport optical breadboard requires $\sim$0.8 metric ton of material. The optical bench alone would consume about 40% of the total mass budget. Without performing exhaustive analysis or optimization, it looked as if additional stiffening elements would bring the total mass usage to over 60% on just the structure alone.

Second, laminated honeycomb designs do not lend themselves to finite-element analysis. They may have mechanical hysteresis, or exhibit other non desirable properties. Depending on the lamination process, these honeycomb designs can degrade over time, which would not just increase flexure, but also introduce mechanical hysteresis. Given our adopted open-loop flexure compensation strategy, this hysteresis may be unacceptable. Without detailed experimentation and prototyping, it will be hard to determine from analysis only if light-weighted honeycomb structures work.

For the aforementioned reasons, we have decided to design the structure around a determinate space frame. Our current space frame design is estimated to use about $\sim$0.3 metric ton of material or about 15% of the total mass budget. Thus, space frame design leaves plenty of mass for the rest of the instrument. Note also that space-frame design lends itself to finite-element analysis. The determinate nature of these structures lends itself to finite element analysis.

Space frame design carries two challenges, though both have been overcome for our GEONIS concept. First, the frame has to package around the instrument; second, the frames are connected via nodes that must have no mechanical hysteresis; this problem was solved for the Levy spectrometer (Vogt et al., 2014) by using a precise six-axis mill and tungsten inert gas tack welding of joints.

We note here that the structure and instrument satisfies Gemini's instrument volume requirements (except for the ADC as described in §D.7.2). These are shown in Figures 13 and 14.

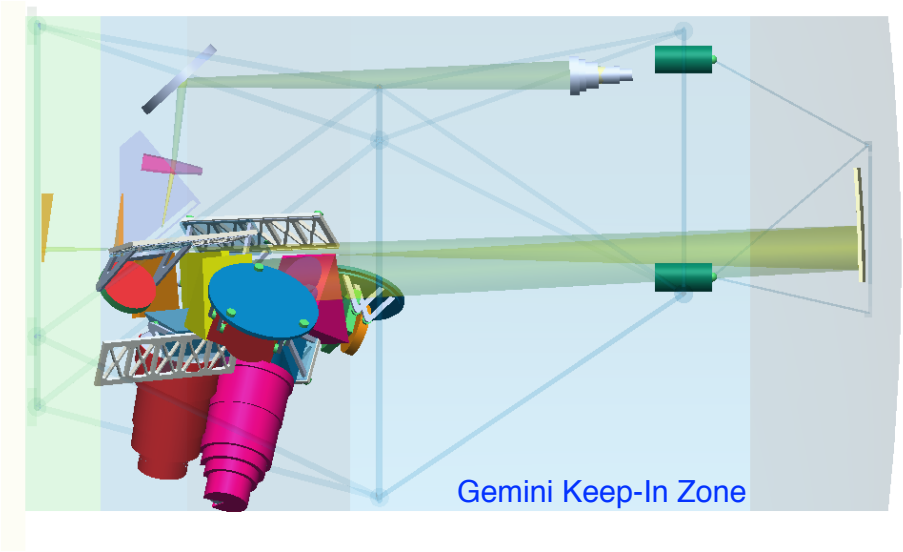


Figure 13: Side view of GEONIS solid model with the Gemini instrument volume indicated. ADC prism1 is shown in its fully extended state where it penetrates the pale green keep-out volume as discussed in §D.7.2 above.

Outline of instrument integration procedure: GEONIS is a large astronomical instrument. In order to manage its complexity GEONIS has been designed as a number of subsystems, nearly all of which may be tested independently to verify their performance prior to integration with the rest of the instrument. Even the space frame can be prototyped and vetted for flexure performance.

The results of subsystem tests are documented, as these results will provide a key tool in analyzing overall performance problems encountered during instrument integration. Each subsystem will have an associated assembly drawing and design note. As the subsystem is built up, it will be checked against the assembly drawings. Technicians are responsible for maintaining a book of "red lines". These redlines are modifications made to the instrument during the course of assembly. Reintegrating the redlines are a critical component of the final documentation of the instrument.

Each subsystem will also have a test plan associated with it. The test plan contains the test configuration and test procedure documentation. As the test plan is performed, a test report is written.

To ensure that there are no interference problems we viewed our solid model at various angles to see if components could be assembled into the frame. No interferences exist that cannot be handled.

GEONIS must be aligned to the telescope. The space frame allows for ease of system alignment. There are six supporting members of the telescope-to-instrument interface using turnbuckles. These can be adjusted to move the instrument in any degree of freedom. A translation and rotation matrix is kept in Excel and when any motions are needed, we can predict how much rotation of the turnbuckle will lead to the desired outcome.

GEONIS Space Envelope: GEONIS has been designed with care to maintain the Gemini mandated volume requirements (except for a small penetration of the keep out zone by the ADC §D.7.2).

Feasibility: The structure is deemed feasible based on comparisons to similar instruments, and on our mass, and volume estimates. Our initial analysis on a simplified space-frame with Frame3DD shows that the structure is stiff, with a first resonant mode higher than 35 Hz and with negligible displacements.

GEONIS requires an open-loop feedback system that delivers 0.1 pix RMS residuals. Thus the mechanical hysteresis of the structure must be negligible. The main contributor to hysteresis in a space frame is slop in the joints, so joint design requires special care, but this problem has been solved by other spectrometers via proper design and implementation.

Next steps: The full structure must be designed to minimize flexure and fit around the optical components. A storyboard of the integration process to ensure that the instrument can be assembled would be useful. The structure must be analyzed for buckling under seismic conditions. Finally, the individual subsystems must be connected to structure in the mechanical design.

D.7.2 Atmospheric Dispersion Corrector

The science requirements to the atmospheric dispersion corrector are that it must operate 400 nm - 1.6 μm in wavelength without adding thermal background, it must fit into the space between the instrument support structure and the focal plane, the ADC must operate over the widest airmass range possible, the ADC must not degrade images by more than $0.06''$, and the ADC must not degrade the precision of GEONIS for exoatmosphere studies. These requirements flow down to technical requirements that dictate its material, the size of the prisms, the length of the trombone system, and wavefront error.

The ADC is an optical system, a mechanical system, and requires software communication with the telescope control system. There are two important notes for the ADC to the Gemini team. First, the ADC will require modifications to the telescope control system. Second, the ADC will penetrate the 200-mm keep-out area extending from the Gemini instrument support structure and will thus require a letter of exception from the observatory.

The ADC is an essential component to success in observing transients, that are often embedded in a galaxy host. Transient host galaxy subtraction requires observations at position angles that may not be aligned with the parallactic angle. Similar

arguments can be made for GEONIS' workhorse capability of observing faint objects. Without an ADC, about 20% of the light ends up out of the 1-arcsecond slit for objects with airmass of 1.1.

In imaging mode, the ADC is essential for the reasons articulated above. The ADC's size is driven by imaging mode, which addresses a large mechanical field. If GEONIS was descoped to a spectrograph only, the ADC would shrink in size.

For exoplanet observations, the benefit of the ADC is not clear on measurement precision. ADCs have two deleterious effects that compromise measurement precision. First, ADCs necessarily move the collimator exit pupil, which means that the optical path through the spectrograph can vary and this can be tough to calibrate. Second, ADCs have both polishing and material inhomogeneities which are also tough to calibrate out if observing over a range of airmass. Both problems are solvable: first, one can add an extra pupil mask that reduces the total amount of light into the instrument by a few percent, but ensures that optical path through the instrument does not vary. Second, it is now possible to purchase high-homogeneity fused silica and polish it to low levels of transmitted wavefront error. Our calculations show at a conceptual level that we can exceed the precision requirement.

Field of view: The GEONIS field of view necessitates a large rectangular prism that is 400 mm x 180 mm x 20 mm. Formally, Gemini's field of view will be vignetted in the corners of the prisms, and for space-constraint reasons we may decided to remove the corners of the ADC prisms.

Material Selection: The GEONIS ADCs are selected to be high-homogeneity fused silica. The selection to fused silica is driven from two directions. First is the exoplanet science case that demands high homogeneity; second, we require that the ADC have low emissivity at thermal-IR wavelengths to reduce the thermal background.

There is no other useful available material for the ADC (CaF2/BaF2 are too expensive and PBM2Y or BK7 have high thermal emissivity) and so material selection is hard to improve upon.

Operating airmass range: The GEONIS baselined ADC operates over a limited range of airmass because it is constrained by the mechanical limits of the ISS. As the instrument's airmass increases PRISM1 in the ADC must piston out from the instrument to the ISS. At airmass of 1.1 or so, the ADC penetrates the keep out zone, until it reaches its mechanical limits. The ADC delivers excellent images up to a zenith angle of 37.5 degree (airmass 1.26). If the slit is orthogonal to the parallactic angle then the light loss increases such that at airmass 1.56 (50 degree) 80% of the light is in the slit, at airmass 1.74 about half the light ends up in the slit, and at airmass 2 only about 30% of the light ends up in the slit.

If one adopts airmass 2 as the sky limit, our ADC design covers 41% of the sky, and works well over 71% of the sky. For the remaining observations beyond airmass 1.56, GEONIS works, but will need to be aligned to the parallactic angle to ensure no light loss.

Image quality impact: The ADC adds about 0.02″ RMS to image diameter deliv-

ered at the telescope and meets its image-quality budget allocation of 0.06″.

Pupil wander considerations: The nature of a linear ADC, such as the one that we advocate, is that ADC displacements shift the collimator exit pupil. To minimize pupil wander, one reduces the apex angle of the prisms; however, by reducing apex angle the required linear-displacement-distance increases. The ISS-to-focal-plane distance is 300 mm, which is not enough linear room to cover correction to airmass 2. Thus we traded apex angle, linear throw distance, and pupil wander. Based on experiences with a variety of ADCs and spectrographs we allow several mm of wander of the collimator exit pupil.

However, for the exoplanet science case, pupil wander changes the optical path through the spectrograph and will impart a signal. The pupil-wander signal can be eliminated by either locking the ADC into a single observing position, or by masking the collimator exit pupil to force a constant optical path through the spectrograph (we discuss the pupil mask later).

Telescope-related issues: As indicated in Figure 15 above, as the ADC trombones, the field shifts laterally along the parallactic angle moving the telescope pointing origin. For this reason, Gemini will have to allow us to modify the pointing on the fly.

The ADC will require a written exception from Gemini observatory. The ADC pierces the keep-out zone as shown in Figure 15. Formally, the issue only exists in the corners of the keep out zone. Note that while the instrument is being installed onto the ISS, the ADC will be retracted.

Electrical and software issues: The ADC has a trombone structure that is actuated by several elements. We have implemented a much larger ADC for the Keck Observatory. The ADC mechatronic design is thus adapted from the Keck ADC.

The ADC trombone mechanism is actuated by a single ball screw mounted at the edge of the prism. Moment forces are absorbed by the ball slides that flank the prism on either side. A rotary encoder is attached to the ball screw. The motor, rotary encoder, and gearbox are standard off-the-shelf items. These items would be controlled by something like a Galil controller.

Next steps: For conceptual design phase, we would develop further the pupil wander and homogeneity specifications further.

D.7.3 Slitmask Removal System

The slitmask removal system moves a slitmask out of the focal plane when transition from the spectroscopy to imaging modes. The science requirements for the slitmask are that it accommodate three observing modes: echelette (short slit), long-slit mode, and imaging. Thus the slit mask system must be able to swap between a variety of slitmasks and clear (imaging).

For this phase, we did not consider the science trade of slits with adjustable widths. Instead GEONIS is baselined with fixed slitmasks. Formally, the exoplanet science case requires a wide $6' \times 13''$ slit. The science team believes that it would be useful

to have a narrow long-slit mode in addition to the exoplanet long slit. Thus, the slitmask removal system should switch between three masks and the open position.

In workhorse spectrographs, spectrophotometric calibrations are derived from standard stars with a wide open slit. GEONIS is not baselined with many slit options; instead; spectrophotometric standards will be observed without a slit. During the next phase, we may change requirements so that we can change slit widths on the fly.

In the proposal, we suggested that we would produce a stray-light specification for thermal emission from the slitmask. At the time, we expected thermal rejection filters with 10^{-4} suppression. After submitting the proposal, we discovered from our colleagues in Toronto that Asahi filters can produce out-of-band rejection filters that suppress long wavelengths at the 10^{-6} level. As a result of this new technology, we became less concerned with stray light.

The slitmask has an optical surface on one side that reflects light into the slit-viewing camera. The backside of the slitmask must be coated in a low-emissivity material (e.g., gold) to reduce the thermal back-ground into the NIR spectrograph.

The slitmask controller is designed at a conceptual level. The controller moves the mask in/out of the focal plane. The controller requires electronics and control software.

Feasibility: The slitmask control system will be inherited from other slitmask controllers such as those found on GMOS (on Gemini) or DEIMOS (for Keck). The slitmask control system is a low risk item.

Next Steps: The slitmask removal system is designed around three slits. It may be necessary for science reasons to carry more slitmasks. The science requirements and technical requirements for the slitmask system must be developed further during the next phase.

D.7.4 Slit-viewing Camera System

The science requirements for the slit-viewing camera are: the camera must have a sufficient field of view for an automated astrometric solution, and that the system can act as a precise on-instrument guider. We have noted that differential flexure between the slit-viewing camera and the guider system can be taken out by using the slit as a fiducial to guide against.

The Slit-viewing Camera (hereafter "slit viewer") is a critical component of GEONIS that is responsible for robotically moving targets into the slit and for on-instrument guiding. It will: acquire the target field of view, derive an astrometric solution, move the targeted RA/Dec into the slit, and guide on a background source. The slit viewer must guide on non sidereal targets. The slit viewer thus refers to the optics, optomechanical mounts, focus mechanism, detector for the slitmask camera system, and observing software.

The slit viewer field of view must be large enough that astrometry solving software can efficiently deliver a robust world coordinate system solution. Lang et al.

(2010) suggest the ideal field size is $4'$ x $4'$, our baseline acquisition system delivers a rectangular $5'$ x $3'$ field onto a 1k x 1k chip with 0.25" pixels (4 pixels = $1''$). The final field size may need to be increased by tens of percent, which should yield a minor cost increase. Note, whatever astrometric software is used, it must not rely on an external internet connection to operate (e.g., astrometry.net database will be stored on the host computer).

For this GIFS phase, we redesigned the acquisition system to package with the slitmask exchange and ADC, sped up the optical system (to f/1.5), and improved the poor image quality. Our goal was to develop a conceptual slit-viewing camera. The concept is shown in Figure 16.

Various fast Canon[4] lenses were simulated in zemax; however, these lenses show significant vignetting at the edge of the field. We are unsure of the impact of corner vignetting on the automatic astrometry solution software. GEONIS relies on automatic astrometry, and for this reason we are reluctant to baseline a commercial-off-the-shelf lens. That said, we are interested in studying this issue further and would prefer an off-the-shelf optical system.

Next Steps: During conceptual phase, we will try to simplify the aforementioned optical system by simulating the impact of vignetting on automated astrometric solutions. It may be valuable to add wavefront sensing capabilities to the acquisition/guider unit, and we will explore this possibility during the next phase.

[4]We used Canon lens prescriptions based on their Patents.

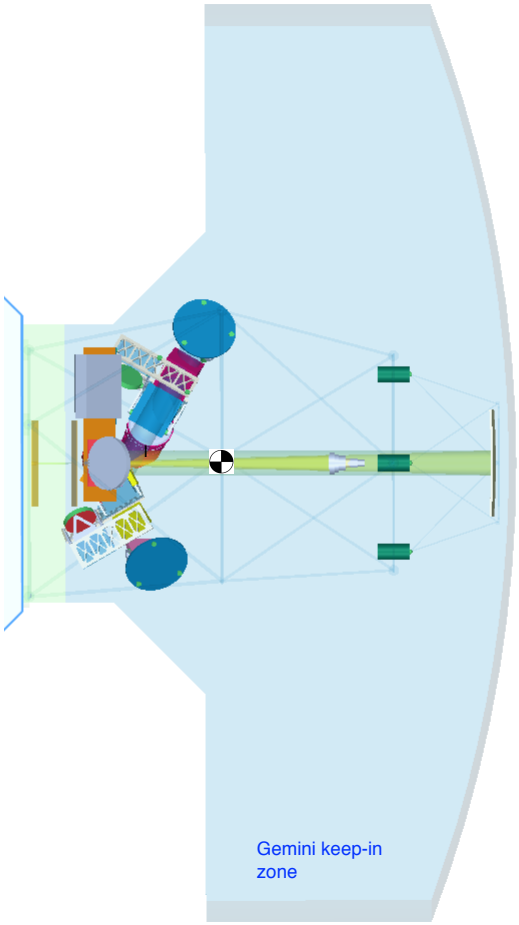


Figure 14: Top view of GEONIS solid model with the Gemini instrument volume indicated. The center of mass is indicated with the ◒ symbol. ADC prism1 is shown in its fully extended state where it penetrates the pale green keep-out volume as discussed in §D.7.2 above.

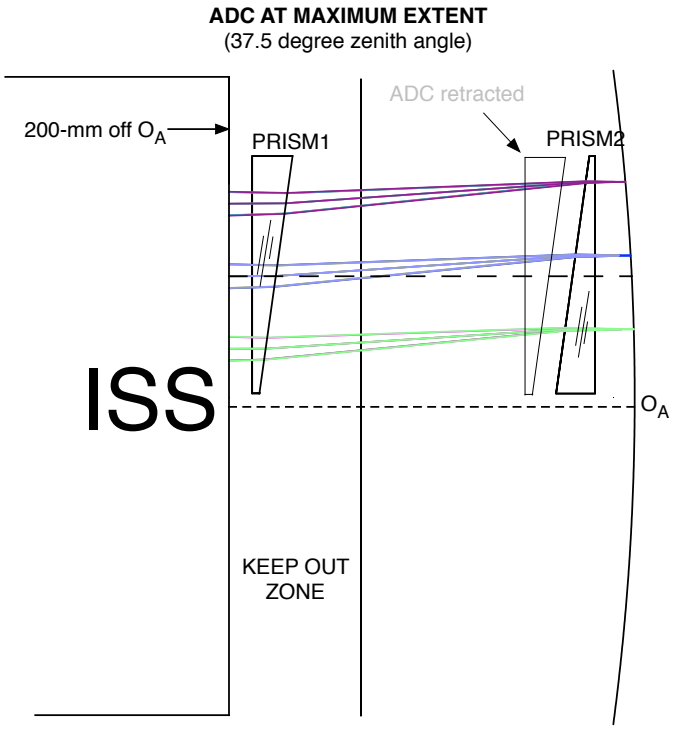


Figure 15: Section view of ADC design and rays. The instrument support structure is shown at left with the 400-mm-diameter field. The configuration shown is with the prisms extended as far as possible. In this configuration, the ADC corrects up to zenith angle of 37.5 degree. The ADC retracts such that prism 1is moved to be pushed against prism 2. The ADC can be retracted for exoplanet work, or for instrument installation.

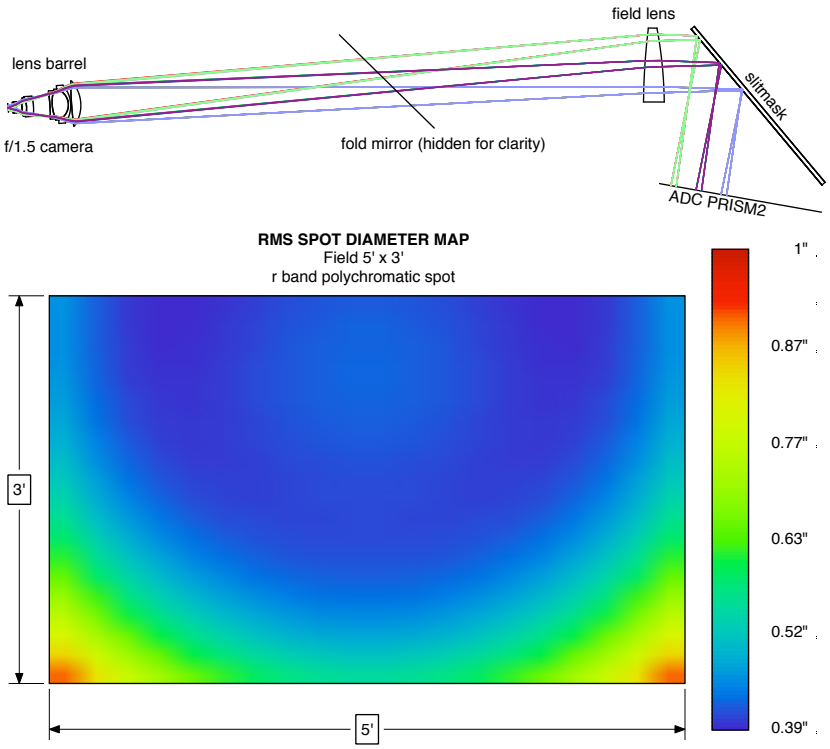


Figure 16: Ray traces and rms spot diameter for a conceptual six-element all-spherical acquisition/guiding camera (field lens not shown) for GEONIS. The guider feeds a 1k x 1k EMCCD with 15 μm pixels. As designed, the pixel scale 0.25″ / pixel. Over most of the field, the RMS image diameter is 0.39"

D.7.5 Collimator

The science requirements passed to the collimator follow: The collimator must support the wavelength, spectral resolution, field, throughput, thermal background, and image quality requirements. The collimator, with its long lever arm, is also the basis for flexure compensation.

To achieve the required spectral resolution, the collimator must deliver a larger than 100-mm-diameter exit pupil with enough pupil relief for gratings, cameras, and pupil mask. Science requirements dictate that the collimator operates over Gemini's full field and over the λ range 400 nm - 1600 nm. The collimator must accept Gemini's curved field and exit pupil. The design must be squat to not torque the center of gravity. Optically, the collimator must produce a sharp image of the pupil (where a pupil mask might be placed), and not add much to the thermal background. Thus the collimator uses a low emissivity coating. Finally, the collimator is used for flexure correction, so it has articulation stages built in.

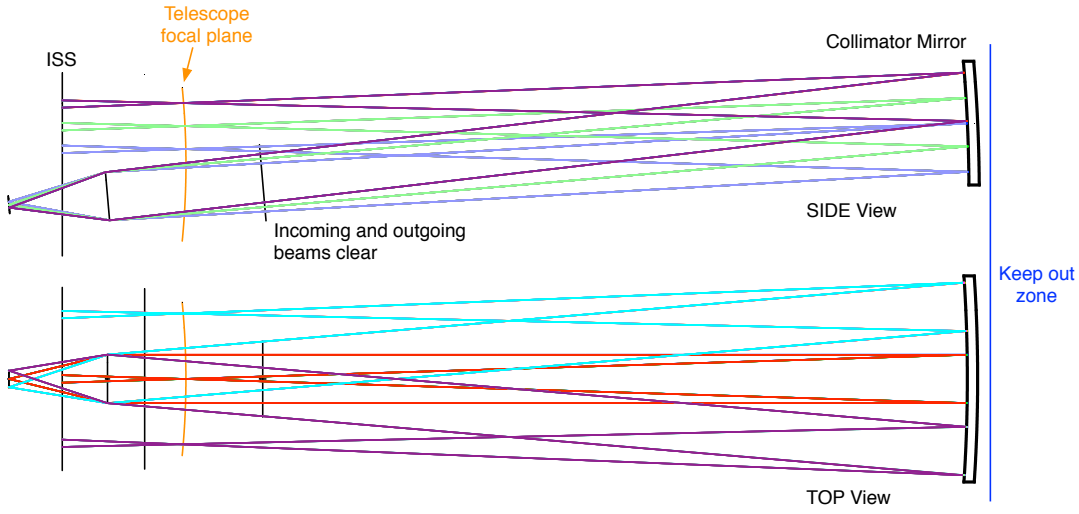


Figure 17: Ray traces for the conceptual single-mirror collimator. The collimator works over the entire Gemini field of view (10') and must meet a variety of conflicting optical, packaging, and mechanical requirements. Furthermore, material use is restricted to low-emissivity crystals and glasses. Note that the pupil delivered by the collimator is sharp (the off-axis rays are compressed due to vignetting) and an appropriate place for a pupil mask (Lyot stop).

Current Design: The collimator is a critical optical component and its design is one of the most challenging aspects of GEONIS' optics. A conceptual collimator has been designed to meet the aforementioned requirements. The raytrace and image quality distribution for the conceptual collimator are shown in Figures 17 and 18. The current conceptual design satisfies the image quality requirement over most of the field.

Given all the constraints, we have adopted the strategy of using a single mirror collimator. It has been shown by H. Epps, that for Ritchey–Chrétien telescopes, one can collimate the field with a single mirror of focal length equal to the radius of the focal plane delivered by the telescope. In the case of Gemini, it is not possible to match that condition exactly because the collimator mirror would be pushed beyond Gemini's volume limits. We thus eased back on the focal length to keep the rear of the collimator mirror to be 75 mm from the required volume limit. At this location, the collimator has a focal length of 1895 mm and produces a roughly 117-mm-diameter exit pupil. The main disadvantage of this approach is that the instrument must work off the telescope optical axis. Thus, the collimator field of view is displaced by 2.5′.

A single-mirror collimator has myriad advantages for GEONIS. It achieves the required image quality. When coated properly the collimator will have high reflectivity and thus low thermal background. Finally, the single-mirror collimator fits Gemini's space envelope. In short, we achieved the goals that we identified during the proposal phase.

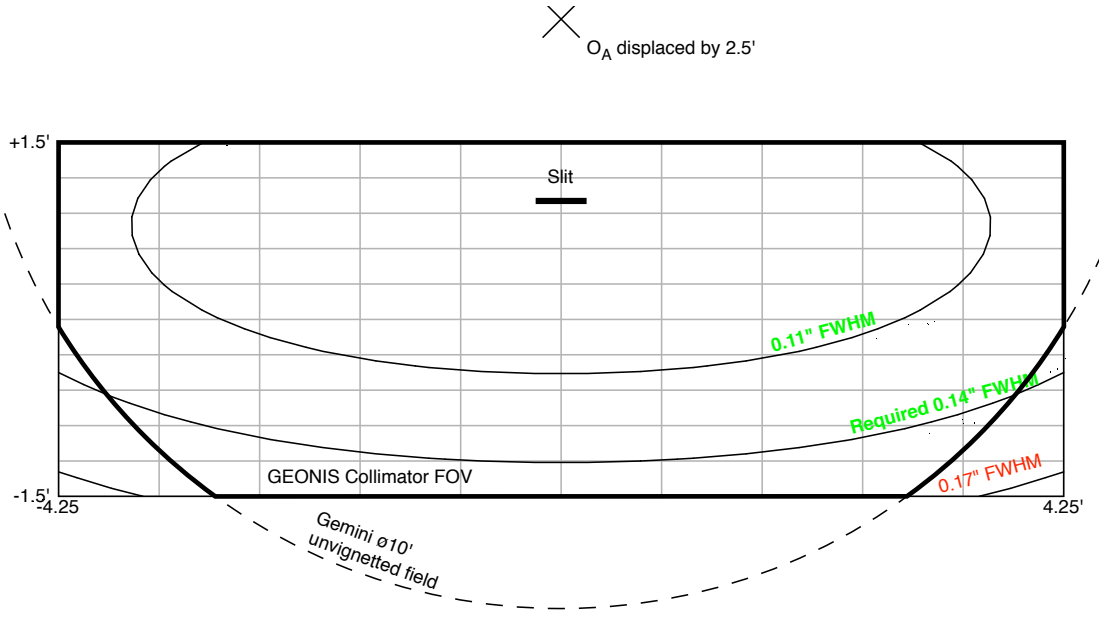


Figure 18: Contour map of delivered image quality from the collimator and telescope expressed in FWHM with the telescope fields of view overlayed. The collimator has a 8.5′ by 3.5′ field of view, although part of the field is vignetted (thin dash line). The telescope optical axis (O_A) is displaced from the center of the instrument's field of view in order to clear the collimated beam. The union of the unvignetted telescope field and the collimator field is represented with a thick line. The location of the short spectroscopic slit is shown for reference. Over most of the field, image quality meets or exceeds the 0.14″ FWHM requirement. At the far edges and corners, the delivered image quality softens to 0.17″ FWHM.

The compound field of views and image quality of the designed collimator are

shown in Figure 18 above. The figure indicates the fields of view of the designed collimator, as well as contours of delivered image quality. The formal requirement for the collimator and telescope is to achieve 0.14″ FWHM images, which the baselined GEONIS collimator does over most of the field.

Optomechanical and flexure design: Based on initial calculations, we believe that a 25-mm thick substrate, with proper supports, should allow us to maintain collimator figure to the required level.

The collimator serves as the main flexure compensation element for GEONIS. Based on experiences with the Echellette Spectrograph and Imager (ESI; Keck Observatory) we have an advanced design for the collimator actuators as shown in a figure from Radovan et al. (1998). The actuator is a lead-screw system run by a motor with a 100:1 gear box reduction. A precision full-ball type actuator is used (THK "Model KR"). Precision Renishaw read heads with 0.1 μm precision determine the tip/tilt of the mirror. The system is run through a Galil motor controller. This actuator system has been running reliably for many years at Keck observatory, and allows the collimator to tip/tilt within 4 arcsecond and focus over a 50-mm range.

Next Steps: During conceptual design we will continue to develop the optical and optomechanical models.

D.7.6 Spectrograph/Imager layout

The spectrographs have numerous science requirements: they must operate in their wavelength range, achieve the required spectral resolution, throughput, and slit length. For the exoplanet case the two channels must deliver precise spectrophotometry.

The spectrographs accept the 117-mm-diameter collimator exit pupil, disperse it, and then send the beam to the two separate cameras. The layout of the optical and infrared spectrographs and imagers are similar, and both are described together. When we proposed GEONIS, we assumed that we could design a grism echelette spectrograph with a layout similar to Subaru FOCAS. Early on in the feasibility process, we realized that grisms are not efficient at the high orders required to achieve the resolutions of interest (see §D.14, and note that we highlighted this as a risk item in the proposal). Furthermore, after we changed the collimation strategy to a reflective collimator we realized that the instrument must fold back on itself, so that traditional ruled gratings become attractive. Here we describe the current layout.

The gratings were selected as follows. Given the desired resolution and pixel scales, we identified the gratings that will achieve the scientific requirements. In the optical, we are baselining a 250 groove/mm grating operating in orders 7-12 blazed to a wavelength of 5.2 μm, while in the infrared the grating we settled on a 133 groove/mm grating operating in orders 6 - 11 blazed to a wavelength of 9.3 μm. Based on the detector sizes, we found that the cameras must operate at faster than f/2.2 in order to put the entire format onto the detector. Based on the predicted spectral format, it should be possible to extend the spectrograph to operate down to 370 without; however, we baseline a camera that operates down to 400 nm.

With the gratings selected, we developed a cross-dispersing strategy for both channels.

Cross dispersion in the optical is always challenging. Because we are covering a broad wavelength range, we cannot cross-disperse with diffractive elements (gratings, grisms, or vph grisms). Thus we must use a prism. There are a handful of available materials in the size necessary. The go to material is fused silica, but we also considered S-BSL7Y, PBM2Y, S-LAM2, and S-LAH53; all of which are available in the required diameters (though some materials would require bonding multiple blanks). The dispersing power of these materials varies by a factor of 4. For cost and blank procurement risk reasons, we settled on PBM2Y for our baselined prism material. PBM2Y has more dispersing power than fused silica, but it is not the most dispersing material available, so there may be further optimizations in this area for the future.

Cross dispersion in the near infrared is well studied and is often accomplished via a mixture of fused silica and ZnSe. These two materials happen to balance dispersion well across the infrared. For GEONIS, we found that we could achieve our cross-dispersion goals with ZnSe only.

With the gratings and cross dispersers set, the goal was to place the prisms, grating, and camera in locations that fold nicely into the spectrograph, maximize geometric throughput, keep the large elements fixed between observing modes, ensure

there is little anamorphic magnification, and minimize angles of incidence onto the prisms. The potential parameter space is vast; nevertheless, we produced a set of layouts that passes the feasibility requirements, even though more design work is needed.

Given that each spectrograph can operate in one of three modes, a significant amount of work was put into system packaging. Our goal was to ensure that as the various modes are changed, the smallest number of elements move, and in particular the large cameras stay fixed in space.

The layouts are shown in Figure 19. The echelle modes require three prism passes to achieve the necessary cross dispersion, with one large prism used in double pass. The low-resolution mode operates without the echelle grating, but with a mirror used in its place. Imaging mode is achieved with a large mirror placed in front of the collimator's exit pupil.

Spectroscopic Formats: The spectroscopic formats of the optical spectrograph are shown in Figure 20 and the formats of the infrared spectrograph are shown in Figure 21. In both figures, the echellette spectral format is displayed on left, while the lowres format is shown at right.

For both echelette formats, one notes the precession of spectra across the various orders. Blue wavelengths correspond to higher orders (the blaze peak scales as $\frac{\lambda_{blaze}}{order}$) and wavelengths within the order increase from right to left. The curved rectangles are sized for a $20''$ slit; note that we adopted a conservative slit length to allow for precise sky subtraction.

For the both lowres formats, the cross-dispersing prisms are the only dispersive elements used. The primary science motivation for lowres is the exoplanet atmosphere science case. The resolution requirements for exoplanets is only about $R \sim 50$, and thus this mode satisfies its main science requirements.

We also explored the possibility of replacing the lowres mirror with a grating (see panel (c) in Figure 19) operating at first order. In this mode the spectrograph would be able to double the spectral resolution, at the expense of some loss in wavelength range. We will study the resolution/wavelength range trade during the GEONIS conceptual phase.

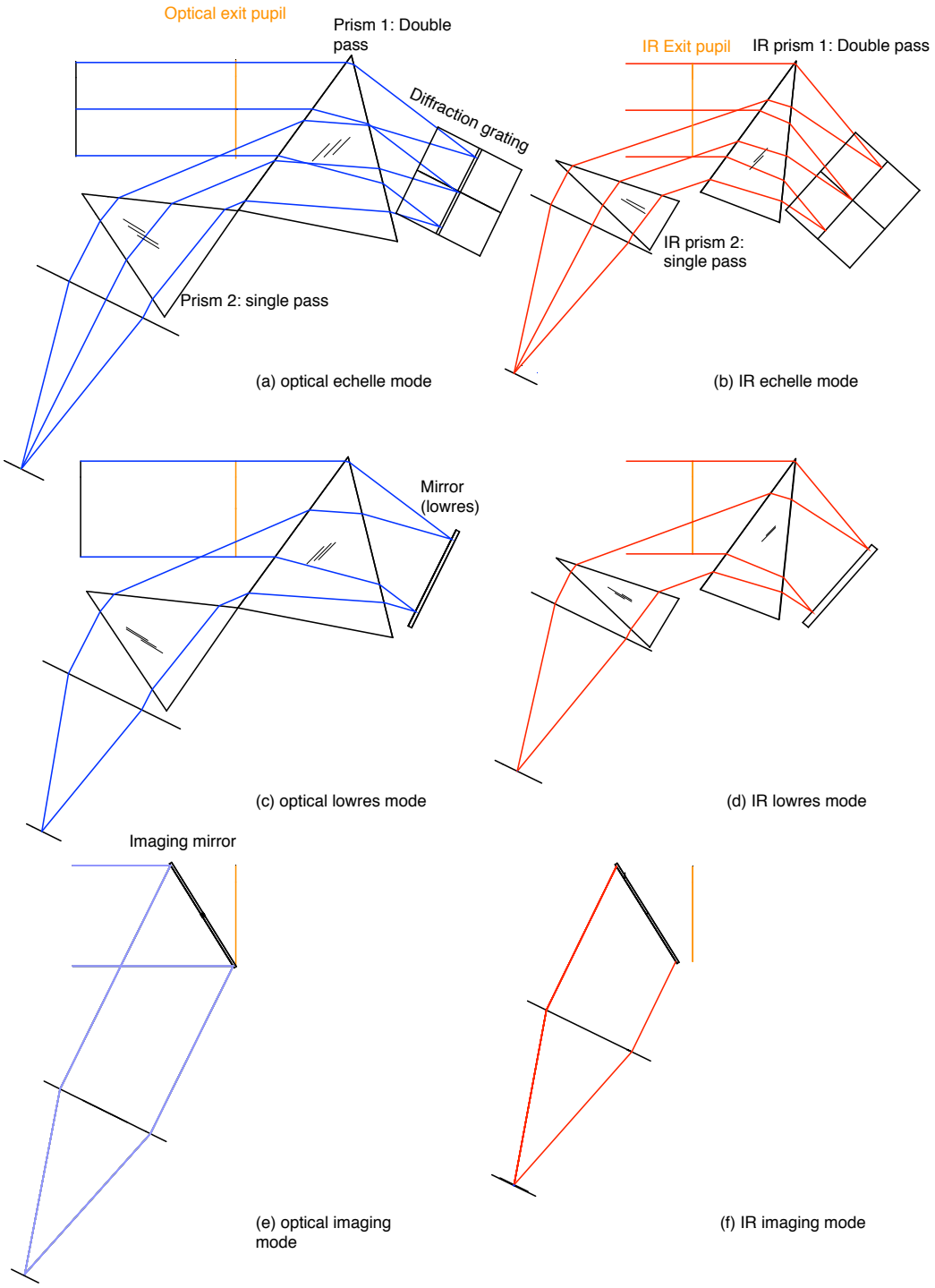


Figure 19: Optical and NIR layouts of the six different instrument operating modes. Optical modes are drawn on the left side; infrared modes are drawn on the right side. Each spectrograph channel can operate in one of three modes independently: echelette, low resolution ("lowres"), or imaging. These mode switches are accomplished by moving elements in the beam path.

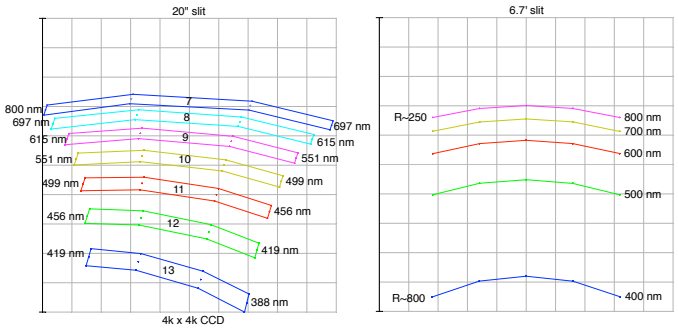


Figure 20: Optical spectral formats in the echelette (left) and lowres (right) modes. These formats correspond to Figure 19 panels (a) and (c). Left: shows the echellette spectral format for orders 7-13 (order numbers indicated on spectrum). The format is defined by the slit width, and the half-power points. Note the spectra extend past the half power points to the edge of the detector. The curved rectangles indicate the slit length of 13.7″ though the final slit length is not fully determined. Note that at order 13 the spectrograph works down to below the limit of GEONIS. It is not clear if we should block this light (to reduce scattered light) or extend the camera performance down to 388 nm. Right: shows lines of constant wavelength in the low-resolution mode. The low resolution mode has a 6.7′ slit length and spectral resolution that varies from 250 to 800 (with a 1-arcsecond slit). In the text we describe how to double this resolution.

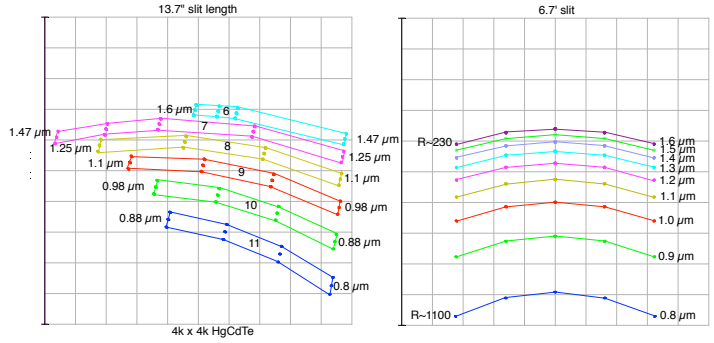


Figure 21: Infrared spectral formats in the echelette (left) and lowres (right) modes. These formats correspond to Figure 19 panels (b) and (d). Left: shows the echellette spectral format for orders 6-11 (order numbers indicated on spectrum) at the half power points. Note that we cutoff about half of order 6. The curved rectangles indicate the slit length of 13.7″. Right: shows lines of constant wavelength in the low-resolution mode. The low resolution mode has a 6.7′ slit length and spectral resolution that varies from 230 to 1100 (with a 1-arcsecond slit).

Spectral Resolution: The average spectral resolution in the echolette mode is listed in Table10 below.

Table 10: Spectral resolution with a one arcsecond slit for each order in the two spectrograph channels in echelette mode. It is possible to scale this to any slit width by dividing the following numbers by the slit width. So for a $0.75''$ slit the delivered spectral resolution is $\sim 5600 = \frac{4200}{0.75}$.

Order	Optical	Near infrared
Typical	4230	4200
13	388–419 nm: 4328–4464	
12	419–456 nm: 4160–4406	
11	456–499 nm: 4153–4422	800–880 nm: 4000–4400
10	499–551 nm: 4145–4442	880–980 nm: 3974–4425
9	551–615 nm: 4136-4465	980–1100 nm: 3957–4442
8	615–697 nm: 4124-4494	1100–1250 nm: 3931–4468
7	697–800 nm: 4109–4532	1250–1470 nm: 3860–4540
6		1470 - 1600 nm:

Exoplanetology and Pupil wander issues The exoplanet atmosphere science case requires high measurement precision. In other words, ignoring varying atmospheric conditions, the ideal version of GEONIS would deliver the same measurement for a given source within the limits of shot noise. Our formal specification from the science team is 200 ppm (§2).

To understand how pupil wander affects the the precision of our instrument, consider Figure 22. Here we show a measurement taken with the instrument at some point in time. Either due to instrument flexure, and due to ADC pistoning, the telescope pupil is displaced. This displacement changes the optical path length through the instrument. GEONIS is not homogeneous, and these optical path changes will affect the wavefront sent to the camera, changing the resulting point spread function, and impacting photometric precision.

We simulated the effect of pupil wander on the precision of the instrument to demonstrate the feasibility of achieving our goal with about one meter of optical path through glass. To perform this simulation, we added extra glass (RMS of about ± 0.005 mm based on reasonable material homogeneity and polishing specifications and our total path length to the surface of a large prism. We then raytraced two perfect 117 mm pupil through this large prism, separated by about 4 mm (a bit larger than the expected amount of pupil wander). The two beams were then imaged with a perfect camera, and the RMS spot radii of both beams was recorded.

To estimate how the RMS spot radius change impacts the precision of the delivered signal, we subtracted both radii from one another and used the residual radius as an estimate of increased spot size. The impact of material homogeneity to the delivered

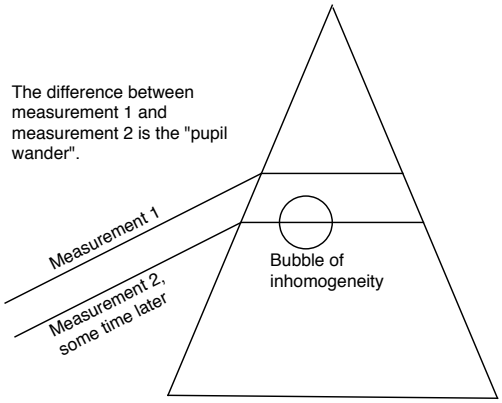


Figure 22: Cartoon diagram illustrating how pupil wander affects optical path length through the system. As the path length changes, the beam is exposed to a variety of imperfections within the prism, and the outgoing signal from the beam is affected. These types of issues have a direct impact on the performance of GEONIS for exoplanet atmospheres.

signal is then just the ratio of the two offset spot areas. We used zemax to simulate 150 Monte Carlo realizations and demonstrated that under reasonable assumptions about the distribution of slope error, the radius of a spot does not change by more than 0.7 μm as the beam is displaced during the course of an observation.

In Figure 23 we plot the estimated fractional signal impact as a function of change in radius. A vertical line is shown at our current estimate of $\Delta radius$ from the aforementioned Monte Carlo simulations (0.7 μm). A horizontal line indicates our precision goal of 200 ppm (§2). The estimated impact is 60 ppm.

If more spectrophotometric precision is needed, or we find that we made incorrect assumptions in our simulations, there are other ways to improve the precision of GEONIS. The first approach is to lock the ADC to a single fixed position during the course of exoplanet observations. While in a fixed position, there is no component of pupil wander from ADC (the leading contributor to wander). The second approach is to baffle down on the collimator exit pupil, which enforces a common optical path; however, this approach loses light.

Our goal during this phase is to demonstrate feasibility that we can achieve the required (tight) specifications through our large amount of glass. Never the less, more work will be performed on exoplanet precision in future phases.

Mechatronics: There are a number of stages required to actuate the systems. We have baselined systems that are already working reliably at Keck observatory. The linear stages that move the prisms or mirrors into or out of the beam are derived from similar stages used in the ESI spectrograph (Sheinis et al., 2002) for the past decade. The rotary stage that selects between echelette and lowres modes are derived from the MOSFIRE spectrograph (McLean et al., 2012). A table of observing modes and

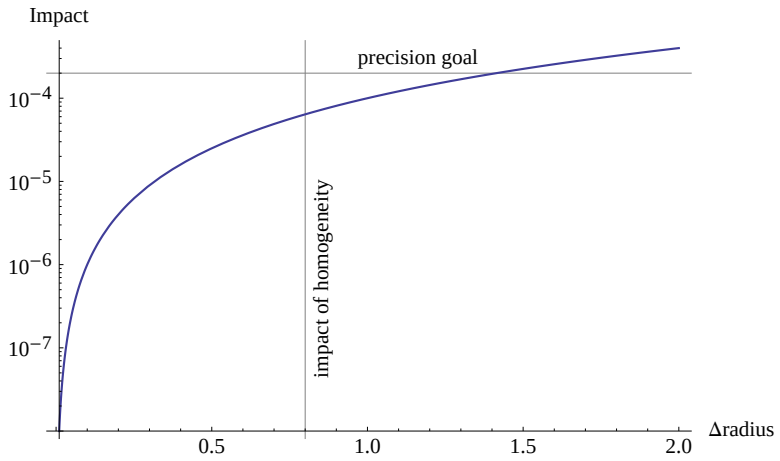


Figure 23: Estimated impact on photometric precision caused by pupil wander. Here we plot the impact of small changes in spot radius to photometric precision. Based on Monte-Carlo simulations of pupil wander on prisms with inhomogeneous substrates, we estimate that typical radius change to be 0.7 μm. The effect of pupil wander from peak-to-valley is on order of 60 ppm.

their optical configuration is shown in Table 11 below.

Table 11: Observing mode configuration index.

Element	Echelette	Lowres	Imaging
Prism 2	In	In	Out
Grating turret	Grating	Mirror	Don't care
Mirror	Out	Out	In

In order to change between the various observing modes, the following motion devices are needed:

- 6 motors: visible+ir mirrors, turrets, and prism.
- 6 actuators
- 12 limit switches
- 6 encoders

all of the aforementioned devices can be purchased off the shelf from companies we have worked with in the past such as Galil and Renishaw.

Conceptual phase: During the upcoming conceptual design phase, we will further develop requirements, budgets, and study pupil wander issues.

D.7.7 Camera Lens Mounting

The optical system in GEONIS consists of lenses manufactured from various materials with a range of hardness, CTE, etc. These lenses will be mounted and aligned using a series of lens mount flexure assemblies that support the outer edge of the lens to achieve the required optical performance. The lens mount assembly design is required to provide stability at varying gravity vectors and maintain acceptable stress levels at the interface to the lenses during handling or during the transition from laboratory to shipping and operations (survived from -33° C to 71° C see Gemini ICD-G0013). The lenses are separated into two major assemblies: optical camera assembly and infrared camera assembly. Both assemblies include the detector.

To achieve these requirements, while minimizing development risk, all optics will be mounted using a ring-flexure system that was devised for the Keck/MOSFIRE spectrograph (which had the same survivability specification). This system allowed for all optics to be aligned to a common optical and mechanical access to better than 25μ m. The expected tolerances of the camera design (based on $f/\#$ considerations) are similar.

The optics use fragile materials such as CaF2, BaF2, ZnSe, and a variety of Ohara i-line glasses, which must function over a wide range of temperatures. All lenses are mounted with multiple thermally-matched metal pads epoxied to the lens girdles. The pads are connected via flexures to metal lens cells, which are stacked and bolted together to form into the collimator and the camera barrels, respectively. The flexure mount system allows our fragile lenses to be held rigidly to the lens cells without accumulating thermal or mechanical stresses.

A single cell is shown in Figure 24. The lens is held in place with a series of flexure assemblies that absorb differential stresses between the barrel. Each lens is connected to the flexure via a bonded mount pad. Each optical material requires a corresponding thermally-matched material for its mount pad.

The lens cells are assembled into barrels using a "stack of poker chips" method. This approach is shown in Figure 25. Here each cell is assembled with an alternating stack of lens cell (described above) and then a baffle/shim, which allows us to fine tune the inter-lens spacing based on the final as built dimensions and optical coefficients of the materials.

We expect that the detailed assembly procedures comprise several hundred steps per lens cell. The total number of individual steps required to assemble a single camera will run into the many thousands. Each key series of steps is signed off by the technician. Alignment is performed in a clean room with a coordinate measuring machine or Opticentric with expert optomechanical technicians as shown in Figure 26.

Current Status/Risks: There are many approaches to bonding lenses into cells to consider. The advantage of the aforementioned bonded flexure procedure is that there is no long-term maintenance or realignment that is required or wanted. Furthermore, the cost and risk of this approach can be estimated from analogy to MOSFIRE.

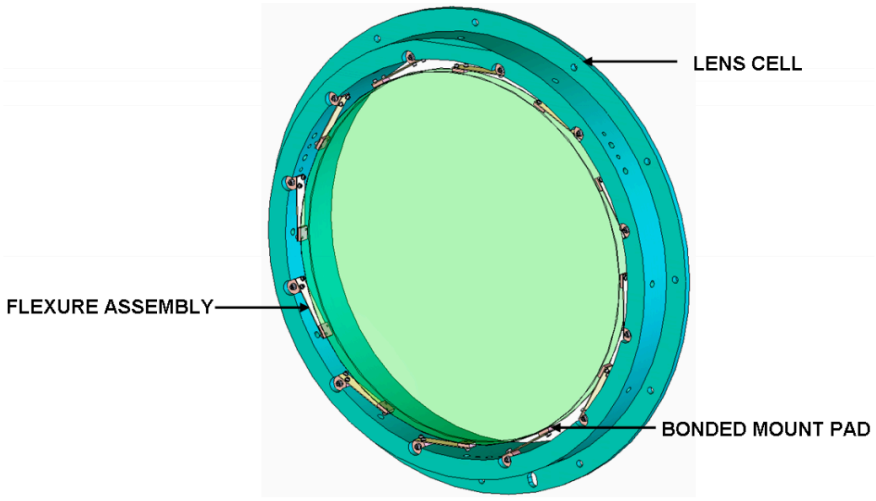


Figure 24: Solid model of a single lens cell assembly. The lens cell is a metal tube that is connected to the lens via a flexure assembly and bonded mount pad. The flexure assembly absorbs any mechanical stress differences between the lens barrel and the lens due to temperature changes. The mount pad is a small block with a radius cut to match the lens girdle radius. This block is bonded to the lens with adhesive.

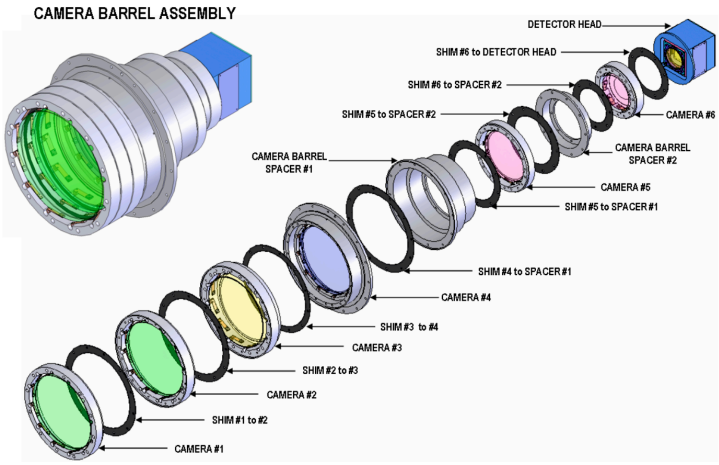


Figure 25: Solid model of a lens barrel assembly. A lens barrel is assembled in a "stack of poker chips" configuration. Each cell is shown and described above (Figure 24). The cells are assembled together with a series of precision flange interfaces. Between each cell is a shim/baffle that controls the inter-lens spacing to the few-micron level.



Figure 26: A picture of two expert technicians bonding a lens into its cell. The required elements for assembly include the clean room, opticentric or coordinate measuring machine (seen as #231 in the picture), and expert machinists and technicians with the expertise to perform a many thousand step procedure.

D.7.8 Optical Camera System

The optical camera system is a lens that refocuses the 117-mm-diameter collimated beam from the collimator. The camera operates at f/2.0 in order to achieve the pixel-scale requirements and covers the wavelength range from 400 nm to 800 nm. It has enough field of view to cover most of the 4k x 4k EMCCD (and it exceeds the collimators full field of view). Based on our systems engineering (§D.6.2) we require the cameras to deliver 8.6 μm RMS images (0.17″ FWHM). This image quality requirement, in order to take advantage of Gemini's excellent delivered image quality, requires GEONIS cameras that deliver twice the image quality of similar cameras at Keck Observatory. Furthermore, GEONIS is mass constrained, and thus we eschew oil-coupling (and their attendant bladders and seals) to keep the camera mass down. The camera is shown in Figure 27.

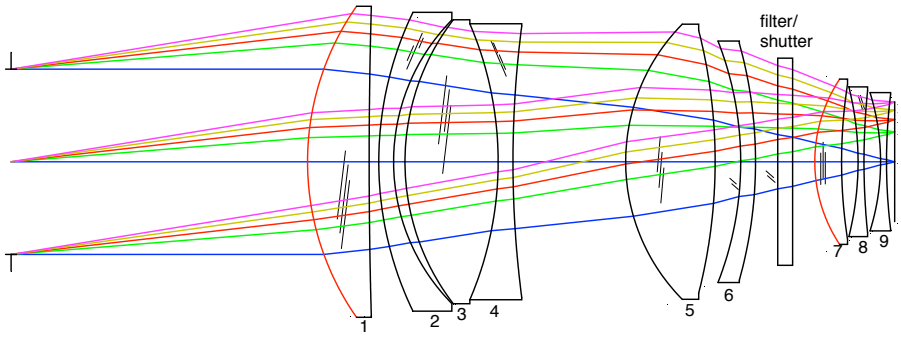


Figure 27: Ray traces for the f/2.0 optical camera system. The ray trace shows the optical path through the camera. Image quality is excellent in this conceptual design with spot FWHM of 0.17". To keep mass low, we use two aspheric elements (marked in red).

Given the strict image-quality and mass requirements, we produced a conceptual camera design to demonstrate design feasibility. The camera concept requires large calcium fluoride elements for positive power, while color correction is offloaded to Ohara i-line glasses. All of the material required for this concept is available in the thickness and diameter required. To keep the mass low, we choose to use aspheres. In the baselined design, there are two aspheric elements on calcium fluoride. The baselined design meets the requisite image quality and also achieves a fraction of an arcsecond of total lateral color. RMS radii are shown in Figure 28.

The camera also requires several moving parts. A filter has been designed in the converging beam of the camera with a fused silica substrate. A filter slide or wheel is required, along with required motors, encoders, and microswitches. Flanking the filter wheel is a shutter, which we intend to purchase from an outside vendor. Finally, the detector itself will require a precise focus stage. In summary:

- 3 motors: shutter, filter, and focus.

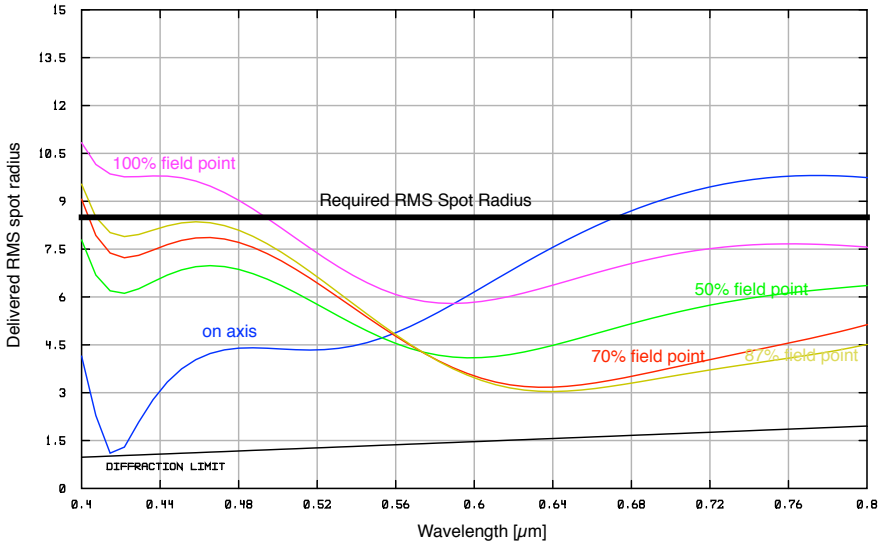


Figure 28: RMS spot radii as a function of wavelength. The budgeted RMS spot radius requirement is met over nearly the entire field.

- 3 actuators
- 12 limit switches
- 3 encoders (these may not be useful or wanted, but we have baselined encoders in).

Current Status/Risk Assessment: The conceptual optical camera (Figure 27) delivers 0.17" FWHM spots over the full field and wavelength range. Furthermore, the camera uses materials available in the sizes required. In short, we have addressed all the issues that were highlighted in our proposal.

Despite the fact that we have a concept that delivers excellent images, the camera system has increased in risk. Our image-quality budget requires cameras that deliver outstanding image quality. Given Gemini's mass constraints, we choose to trade mass by adding two aspheres to the design. During the next phase we will perform a mass versus asphere tradeoff study. Aspheres on calcium fluoride have been demonstrated on (at least) Magellan.

Steps during the conceptual phase: The camera is a critical system, and the baselined design provides an excellent starting point. During the conceptual phase we must develop ghost and scattered light requirements, and ensure the baselined camera meets those requirements. Because camera has a number of long-lead items, its design should be advanced to pre construction levels, so that the long-lead items will not impact final delivery schedule.

The science team is pushing to extend GEONIS to work at wavelengths below 400 nm. Thus, during the conceptual phase we may choose to extend performance down to about 370 nm (to include coverage of the [O II] emission line).

D.7.9 Near-Infrared Camera System

The near-infrared camera system is analogous to the optical camera system (see Figure 29). However, because the NICS is addressing a larger detector, we have designed the system to operate at f/2.2 with respect to the 117-mm-diameter-beam. There are several major differences due to thermal-background considerations. First, the NIR system camera must allow for stray-light rejection. The infrared camera is designed with materials of low emissivity to $\lambda 2.5\ \mu m$ so that the camera lenses themselves do not increase thermal background.

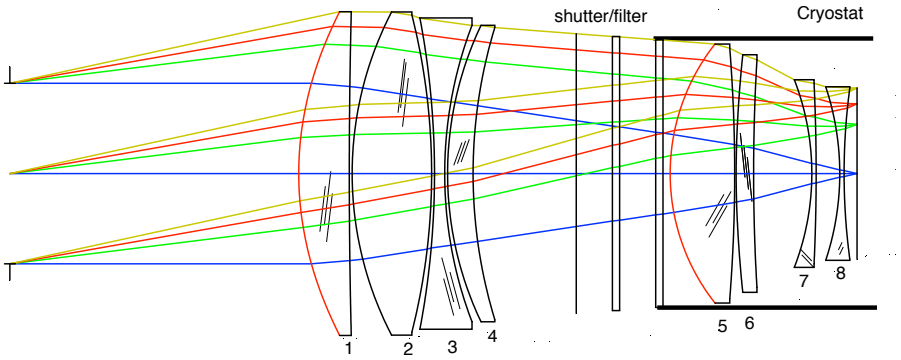


Figure 29: Ray traces for the f/2.2 infrared camera system. The ray trace shows the optical path through the camera. Image quality is good in this conceptual design, with FWHM of 0.17" over about half the field. In future phases this camera design needs to be improved. To keep mass low, we use two aspheric elements (marked in red). The cryostat extends outwards from the detector to block stray light. An out-of-band thermal infrared blocking filter with 10^6 rejection is used as the cryostat window.

In the past few months, we have discovered that there are out-of-band rejection filters that reject thermal infrared at the 10^6 level. Thus, we have changed the near-infrared camera design to be shorter, stouter, and without the large "cold snout" that was advocated at the proposal phase.

The baselined near-infrared camera delivers $0.17''$ ($9.5\ \mu m$ RMS) images over about half the field and wavelengths. Formally, the camera does not meet its budgeted requirements; however, it is close enough to demonstrate feasibility, a useful design for cost-estimating, and sufficient for mass estimates. RMS image sizes in microns are shown in Figure 30.

Next Steps: The near-infrared camera system has been demonstrated to be feasible, at least at the level needed at this phase of the GEONIS project. Unlike the optical camera system, the near-infrared system requires more design work to achieve

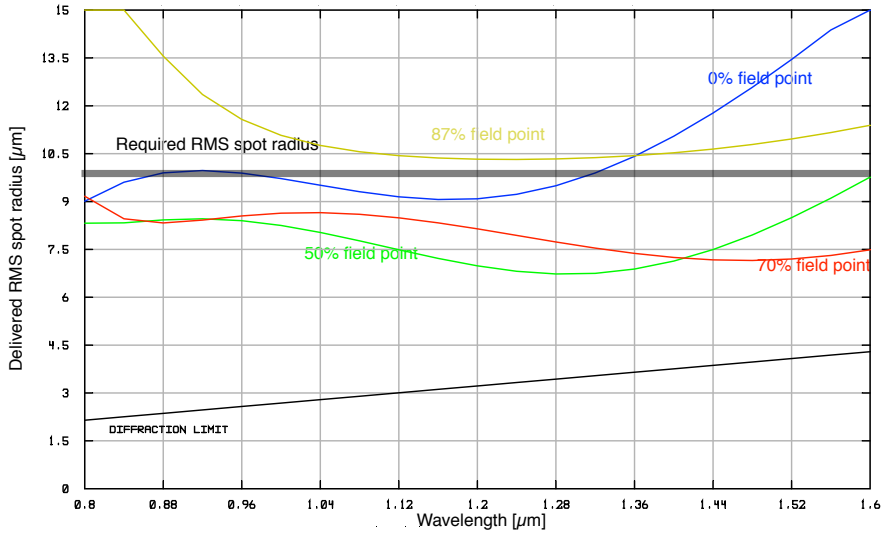


Figure 30: RMS spot radii as a function of wavelength. The budgeted RMS spot radius requirement is met over most but not all field and wavelengths.

the required image quality. After the design is converged, the following work must be performed: First, stray-light requirements must be derived. Second, a conceptual stray light analysis must be performed to understand where the cryogenic system begins. Finally, there is a potential issue with the development risk associated with Hawaii 4RGs and GEONIS may need to descope to a smaller detector. The detector size will affect camera field of view, focal ratio, and cost.

D.7.10 Optical / Near Infrared Detector System

The science requirements passed down to the detectors are as follows: the detectors must be able to deliver $> 90\%$ duty cycle at one-minute exposure time, they must have high quantum efficiency, and must enable the software-tunable spectral resolution. Aside from the science requirement, the optics design requirements flowed from detector selection.

One area where the team is most excited is the real-time classification of transients. Here, we would like to make sure we operate detectors at high readout speed, but with low read noise. Thus, we are baselining devices with as many amplifiers as possible, and readout electronics with the highest levels of performance.

The detector system comprises of a detector, detector electronics, dewar, and tip/tilt/shift system for focus and flexure compensation. The optical detector is baselined as an e2v CCD282 device with 13 μm pixels, while the near-infrared detector is baselined as a Hawaii 4RG with 15 μm pixels.

Current Status/Risk Assessment: The optical detector and readout electronics have some risk as they are a development program (Gach et al., 2014). Given the

typical lead time of a CCD, the GEONIS project is probably several years away from purchasing the optical detector. Thus, we are in a wait and see mode. Two vendors exist for providing the EMCCD readout electronics (one in Canada, one in France).

If the EMCCD is not ready by the time GEONIS moves forward, we can simply purchase the corresponding non-electron-multiplying 4k x 4k E2V device. There are two such devices available, and both cost less than the EMCCDs.

EMCCDs generate more heat because they are continuously clocked at MHz levels. We have now been running several EMCCDs in the laboratory and know how to remove this waste heat without destabilizing the device.

The H4RG and its electronics have development risk. Though it is possible to tile 4 H2RGs, the cost of GEONIS increases by several hundred thousand USD. The other option is to descope to either 2 H2RGs or 1 H2RG. The final selection depends on trades between budget and science capabilities. We have not predicted how such a large loss in detector area would impact the science productivity of GEONIS, and would urge a mitigation plan to be developed during the next phase.

Next Steps: For the conceptual design phase, we will continue to refine detector requirements, including AR coatings.

D.7.11 Open-Loop Flexure Compensation System

All Cassegrain-style mounted instruments exhibit flexure. A variety of science requirements are passed to the flexure compensation system. First, the flexure compensation system must be able to correct up to ten pixels of flexure. Second, the RMS residuals of such flexure must be at the 0.1 pixel level. These requirements are imposed for scientific throughput reasons, as well as for exoatmosphere precision.

Our desire for open-loop flexure has been driven by successes and failures in flexure at Keck observatory. Both ESI and MOSFIRE are large (2.5 to 3 ton mass) Cassegrain-style mounted spectrographs. Both spectrographs exhibit residual flexure of about 0.1 pixel RMS across the entire sky.

Our strategy is to correct flexure at the collimator, where tip/tilts at the collimator shift the entire image on the detector. Our RMS goal is 0.1 pixel, and so the collimator must have at least 3× the resolution of our RMS goal. Here we baseline 10× to ensure good margin. A 0.1 pixel rotation on our cameras corresponds to tip-tilts at the collimator mirror of $0.6''$. Given spacings of 400 mm between mirror actuation points we need steps of 2.3 μm to achieve the articulation resolution requirement of 0.1 pixel. The collimator actuation system must keep hysterisis and slip far below 2.3 μm, and this specification drives our requirement for high-precision 0.1 μm Renishaw read heads and THK KR actuators. The open-loop actuation system will achieve the required levels of actuation with off-the-shelf components.

Demonstrating the open-loop flexure compensation system will require a ISS simulator that can tip, tilt, and rotate. During integration phase we will move GEONIS to thousands of positions and measure flexure. For Keck instruments we build test stands that mimic the telescope mount points; for GEONIS we have budgeted for

such a stand.

Exoplanetology Impact: The flexure compensation system is designed to correct less than a few pixels of flexure (we will aim for three pixels). The nature of a FCS is that it introduces pupil wander, and pupil wander impacts exoplanetology precision (§D.7.6). The focal ratio of the collimator to the cameras is smaller than 10x, and thus three 45 μm pixel maps to a pupil wander of about 0.45 mm at the collimator exit pupil. Compared to the the ADC (§D.7.2), 0.45 mm of pupil wander is significantly less than that predicted by the ADC system.

Mechatronics: The design, cost estimation, and mass estimate of our flexure compensation system is derived from the work of Radovan et al. (1998). The collimator requires three 120°-separated actuator systems. Each actuator system is comprised of a motor, 100:1 reduction gear box, linear actuator, two switches, and encoders. The total number of elements needed is:

- 3 × motor
- 3 × 100:1 reduction gear box
- 3 × linear actuators
- 6 × limit switches
- 3 × encoders

These items will all be purchased off the shelf from companies like Galil, THK, and Renishaw.

Current Status & Risk: Low implementation risk, but medium risk the flexure compensation strategy cannot remove flexure in both channels at the same time.

Conceptual Design Phase: Our first deliverable is requirements development for the FCS. Based on these requirements we will perform a cost estimate for measuring and implementing the open-loop flexure compensation system via analogy.

D.7.12 Electronic and Interfaces Design

There are no specific science requirements passed down to the electronics and interface systems. There is a high-level scientific requirement to ensure that GEONIS has high total system throughput, and so these systems must be robust and invisible to the observer.

GEONIS' electronics and interface design is based on the design heritage of recent WMKO instruments including OSIRIS, NIRSPEC, NIRC2, MOSFIRE, and ESI. Most of the electronics consist of commercial off the shelf equipment with the required interconnections. No custom equipment is anticipated except for a few printed circuit boards used to simplify various high pin count interconnections and cabling. We consider GEONIS' electronics to be low risk. Based on similar instruments, we anticipate that GEONIS will require two racks of equipment and plumbing.

In the previous sections, we described all the relevant axes of control (e.g., the collimator has three axes for tip/tilt/focus). Summing the aforementioned axes of control, GEONIS needs the following: 13 axes of motion control including encoders, limit switches, and the like.

To ensure that the waste heat generated by our electronics is disposed of, GEONIS employees two Electronics Cabinet Cooling Systems (EECS) heat-exchange units, one in each of the electronics racks inside the dual cabinet mounted on the side of the space frame. In order that image quality is not disturbed by air convection, it is necessary to limit the heat radiated by the electronics. As GEONIS will be exposed to the elements, the electronics cabinet is a NEMA4 unit, sealed against dust and rain. In order to limit the total radiated heat, and also prevent catastrophic heat buildup inside the cabinet, we utilize the ECCS units to remove internally generated heat and dump it to the chilled facility glycol.

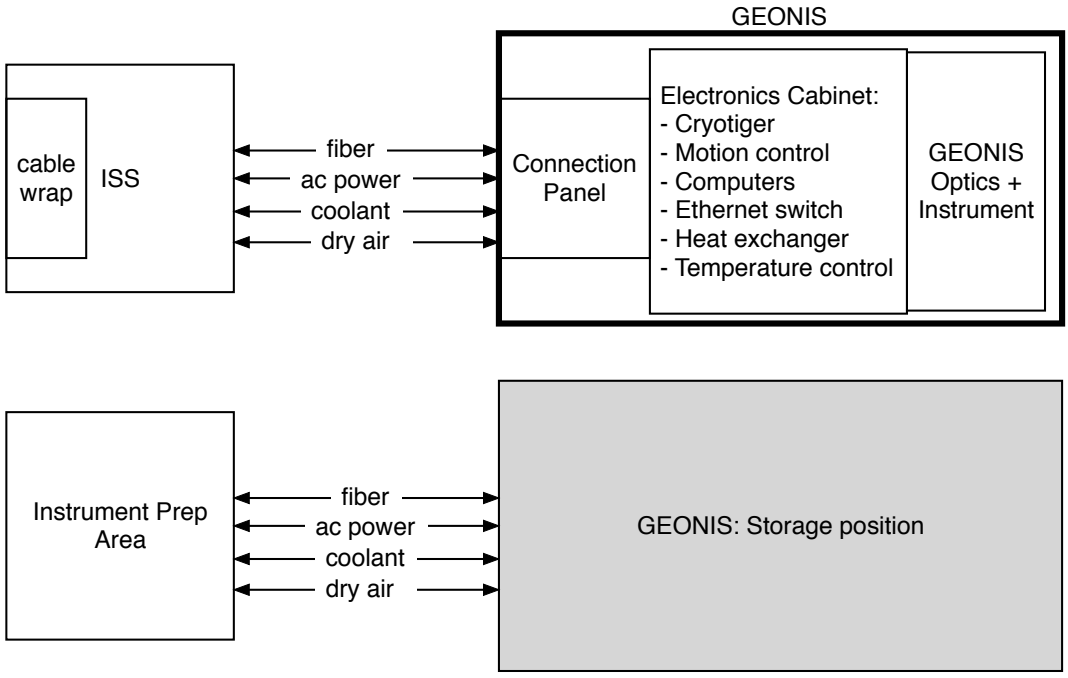


Figure 31: GEONIS electronic interfaces. Interfaces are made as per specified ICDs at a single interconnect panel on the side of the instrument. From the interconnect, a variety of interfaces are sent to the NEMA enclosure. Within the NEMA enclosure is a EECS heat exchange system, that takes waste heat generated by the electronics.

The following electronics boards, and equipment are needed for the baselined instrument. These interfaces are shown in the schematic shown in Figure 31.

1. Optical detector – E2V 4k x 4k CCD with frame transfer region. An electron multiplication register device is baselined.
2. 2× shutter – Bonn shutter, the standard 200 × 200 mm product line.
3. 2× Bonn shutter controller – High precision controller for blade movement. Interfaces to power and RS232.
4. IR detector – Hawaii 4RG or equivalent.
5. Teledyne sidecar server – Reads Hawaii 4RG.
6. Galil control system
   (a) FCS
   (b) Slit exchange
   (c) ADC
   (d) Collimator
   (e) Linear
   (f) Detector focus
7. Paluzzi network power switches.
8. Telemetry devices: temperature, humidity, and vibration.

D.7.13 Control Software

GEONIS will be a fourth generation Gemini instrument and therefore will inherit a wealth of software infrastructure, and will benefit from previous experiences on a variety of instruments for setting requirements. The Caltech Optical Observatories (COO) has experience with four generations of Keck instruments, and we intend to leverage our previous experience

GEONIS instrument software will follow the requisite Gemini ICDs requires three software components: the Components Controller (CC), Detector Controller (DC), and Instrument Sequencer (IS). Here we discuss the key high-level requirements for the GEONIS instrument control software.

- GEONIS software will conform to all ICDs specified by Gemini.
- GEONIS will provide command-line engineering interfaces for checking out the instrument.
- All GEONIS mechanisms will be controlled through the components controller.
- GEONIS software will not impact the total system throughput of exposures, signal to noise, or classification by more than a fraction of a percent.
- GEONIS will be responsible for protecting GEONIS hardware. No command issued by the observatory can cause damage to GEONIS. GEONIS will return meaningful errors if the commands are not allowed.
- Detectors
  - GEONIS software will control cool down and warmup rates of detectors to a level that will be specified in the future.
  - GEONIS software will control optical and infrared science detectors and shutters. The observatory will be allowed to configure these devices.
- Acquisition/guiding
  - The observatory will provide software to plate solve the acquisition image and move the requested RA/Dec into the slit within one spectrograph pixel ($0.17''$).
  - The observatory will provide software to guide on the slit-viewing camera images either from spillover light in the slit, or from field objects. To support exoplanet science, the precision of such guiding will be $0.04''$ (0.25 pixel) RMS.
  - The observatory will provide software to guide on non-sidereal targets.
- Real time systems – these require communication with TCS.

  - The GEONIS software will control the ADC. The ADC software will communicate with TCS. When the airmass exceeds the ADC limits, the GEONIS software will issue warnings to the observatory.
  - The GEONIS software will control the slitmask exchanger.
  - The GEONIS software will control the spectrograph setup via high-level commands that are exposed to Gemini (e.g., configure echelette mode). The high level software will coordinate with the devices.
  - GEONIS will report telemetry at a reasonable update rate (a few times per minute).
  - GEONIS flexure control system will update at a reasonable update rate (a few times per minute), or what is necessary to maintain the fraction of a pixel performance requirement.
  - GEONIS flexure control will be represented as a parametrizable function. The parameters will be adjustable, though we expect the parameters will never need to be changed.

- GEONIS control GUIs are the responsibility of Gemini.

- Real Time Classification of science events is a powerful concept and of tremendous value to GEONIS in specific and Gen4#3 in general (§D.5). At this point, given the scope of work, neither Gemini nor GEONIS are responsible for providing the ability to perform real-time classification. Never the less, the software will be designed so that it will not preclude real time classification.

Hardware Platforms: Only the near-infrared science requirement impacts hardware platform requirements. In general, Teledyne's control software runs on a Windows PC host. All other hardware runs well on PCs running Linux, and our preference is to stick to Linux where possible. We will conform to Gemini ICDs here.

High level software design: COO observing software systems are generally client/server programs that communicate to clients via RPC. Our software server layer consists of a generic server module that is configured by a hardware dependent function library to control each GEONIS hardware subsystem though a variety of hardware interfaces (Ethernet, RS-232, etc.). For Keck, a custom-purpose library called Keck Task Library or KTL (pronounced kettle) is used. Such a system would make sense for GEONIS; however, we intend to conform to Gemini standards as required.

GEONIS servers provide keyword control of the servers. Instrument specific keywords are defined in a keyword list. Common practices and standards exist for the development of keyword lists, and the keyword lists for GEONIS would be based on existing keyword lists. An important feature of this architecture is that the GEONIS hardware can be controlled and tested using keywords and keyword scripts once the

servers are complete. This avoids the interdependencies between hardware assembly/test and user interface development, which often lead to development schedule problems.

The following servers would be needed for the baselined instrument. All software communicates via RPC, except where noted:

- Global server – coordinates moves, is the interface point for all commands.
- Optical detector server – configure, start, stop, switch modes (linear, high gain, and photon counting). Coordinates with shutter.
- IR detector server – configure, start, and stop. Coordinates with shutter.
- IR sidecar server – Runs on Windows host and provides wrapper around ASIC. Uses ICE and note IPC for communications.
- Slit viewing camera server – configure, start, and stop.
- Rotary Server – Controls filter wheels using serial commands to Galil.
- Flexure compensation server – starts/stops flexure compensation server; and configures flexure compensation for a given azimuth, elevation, and rotator position based on lookup table.
- Slit exchange server – Selects between slits and imaging mode, communicates using serial commands to Galil, communicates using serial commands to Galil.
- Atmospheric dispersion server – on/off control, airmass control. Is updated several times per minute, communicates using serial commands to Galil.
- Collimator focus and tip/tilt server – Controls collimator's 6 degrees of freedom, communicates using serial commands to Galil.
- Linear Server – Controls mode selection slides, communicates using serial commands to Galil.
- IR focus server – Controls IR camera focus motor, communicates using serial commands to Galil.
- Optical focus server – Controls optical camera focus motor, communicates using serial commands to Galil.
- Power control server – Controls power to various subsystems, communicates using serial commands to Puluzzi.
- Glycol monitoring server – Monitors glycol flow and temperature.

- Temperature control server – Monitors and controls temperature control subsystem, communicates using serial commands to Lakeshore.
- Vibration measurement server – Monitors vibrations

Algorithms and Tools: COO observing software is developed using standard unix-based software (make, vi, and emacs). Java code is often developed in Eclipse software.

D.7.14 Data Reduction Pipeline

GEONIS is designed with the data reduction pipeline in mind. First, we are employing a slit-viewing camera to ensure the object stays fixed relative to the slit edges. Second, we have an ADC which will ensure the trace does not rotate with airmass. Third, we employ fast cameras that will achieve background-limited operations in a matter of minutes, and so operation modes like A-B or precise sky-subtraction methods using splines and the like are enabled.

The GEONIS team has experience writing data reduction pipelines for a variety of instruments (multi object, IFU, imaging, slit spectrographs, etc). Based on our experience, GEONIS spectra can be reduced with tools astronomers are familiar with today.

If EMCCDs are used, then further thought will be required for pipeline development. We note that "Hawaii" detectors with their non-destructive reads and "up the ramp" sampling have a minimal impact on data reduction pipelines as the readout and reduction are partitioned into separate problems.

D.8 Design Orthogonality

The GEONIS review panel asked a series of questions about the cost breakdown of the three operating modes. The rational is that it may be possible to descope the instrument by removing a mode. In this subsection, we show that the design of the various modes is not orthogonal. The lack of orthogonality makes it difficult to decouple the cost of one of the three modes. For the purposes of discussion, if GEONIS had three orthogonal modes then the cost of removing a mode would reduce the cost of GEONIS by $\frac{1}{3}$.

Table 12: GEONIS design orthogonality. The three major GEONIS cost drivers (enormous cameras, wide field of view, and dual-beam operations) are indicated against the three modes of operation.

	Large Camera	Wide field of view $	Two detectors
Echelette	Yes	No	Yes
Long slit	Yes	Yes	Yes
Imaging	No	Yes	Yes

In Table 12 we show that it is not cost effective to drop a single mode of operations. The table shows GEONIS' three main cost drivers (large camera, wide field of view, and dual-detectors) and how each mode of operations relies on these features. To realize the most cost savings, one would have to drop two operational modes. A version of GEONIS with only one mode is different enough that our costing methods would have to be reapplied.

D.9 EMCCDs - Mass, Budget, and Risk Savings

In the optical, instead of a grating-exchange system, GEONIS is baselined with an EMCCD that will achieve background limited operation in seconds. The user selects the spectral resolution of interest when running the data reduction pipeline. Of course, there are trades associated with EMCCDs and their various modes of operation. In this subsection we both review EMCCD operation, and describe how we plan to take advantage of EMCCDs given their limitations.

Conventional wisdom when designing a spectrograph is to achieve the minimum useful spectral resolution. The minimum useful resolution is one where the sky lines are sufficiently unblended, and where the signal per read noise from the science target is at least three. Our proposal is to use EMCCDs to do precision sky subtraction on background-limited, and short, exposures and then stack and rebin the spectra to the resolution of interest.

For GEONIS, precision sky subtraction is one of its workhorse capabilities, thus it is important to consider sky subtraction as part of the system design process (from hardware to software levels). To understand night sky variations, we took several nights of data above Palomar in 2009 and measured the exposure-to-exposure variation of the night sky. We "rediscovered" that the night sky variations can be several percent over just a couple of minutes. Thus, it is valuable for spectrographs to take as short as exposures as possible in order to freeze the night sky (Figure 32).

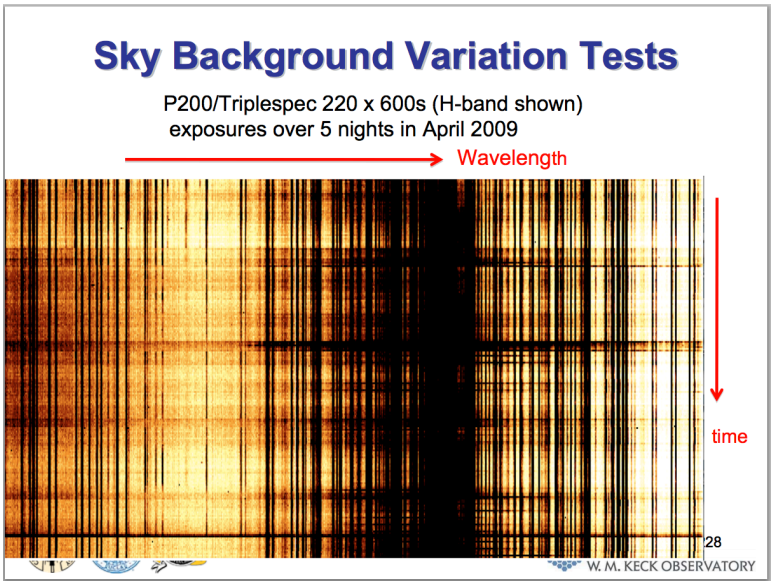


Figure 32: Sky background above Palomar in the infrared as a function of time. Each row represents a reduced spectrum taken over ten minutes above Palomar. Typical variations from exposure-to-exposure are on order of a fraction of percent. The biggest variations are at the several percent level. The point is that by using short exposures it is possible to "freeze" the night sky and perform clean subtraction.

Electron multiplying charge coupled devices (EMCCDs) are well known in astronomy, but perhaps most famous for Lucky Imaging (Law et al., 2009). Yet it is still rare to see EMCCDs used in astronomical spectrograph, although there are some examples (e.g., ULTRASPEC, Dhillon et al., 2007, 2014). While EMCCDs behind spectrographs have myriad advantages for observations, here we focus on their use in observing faint objects efficiently. EMCCDs are conventional frame transfer CCDs but with an extended high-gain register. An example of an e2v CCD282 device (Gach et al., 2014) is shown in Figure 34.

EMCCDs can increase the dynamic range of a spectrograph by about 30×. This allows EMCCDs to probe new scientific territory. To show this increase, we have performed simulations of an EMCCD shown in Figure 33. The simulations express the delivered signal to noise of the device divided signal to noise as expected from pure shot noise. Conventional CCDs (blue) perform poorly for signals less than a few photon per pixel; however, this is made up for in switching over to the EMCCD amplifier (red).

One of the most prominent problems with EMCCDs is they have been limited to a 1k x 1k active area. Recently, E2V has produced CCD282 (Gach et al., 2014) in an 8k x 4k format. Half of the detector is the frame transfer region, so that when an exposure is complete, the charges in the active area are shifted into the frame transfer area and a new exposure can begin. Thus, the duty cycle of operation can be kept near 100%. Finally, the device has 8 amplifiers that each read a 2k x 1k region of the frame transfer area. Each amplifier can do electron multiplication.

EMCCDs can be operated in one of three modes. Classical mode: Just like all CCDs that we know and love, an EMCCD can operate in a classical integrating mode with 20-s readout time, and ∼4 e- read noise. This mode is well understood and will not be discuss further. Analog mode: The CCD operates with an electron multiplying gain of about 100 thus the effective read noise per pixel is now 0.04 e- and the detector can be read out in 0.2 s. The disadvantage of this mode is the excess noise that comes from gain instability (Robbins and Hadwen, 2003). The excess noise limits the usefulness of this mode to very-high-speed transit work. We intend to explore the scientific use of analog mode during feasibility phase, but for this proposal, we do not intend to discuss analog mode further. Photon counting mode: The CCD operates with an electron multiplying gain of about 5,000 yielding an effective read noise per pixel of about 0.009 e-. Like the analog mode, the detector can be read out at 5 Hz. The disadvantage of this mode is two fold: First, the high gain amplifies clock-induced charge (CIC), which is a normal, but orders of magnitude too weak, source of noise in conventional CCDs. The result is that the faintest signals are dominated by CIC noise. Second, as a photon-counting device a pixel may receive more than one photon per frame and this second pixel is lost. The coincident loss limits EMCCDs efficiency at the bright end. In short, EMCCDs in photon counting mode have a sweet spot.

Computing the sweet spot for EMCCD photon-counting mode is based on the traditional SNR equation with some minor modifications (Tulloch & Dhillon, 2011)

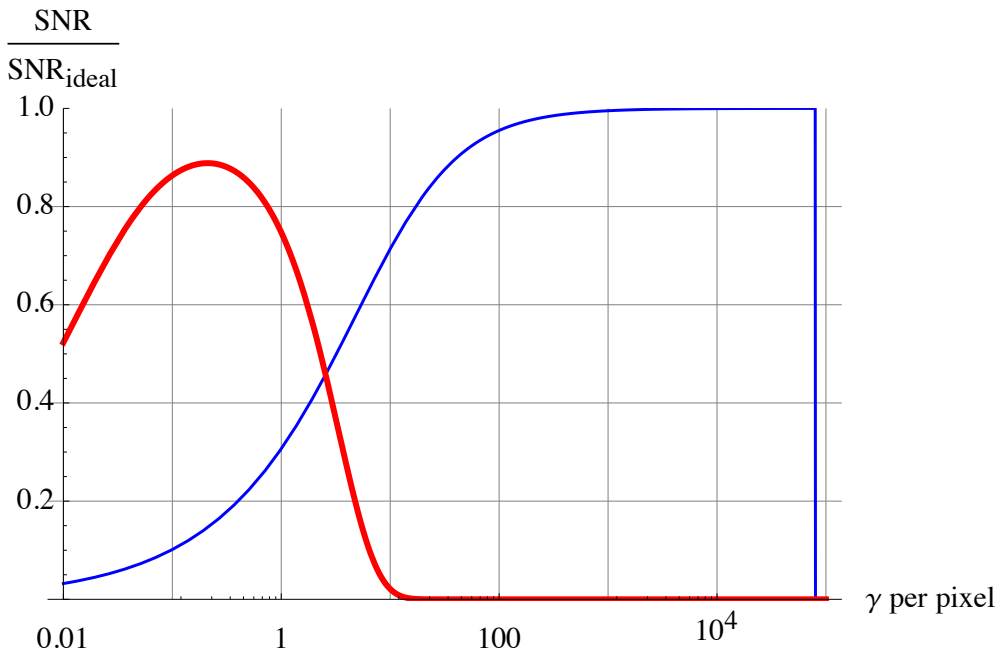


Figure 33: The signal to noise of an EMCCD in photon counting mode (red) and in conventional mode (blue). The device's full well is specified at 80,000 counts. In this figure, signal to noise is expressed as a ratio between the delivered signal to noise relative to that of an ideal photon-counting device. What is apparent is that EMCCDs can operate as traditional CCDs (indeed, we can descope to conventional CCDs with little disadvantage; however, they increase the dynamic range by a factor of ~ 30.

based on expected sky backgrounds, resolution, CIC, dark current, and read noise. For GEONIS, the regimes are as follows: Below 16.5 mag pixels saturate because of a high coincidence rate of photons; we are not concerned because the device can be operated in conventional mode and GEONIS will deliver excellent spectra. Between 16.5 mag to 21st mag GEONIS is in the photon-counting sweet spot. The observing software adjusts the exposure time until the typical pixel receives 0.3 photon / pixel / exposure. Above 21st mag the exposure time in conventional mode is long enough that the observation is background limited in both modes. For faint targets that require exposures of 5 hours, there is only a small gain photon-counting mode. The above is illustrated in Figure 35 where these calculations are shown for CCD282 (the baselined EMCCD) assuming the published clock induced charge, gain, and our baseline spectral resolution.

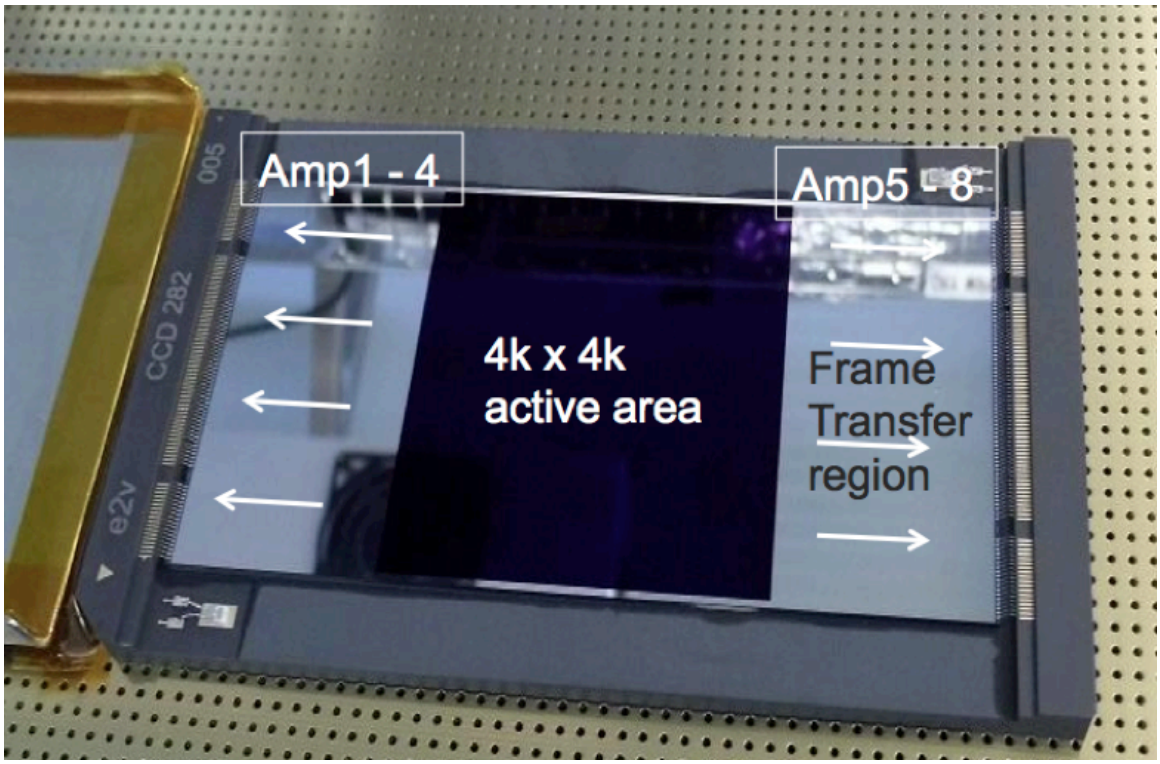


Figure 34: A picture of EMCCD e2v CCD 282 (the baselined device for GEONIS). The picture is from Gach et al. (2014). The active area of this device is the black region in the center, the reflective areas to the left and right of the active area is the frame transfer region. The frame transfer region is a conventional CCD with a reflective coating that prevents signal from reaching the pixels. During readout, the active area is transferred to the frame transfer region (10 ms total), then the eight amplifiers read 2k x 1k segments from the frame transfer region. Observers can choose between conventional amplifier only, analog mode (medium gain), or photon counting mode (high gain). Most observers will use photon counting or conventional modes.

An example image taken in photon counting mode is shown in Figure ??. The figure left panel is a single 90-s exposure in photon counting mode. The right figure is a coadd of 120 such 90-s frames. The faintest "square" in the three hour image has an average of 6 photon / pixel.

The main disadvantage of photon counting mode is loss of dynamic range. Photon counting mode is thus not useful in where there are hundreds of sources and, it is impossible to tune the exposure time to the aforementioned sweet spot. When imaging, the detector will operate in conventional frame-transfer mode. In spectroscopy mode, the focal plane is masked down to the slit, which selects individual targets and thus the dynamic range of the observation is known a priori.

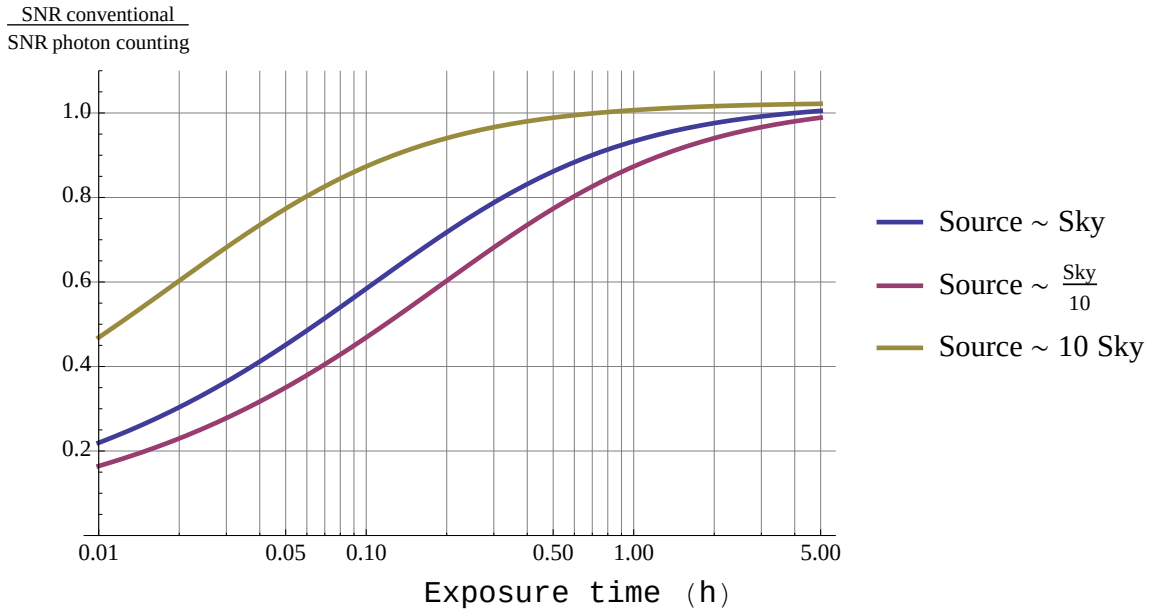


Figure 35: The difference between delivered signal to noise in conventional and photon counting modes. In photon counting mode, tens or hundreds of individual frames are stacked with CIC noise included. In conventional mode, a single long exposure is used and signal-to-noise is computed as $S/N = source\ signal/\sqrt{sky\ shot\ noise + source\ shot\ noise + RN^2}$. The ratio of the two is plotted as a function of exposure time in hour. Three signals representing 10x, 1x, and 0.1x the sky signal are shown. When the target is bright ($> 10\times$ sky) it is better to observe the target in conventional mode. For faint objects with a several-hour exposure time, photon counting mode is roughly as good as conventional mode. Photon counting mode is in the "sweet spot" with several-minute exposures of objects about as bright as the sky background. When in the sweet spot, photon counting mode is thus perfect for binning to a lower spectral resolution.

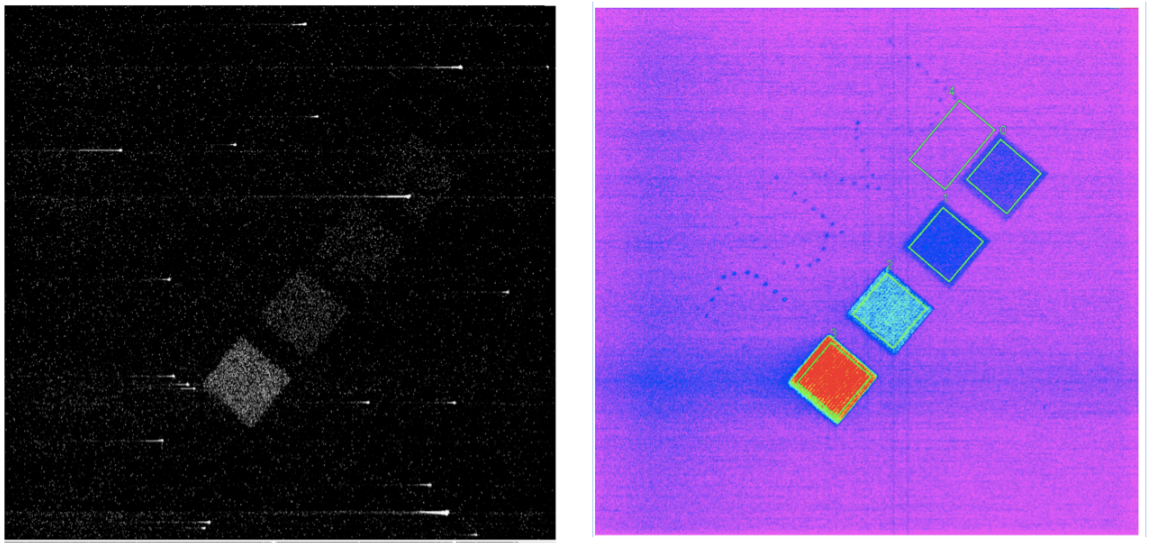


Figure 36: Two EMCCD images from Daigle et al. (2014). Left: is a 90-s exposure of a frame in photon counting mode (the streaks are cosmic rays). The right image is a three-hour stack of images taken in the left frame. Right: the bottom-left red square represents a 20 pho-ton/hour signal while the upper-right blue square is a 2 photon/hour signal. Notice, the name of Daigle's company nüvü can be seen.

D.10 Description of Known Risks for GEONIS

The major risks for GEONIS are listed in the risk table below. The table shows risk probability rated in low (L), medium (M), or high (H), risk impact (same rating), and description of the risk and its mitigation strategy. For this table we focus on the riskiest and/or most impactful risks.

The feasibility of achieving the $12 M cost cap is demonstrated in the next section (§E). There we show that our current baselined instrument is estimated to cost $9.8 M. The estimate is based on analogy to other instruments, and carries an inherit risk and uncertainty.

Table 13: Risk Table - risk level, impact, and description/mitigation strategy.

R	I	Description and Mitigation
M	H	Risk: Stray light analysis shows that the stray-light background is unacceptably high and there is no affordable way to reduce the background. Mitigation: Descope to the optical arm.
H	M	Risk: Instrument is 10% over cost limit. Mitigations: (a) Phase delivery of instrument channels, (b) 10% level descopes on scientific performance in all areas.
H	L	Risk: Instrument is 10% over mass limit. Mitigations: mass exception from Gemini.
M	M	Risk: Instrument is over mass limit plus 10% exception. Mitigations: descope field size.
L	H	Risk: Instrument is significantly over the $12 M cost cap. Mitigations: Major descope includes dropping a major mode (a) dropping the infrared arm, (b) dropping exoplanet longslit and imaging modes.
L	H	Risk: Hawaii 4RG devices are not available. Mitigation: Phase delivery of NIR arm or descope to a Hawaii 2 RG.
L	M	Risk: EMCCD electronics not available. Note: Caltech has a number of groups working on EMCCDs and there are at least three known vendors for EMCCD readout electronics, we thus assign this a low risk.

D.11 GEONIS is a Workhorse Instrument

We confirm that GEONIS is a workhorse instrument. GEONIS is designed around a broad science cases by expert instrumentalists.

D.12 Optical Drawing Tree

GEONIS is currently separated into several ZEMAX files. The drawing tree is summarized in Table 14.

Red side	20150801b	
	Mirror	20150801g
	Lowres	20150801e
	Highres	20150801d
	Camera	20150801n
IR side	20150801c	
	Mirror	20150801k
	Lowres	20150801i
	Hires	20150801h
	Camera	20150801o
Acquisition	201508011	
ADC	20150801m	

Table 14: Optical drawing tree. Item name and zemax file name are shown for the various optical systems.

D.13 Organization of Mechanical Drawings

We have used Solidworks to create the solid models for GEONIS. Associated with this report is a zip file containing the solid models. The models are comprised of STL exports from zemax.

The models are organized under a top-level file called GEONIS. GEONIS is in turn composed of the following five elements:

- The ISS cube
- The ISS frame
- Keep out zone (external)
- Keep out zone (between GEONIS and ISS)
- Optics – The key optical components are:
  - RED [optical side]. Comprised of all opticalside zemax files.
  - IR [IR side]. Comprised of all IR side zemax files.
  - slit viewer: 201508011 (imported from associated zemax file)
  - ADC: 20150801m (imported)
  - Red camera: 201508101n (imported)
  - IR camera: 20150801o (imported)

D.14 Summary of Changes from GEONIS Proposal

The GEONIS final concept achieves the same scientific goals as we proposed; however; the instrument layout change substantially. In this subsection we describe the changes against the proposal.

Proposal risks identified and mitigated:

1. The proposed collimator was a heavy dioptric lens (estimate of 10% of the mass budget). The proposed collimator could not be folded to bring mass towards the required center of gravity of the instrument and underperformed in terms of image quality. Predicted Risk: This item was identified as high risk during the proposal phase. Mitigation: We sacrificed field of view and created a reflective collimator. The reflective collimator naturally folds the center of mass of the instrument onto itself. The reflective collimator is also simpler to build, test, and integrate.

2. The proposed dispersing systems were grating-prism combinations ("grism") operating at high incidence angle and high order. Predicted risk: This item was identified as high risk during the proposal phase. Mitigation: Based on

GSOLVER rigorous coupled wave analysis simulations, we discovered that grisms operating at high order have half the throughput of reflective gratings due to shadowing effects. Throughput is an essential component of GEONIS, so the current version of GEONIS uses reflective gratings.

3. The proposed slit length was $15''$, which we proposed would be enough for exoplanetology. Predicted risk This item was predicted as low risk during the proposal phase. Mitigation: Based on simulations, we show that a slit length of $5'$ covers about 20% of predicted significant targets in the TESS era. We thus added a new "low resolution" observing mode with a slit that is at least $5'$ in length.

4. The proposed cameras were required to deliver $0.3''$ images. Predicted risk: This item was identified as low risk. Mitigation: During systems engineering, we showed that to respect Gemini's excellent image quality, the cameras must deliver much sharper images (§D.6.2). Given the dramatic change in required image quality, and in order to demonstrate feasibility, we designed new cameras for the optical and near infrared channels.

5. Proposed ADC did not fit into space envelope between the instrument support structure and slitmask. Predicted Risk: This item was identified as low risk during the proposal phase. Mitigation: Field of view reduced, ADC now fits into the space between ISS and slitmask. However, the ADC does penetrate the keep out zone during operations.

6. The proposal required a cold enclosure around the infrared arm of the spectrograph. Given the performance of a new infrared-blocking filter from Asahi corporation ($\sim 10^{-6}$) we do not need this cold enclosure anymore.

A side-by-side comparison of GEONIS as proposed to the current concept is shown in Figure 37.

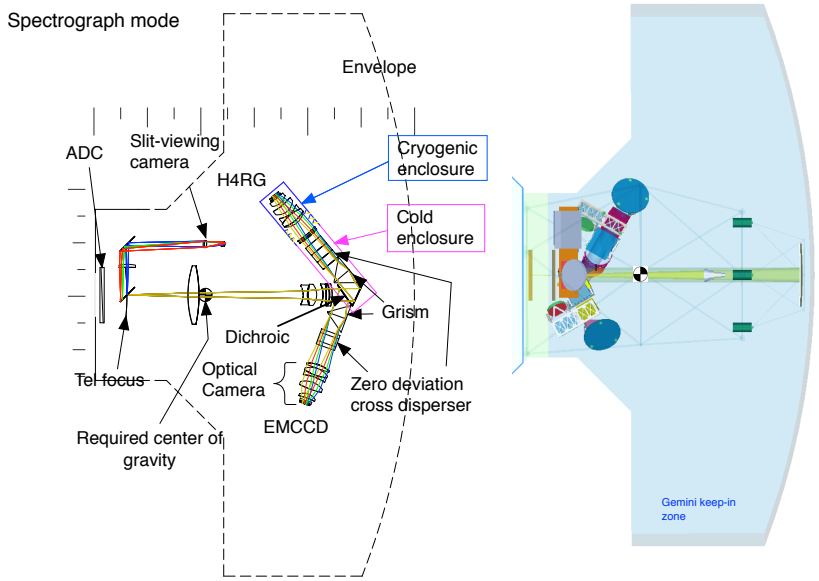


Figure 37: Comparison of instrument layouts between proposal and conceptual design. Note that the instrument is folded and packaged to respect the center of mass requirement.

References

LIGO Scientific Collaboration, Virgo Collaboration, Aasi, J., et al. 2013, arXiv:1304.0670

Barnes, J., & Kasen, D. 2013, Astrophysical Journal, 775, 18

Bingham, R. G. 1979, Royal Astronomical Society, Quarterly Journal, 20, 395

Cenko, S. B., Kulkarni, S. R., Horesh, A., et al. 2013, Astrophysical Journal, 769, 130

Chen, H.-W., Perley, D. A., Pollack, L. K., et al. 2009, Astrophysical Journal, 691, 152

Chornock, R., Berger, E., Fox, D. B., et al. 2013, Astrophysical Journal, 774, 26

Cucchiara, A., Levan, A. J., Fox, D. B., et al. 2011, Astrophysical Journal, 736, 7

Daigle, O., Djazovski, O., Dupuis, J., Doyon, R., & Artigau, É. 2014, Proceedings of the SPIE, 9154, 91540D

Dhillon, V., Marsh, T., Copperwheat, C., et al. 2007, The Messenger, 127, 41

Dhillon, V. S., Marsh, T. R., Atkinson, D. C., et al. 2014, Monthly Notices of the Royal Astronomical Society, 444, 3504
A. J., Fruchter, A. S., et al. 2012, Astrophysical Journal, 754, 46

Totani, T., & Panaitescu, A. 2002, Astrophysical Journal, 576, 120

Gach, J.-L., Carignan, C., Hernandez, O., et al. 2014, Proceedings of the SPIE, 9154, 91540A

Gal-Yam, A., Arcavi, I., Ofek, E. O., et al. 2014, Nature, 509, 471

Kasen, D., Badnell, N. R., & Barnes, J. 2013, Astrophysical Journal, 774, 25

Kasliwal, M. M. 2011, Ph.D. Thesis,

Lang, D., Hogg, D. W., Mierle, K., Blanton, M., & Roweis, S. 2010, The Astronomical Journal, 139, 1782

Laskar, T., Berger, E., & Chary, R.-R. 2011, Astrophysical Journal, 739, 1

Law, N. M., Mackay, C. D., Dekany, R. G., et al. 2009, Astrophysical Journal, 692, 924

Matheson, T., Fan, X., Green, R., et al. 2013, arXiv:1311.2496

McLean, I. S., Steidel, C. C., Epps, H. W., Konidaris, N. P. et al. 2012, Proceedings of the SPIE, 8446, 84460J

McQuinn, M., Lidz, A., Zaldarriaga, M., Hernquist, L., & Dutta, S. 2008, Monthly Notices of the Royal Astronomical Society, 388, 1101

Mesinger, A., & Furlanetto, S. R. 2008, Monthly Notices of the Royal Astronomical Society, 385, 1348

Miralda-Escudé, J. 1998, Astrophysical Journal, 501, 15

Nelson, J. 2005, NATO ASIB Proc. 198: Optics in astrophysics, 49

Phillips, A. C., Miller, J., Cowley, D., & Wallace, V. 2008, Proceedings of the SPIE, 7014, 701453

Prochaska, J. X., Chen, H.-W., Dessauges-Zavadsky, M., & Bloom, J. S. 2007, Astrophysical Journal, 666, 267

Robbins, M. and Hadwen, B., "The noise performance of electron multiplying charge-coupled devices," Electron Devices, IEEE Transactions on 50, 1227?1232 (May 2003).

Radovan, M. V., Bigelow, B. C., Nelson, J. E., & Sheinis, A. I. 1998, Proceedings of the SPIE, 3355, 155

Saha, A., Matheson, T., Snodgrass, R., et al. 2014, Proceedings of the SPIE, 9149, 914908

Sheinis, A. I., Bolte, M., Epps, H. W., et al. 2002, Publications of the Astronomical Society of the Pacific, 114, 851

Tanvir, N. R., Fox, D. B., Levan, A. J., et al. 2009, Nature, 461, 1254

Tanvir, N. R., Levan, A. J., Fruchter, A. S., et al. 2012, Astrophysical Journal, 754, 46

Tulloch, S. M., & Dhillon, V. S. 2011, Monthly Notices of the Royal Astronomical Society, 411, 211

Vogt, S. S., Radovan, M., Kibrick, R., et al. 2014, Publications of the Astronomical Society of the Pacific, 126, 359

Wolf, M. J., Mulligan, M. P., Smith, M. P., et al. 2014, Proceedings of the SPIE, 9147, 91470B